TonEBP in macrophages and adipocytes contributes to obesity and type 2 diabetes

Hwan Hee Lee

Department of Biological Sciences

Graduate School of UNIST

TonEBP in macrophages and adipocytes contributes to obesity and type 2 diabetes

A thesis/dissertation submitted to the Graduate School of UNIST
in partial fulfillment of the requirements
for the degree of Doctor of Philosophy

Hwan Hee Lee

6. 19. 2017

Approved by

Hyug Moo Kwon

Advisor

Hyug Moo Kwon

TonEBP in macrophages and adipocytes contributes to obesity and type 2 diabetes

Hwan Hee Lee

This certifies that the thesis/dissertation of Hwan Hee Lee is approved.

6. 19. 2017

Hyug Moo Kwon

Advisor: Hyug Moo Kwon

Byoung Heon Kang

Myunggon Ko

Jiyoung Park

Jang Hyun Choi

Abstract

The global epidemic of obesity poses serious burden to human health due to its associated risks of chronic diseases including type 2 diabetes and cardiovascular diseases. Adipose tissues have received a lot of attention since as it has become clear that adipocytes and macrophages in them are important integrators of diverse physiological pathways regulating systemic insulin sensitivity and energy homeostasis. It is therefore urgently necessary to identify regulatory convergence points that can be therapeutic targets to improve insulin resistance and impaired energy homeostasis in obesity.

Tonicity responsive enhancer-binding protein (TonEBP), also known as NFAT5, is a critical regulator in cellular adaptation to hypertonic stress, macrophage activation, and T-cell development. In this study I found that adipocyte *TONEBP* expression correlated with body mass index in subcutaneous fat tissues from human subjects. In addition, *TONEBP* expression in leukocytes correlated with fasting blood glucose in patients with type 2 diabetes. In subcutaneous adipose tissues of mice *TonEBP* expression increased >50-fold in response to feeding with high fat diet (HFD). In order to understand the role of TonEBP in obesity, I examined a line of mice with TonEBP haplo-deficiency. These animals showed resistance to HFD-induced weight gain and insulin resistance in association with higher energy expenditure and lower adipose tissue inflammation. To delineate TonEBP action mechanisms in adipose tissues, I studied the role of TonEBP in both adipocytes and macrophages further.

In order to investigate the role of TonEBP in macrophages, a line of mice with myeloid-specific deletion of TonEBP was generated. When fed with HFD, these animals displayed improved insulin resistance without changes in body weight. Their adipose tissue contained fewer M1 macrophages and more M2 macrophages indicating reduced inflammation. Lipopolysaccharide (LPS)-induced assembly of NFκB enhanceosome was found. In this enhanceosome, TonEBP was required for the recruitment of p300 and RNA polymerase II. TonEBP was rate-limiting in that increased expression of TonEBP enhanced the NFκB activity and reduced TonEBP expression lowered it without affecting NFκB itself. LPS induced the expression of TonEBP leading to elevated assembly of the NFκB enhanceosome. Recombinant TonEBP molecules incapable of recruiting p300 did not stimulate NFκB. A natural small molecule cerulenin was found to specifically disrupt the enhanceosome assembly without altering NFκB. Cerulenin dramatically suppressed the inflammatory activation of macrophages and prevented death by septic shock. Thus, the TonEBP-mediated NFκB enhanceosome offers a promising target for useful anti-inflammatory agents. In addition, TonEBP deficiency promoted M2 macrophage polarization with enhanced PPARγ expression. These data suggest that variations in the level of TonEBP expression determine individual variations in insulin resistance and inflammation regulated by NFκB and PPARγ. Taken together the findings reveal that TonEBP promotes insulin resistance through the stimulation of NFκB in combination with the suppression of PPARγ.

To address the role of TonEBP in adipocytes, another line of mice with adipocyte-specific deletion of TonEBP was produced. When fed with HFD these animals displayed improved insulin resistance and lower body weight much like the TonEBP haplo-deficient animals. They also showed elevated energy expenditure and resistance to hypothermia when exposed to cold. In subcutaneous white adipose tissues (WAT) higher levels of beige fat markers and thermogenic genes such as uncoupling protein-1 (UCP-1) and peroxisome proliferator-activated receptor gamma coactivator 1-alpha (PGC-1α) were expressed. This was due to an enhanced expression of the β3-adrenergic receptor (Adrb3). TonEBP recruited DNA methyltransferase 1 (DNMT1) to the *Adrb3* promoter and promoted DNA methylation leading to the suppression of the promoter. These data indicate that TonEBP in adipocytes promotes obesity and insulin resistance by the suppression of the Adrb3 expression and blocking the beiging of WAT.

In conclusion, TonEBP in adipocytes and macrophages contributes to obesity and insulin resistance due to the suppression of WAT beiging and the promotion of inflammation, respectively. As such, TonEBP offers an attractive therapeutic target for obesity and type 2 diabetes.

Contents

Abstract ····· 1

Contents ····· 3

List of figures ····· 5

Abbreviations ····· 7

Chapter1. Background ····· 9

1-1. Obesity and its related metabolic disorders ····· 9

1-2. Adipose tissue inflammation in obesity ····· 9

1-3. Adipose tissue macrophages (ATMs) ····· 9

1-4. Beiging of white adipose tissue (WAT) ····· 10

1-5. Tonicity-responsive enhancer binding protein (TonEBP) ····· 11

Chapter2. Macrophage TonEBP promotes inflammation and insulin resistance by regulating M1/M2 polarization ····· 24

2-1. Introduction ····· 24

2-2. Materials and methods ····· 26

2-3. Results ····· 32

2-4. Discussion ····· 40

2-5. References ····· 64

Chapter3. Adipocyte TonEBP promotes obesity through the suppression of WAT beiging ····· 68

3-1. Introduction ····· 68

3-2. Materials and methods ····· 70

3-3. Results ····· 75

3-4. Discussion ····· 81

3-5. References ····· 104

Conclusion ····· 107

Acknowledgements ····· 109

List of Figures

Figure 1-1. Obesity and its related complications
Figure 1-2. Obesity-induced inflammation and insulin resistance
Figure 1-3. Inflammation and immune cells in obese adipose tissue
Figure 1-4. Crosstalk between macrophages and adipocytes in adipose tissue
Figure 1-5. Three types of adipocytes: Brown, Beige and White adipocyte
Figure 1-6. Adipose tissue beiging and metabolic health
Figure 1-7. Scheme of NFATs and NFκB structure
Figure 1-8. Physiology of TonEBP in hypertonic stress
Figure 1-9. TonEBP in inflammatory diseases

Figure 2-1. Reduced inflammation and septic death in mice with myeloid-specific deletion of the *TonEBP* gene.
Figure 2-2. TonEBP binds to the κB site of the *TNFα* promoter without direct interaction with DNA.
Figure 2-3. TonEBP interacts with p65.
Figure 2-4. TonEBP interacts with p65 via respective RHDs.
Figure 2-5. Stimulation of NFκB by TonEBP requires the TonEBP-p65 interaction.
Figure 2-6. Reduced NFκB activity in *TonEBPΔ/Δ* MEF cells despite normal expression and regulation of NFκB.
Figure 2-7. TonEBP knockdown does not affect DNA binding of p65.
Figure 2-8. The TonEBP Δ protein is unable to recruit p300 co-activator to p65.
Figure 2-9. The transactivation domain of TonEBP mediates the NFκB activation.
Figure 2-10. TonEBP-p300 interaction is independent of p65.
Figure 2-11. TonEBP deficiency breaks down the LPS-induced NFκB enhanceosome assembly on *TNFα* promoter.
Figure 2-12. Cerulenin breaks up the TonEBP-p300-p65 interaction and reduces inflammation.
Figure 2-13. Cerulenin reduces inflammation without cytotoxicity.
Figure 2-14. Cerulenin reduces inflammation and septic death in mice.
Figure 2-15. Cerulenin does not affect nuclear localization, DNA binding, and phosphorylation of p65.
Figure 2-16. IL-4 diminishes the expression of TonEBP which reduces the expression of M2 genes in macrophages
Figure 2-17. TonEBP deficiency enhances the expression and signaling of IL-10 in M1 macrophages

Figure 2-18. TONEBP deficiency enhances the expression of IL-10 in primary human macrophages obtained from 3 donors
Figure 2-19. β-lapachone reduces TonEBP expression and enhances IL-10 expression
Figure 2-20. TonEBP deficiency increases PPARγ1 expression in RAW264.7 cells
Figure 2-21. Myeloid specific TonEBP deficiency improves metabolic profiles in obesity
Figure 2-22. Myeloid specific TonEBP deficiency reduces adipose tissue inflammation by regulating macrophage polarization
Figure 2-23. Schematic model for the role of TonEBP in obesity-induced insulin resistance

Figure 3-1. *TonEBP* mRNA expression in metabolic tissues.
Figure 3-2. Adipocyte TonEBP expression was induced in obesity
Figure 3-3. TonEBP haplo-deficient mice resist the development of obesity
Figure 3-4. TonEBP deficiency protects obesity in db/db mice
Figure 3-5. TonEBP deficiency promotes energy expenditure
Figure 3-6. TonEBP deficiency enhances thermogenesis and beiging of WAT
Figure 3-7. Effects of TonEBP knockdown or overexpression on thermogenic gene expression in 3T3-L1 cells
Figure 3-8. TonEBP deficiency ameliorates obesity-induced insulin resistance
Figure 3-9. TonEBP deficiency ameliorates obesity-induced metabolic dysfunction
Figure 3-10. TonEBP deficiency protects fatty liver in obesity
Figure 3-11. TonEBP deficiency ameliorates obesity-induced hyperlipidemia
Figure 3-12. TonEBP suppresses *Adrb3* gene expression
Figure 3-13. TonEBP suppresses *Adrb3* promoter activity by binding to TonE element
Figure 3-14. TonEBP promotes DNA methylation on *Adrb3* promoter
Figure 3-15. TonEBP recruits DNMT1 to *Adrb3* promoter through the interaction
Figure 3-16. DNMT inhibition protects HFD-induced obesity
Figure 3-17. DNMT inhibition enhances energy expenditure by inducing WAT beiging and Adrb3 expression
Figure 3-18. DNMT1 deficiency increases *Adrb3* expression
Figure 3-19. TonEBP is a direct target of miR-30b and miR-30c.
Figure 3-20. Improved metabolic phenotype of adipocyte-specific TonEBP knockout mice
Figure 3-21. Schematic model for the role of TonEBP in obesity

Graphical summary

Abbreviations

WHO: World Health Organization

TNF-α: tumor necrosis factor-α

IL-10: interleukin-10

ATMs: adipose tissue macrophages

M2 macrophages: alternatively activated macrophages

SVCs: stromal vascular cells (SVCs).

M1 macrophages: classically activated macrophages

NFκB: nuclear factor κB

PPARγ1: peroxisome proliferator-activated receptor γ1

WAT: white adipose tissue

BAT: brown adipose tissue

UCP1: uncoupling protein 1

TonEBP: Tonicity-responsive enhancer binding protein

NFAT5: nuclear factor of activated T cells 5

CBP: CREB binding protein

LPS: lipopolysaccharide

HFD: high fat diet

LysM: lysozyme M

MEFs: mouse embryo fibroblasts (MEFs),

EMSA: electrophoretic mobility shift assay

GalN: D-galactosamine

PECs: peritoneal macrophages

ChIP: chromatin immunoprecipitation

DAPA: DNA affinity purification analysis

RHD: rel homology domain

TAD: transactivation domain

SOCS3: suppressor of cytokine signaling-3

STAT3: signal transducer and activator of transcription 3

BMDM: bone marrow derived macrophage

iNOS: inducible nitric oxide synthase

AQ: adiponectin

AIM: adipogenesis inducing medium

TG: triacylglyceride

FFA: free fatty acid

iWAT: inguinal white adipose tissue

eWAT: epididymal white adipose tissue

PGC1α: PPAR γ coactivator 1α

BMI: body mass index

HSL: hormone sensitive lipase

GTT: glucose tolerance test

ITT: insulin tolerance test

ALT: alanine aminotransferase

LDL: low density lipoprotein

Adrb3: β3-adrenergic receptor

DNMT: DNA methylatrasferase

Chapter1. Background

1-1. Obesity and its related metabolic disorders

Obesity is epidemic in the worldwide, with rapidly and steadily rising rates. Obesity and related diseases are the biggest threats to human health in the world. Obesity is associated with complex metabolic disorders such as certain types of cancer, type 2 diabetes, non-alcoholic fatty liver, dyslipidemia, hypertension, cardiovascular disease and stroke [1-3]. In addition, obese people of all ages are often psychological and social problems, such as low self-esteem and depression. According to World Health Organization (WHO) analysis, overweight and obesity are linked to more deaths worldwide than underweight. The deaths are caused by 44% of diabetes, 23% of ischemic heart disease and 7-41% of certain cancers [4]. Many studies suggested that obesity might be causative factors for these complications by several mechanisms (Fig. 1-1) [5].

1-2. Adipose tissue inflammation in obesity

One of the most reliable links between obesity and its complication is inflammation. Obesity induces low-grade inflammation in metabolic tissues including adipose tissue, liver and skeletal muscle. Obesity-induced inflammation causes systemic insulin resistance by inhibiting insulin signal transduction in metabolic tissues (Fig. 1-2) [6]. Abdominal adipose tissue inflammation is mainly occurred and it is a central mediator for systemic insulin resistance in obese condition. The imbalance between energy intake and outputs causes large amounts of lipid accumulation in adipocytes, leading to white adipose tissue expansion in the processes such as adipose tissue hyperplasia and hypertrophy. In this adipose tissue expansion, several adipocytes located in a region at a distance from the blood vessel undergo hypoxia and necrosis leading to secretion of chemokines for immune cell infiltration. After that, they are surrounded by immune cells initiating a local inflammatory responses characterized by an enhanced Tumor necrosis factor-α (TNF-α) and leptin levels, and reduced Interleukin-10 (IL-10) and adiponectin levels (Fig. 1-3) [7-8]. Stressful conditions such as hypoxia induce adipocyte dysfunction and reduced insulin action in adipocytes with apoptosis.

1-3. Adipose tissue macrophages (ATMs)

In adipose tissue and other metabolic tissues, macrophage has an important role in metabolic functions. The number and polarization of adipose tissue macrophages (ATMs) actively cross-talk with adipocytes in adipose tissue and reflect the metabolic profiles. For example, in lean mice, ATMs have alternatively activated (M2) phenotype comprising about 10% of stromal vascular cells (SVCs). However, classically activated (M1) macrophages are infiltrated to about 50% of SVCs and ATMs are polarized from M2 type to M1 type in obese mice [9]. The population of M1 and M2 ATMs is important

to determine the level of inflammatory and metabolic states in adipose tissue of obesity (Fig. 1-3). The M1 macrophages infiltrated by obesity secrete pro-inflammatory cytokines such as TNFα and promote insulin resistance in adipose tissue. M1 activation and pro-inflammatory responses are mainly promoted by transcriptional factor nuclear factor κB (NFκB). However, M2 macrophages enhances insulin sensitivity of adipocytes by secreting anti-inflammatory cytokines such as IL-10 and this polarization is enhanced by peroxisome proliferator-activated receptor γ1 (PPARγ1) (Fig. 1-4) [10]. Therefore, macrophage polarization in adipose tissue is critical for the development of insulin resistance in obesity.

1-4. Beiging of white adipose tissue (WAT)

Adipocytes are classically divided into white adipose tissue (WAT), which stores energy by accumulating lipids, and brown adipose tissue (BAT), which controls energy expenditure through nonshivering thermogenesis. Recently, a new type of brown-like adipose tissue was discovered in human that are called 'beige' and 'brite' from brown in white [11] (Fig. 1-5). The three types of adipocyte have many distinct characteristics associated with different colors, morphology, localization, cell composition (lipid droplet, mitochondria content) and gene expression [12]. WAT is either ivory or yellow due to unilocular/large lipid droplets with few mitochondria and stores excess energy as triglycerides to regulate energy homeostasis.

Brown adipocyte has different phenotypes including brownish color with high amount of mitochondria and multilocular small lipid droplets and regulates thermogenesis which is important for human in cold environment [13]. The thermogenesis process in brown adipocyte is mainly activated by uncoupling protein-1 (UCP1) in mitochondria. UCP1 mediates regulated proton leak across the mitochondrial inner membrane and thus dissipate the proton electrochemical gradient built up by converting chemical energy into the heat [14]. BAT is mainly localized in paravertebral, suprarenal, supraclavicular regions. In human, BAT generally represents in large depots during infancy but, only small amounts of BAT are remained in adults [11].

Beige adipocyte has combined features of white and brown adipocyte. Beige adipocytes are differentiated from beige precursor or trans-differentiated from white adipocyte in white adipose tissues [14]. Specific WAT depots can develop high numbers of beige adipocytes (beiging) induced by cold exposure, exercise, PPARγ ligands and β3-adrenergic agonists [15]. The beiging of WAT induced by stimuli makes healthy metabolic profiles with enhanced energy expenditure. However, excess energy intake and thermoneutrality increase lipid storage in adipocytes that morphologically resemble classic white adipocytes (whitening) [15]. The whitening of adipose tissue causes adipocyte dysfunction, inflammation and impaired thermogenesis leading to obesity and type 2 diabetes. (Fig. 1-6)

In this obese state, the increased number or activity of beige adipocytes by stimuli improves metabolic disorders and prevents obesity through the enhanced energy expenditure. Thus, there has

been emerging interest in “beiging” as a platform for anti-obesity therapeutic approaches.

1-5. Tonicity-responsive enhancer binding protein (TonEBP)

TonEBP, also known as nuclear factor of activated T cells 5 (NFAT5), belongs to the Rel family of transcriptional factors including NFκB and NFAT1-4 [16, 17] (Fig. 1-7). TonEBP has a variety of molecular and physiological functions. TonEBP was initially identified as the central DNA binding transcription factor of cellular response to hypertonic stress by regulating genes such as *BGT1, SMIT, AR* and *HSP70* [16, 18-20] (Fig. 1-8).

Recent studies have revealed that TonEBP act as a transcriptional co-activator in activation of NFκB and it promotes the M1 activation of macrophages and pro-inflammatory responses [21-22]. Consequently, TonEBP haplo-deficiency is associated with reduced inflammation leading to prevention of inflammatory and autoimmune diseases including diabetic nephropathy [23], diabetic retinopathy [24], rheumatoid arthritis [25], atherosclerosis [26] and encephalomyelitis [27] and seizure [28] in mouse models (Fig. 1-9).

The more recent study showed that TonEBP inhibits adipogenesis through the suppression of PPARγ2 expression, suggesting that TonEBP is one of the key transcription factors that control adipogenesis [29]. In this regulation, TonEBP is a transcriptional co-suppressor in *PPARγ2* transcription by recruiting histone methyltransferase to the promoter.

These studies demonstrated that TonEBP has pleiotropic functions including DNA binding transcription factor, transcriptional co-activator and transcriptional co-repressor in inflammation and adipocyte differentiation. Inflammation and adipocyte differentiation is critical for obesity and type 2 diabetes development. However, the role of TonEBP in obesity and type 2 diabetes was uncovered.

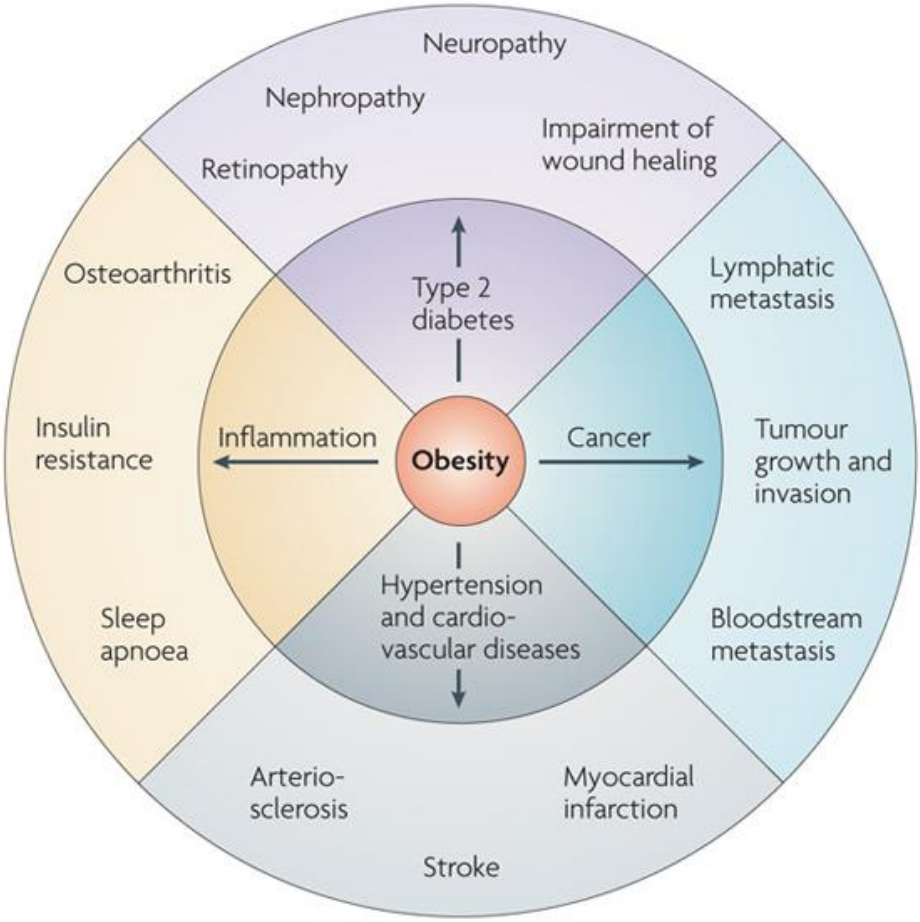

Figure 1-1. Obesity and its related complications

Nature Reviews Drug Discovery 9; 107-115 (2010)

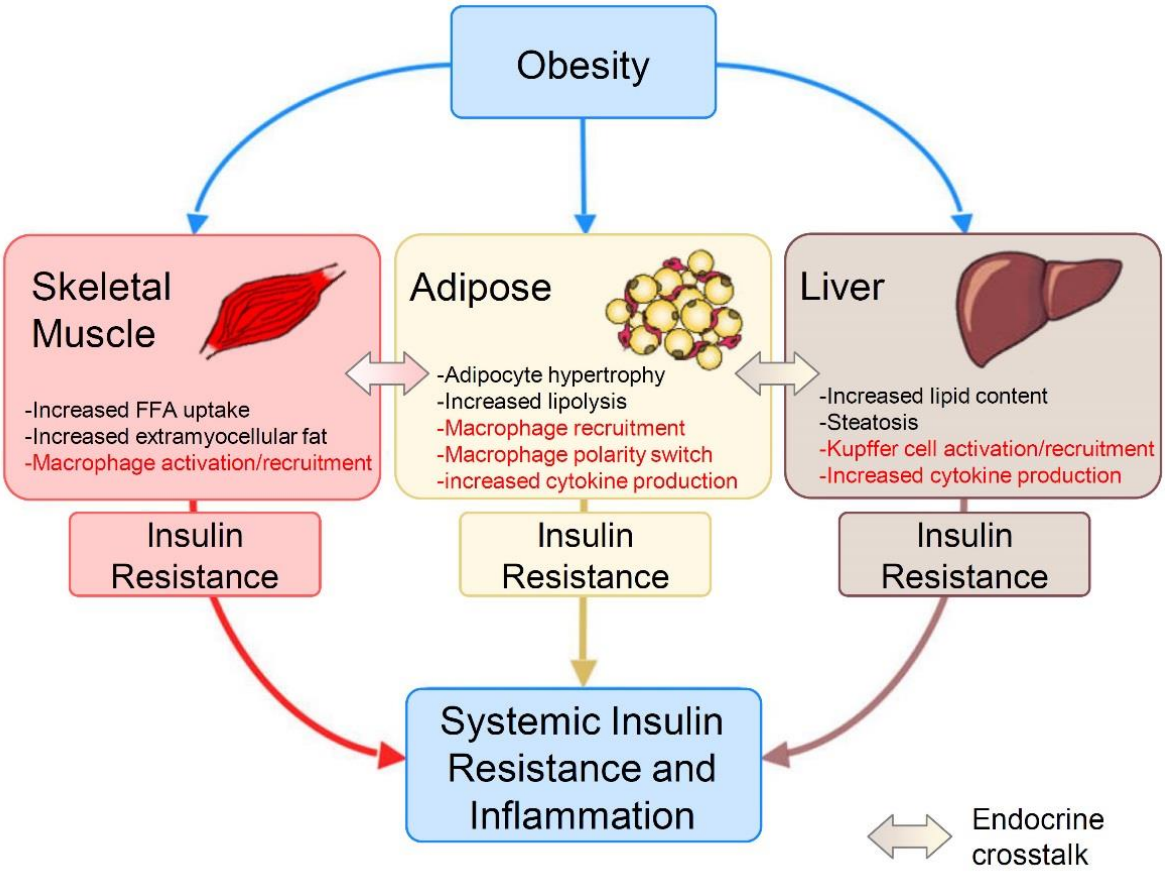

Figure 1-2. Obesity-induced inflammation and insulin resistance

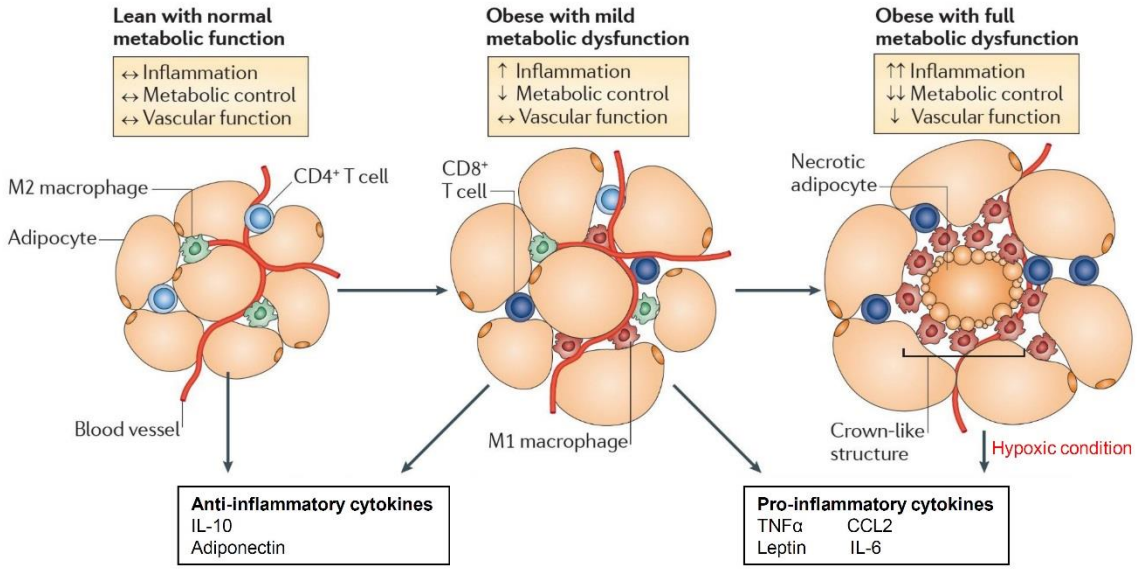

Figure 1-3. Inflammation and immune cells in obese adipose tissue

Nature Reviews Immunology 11; 85-97 (2011)

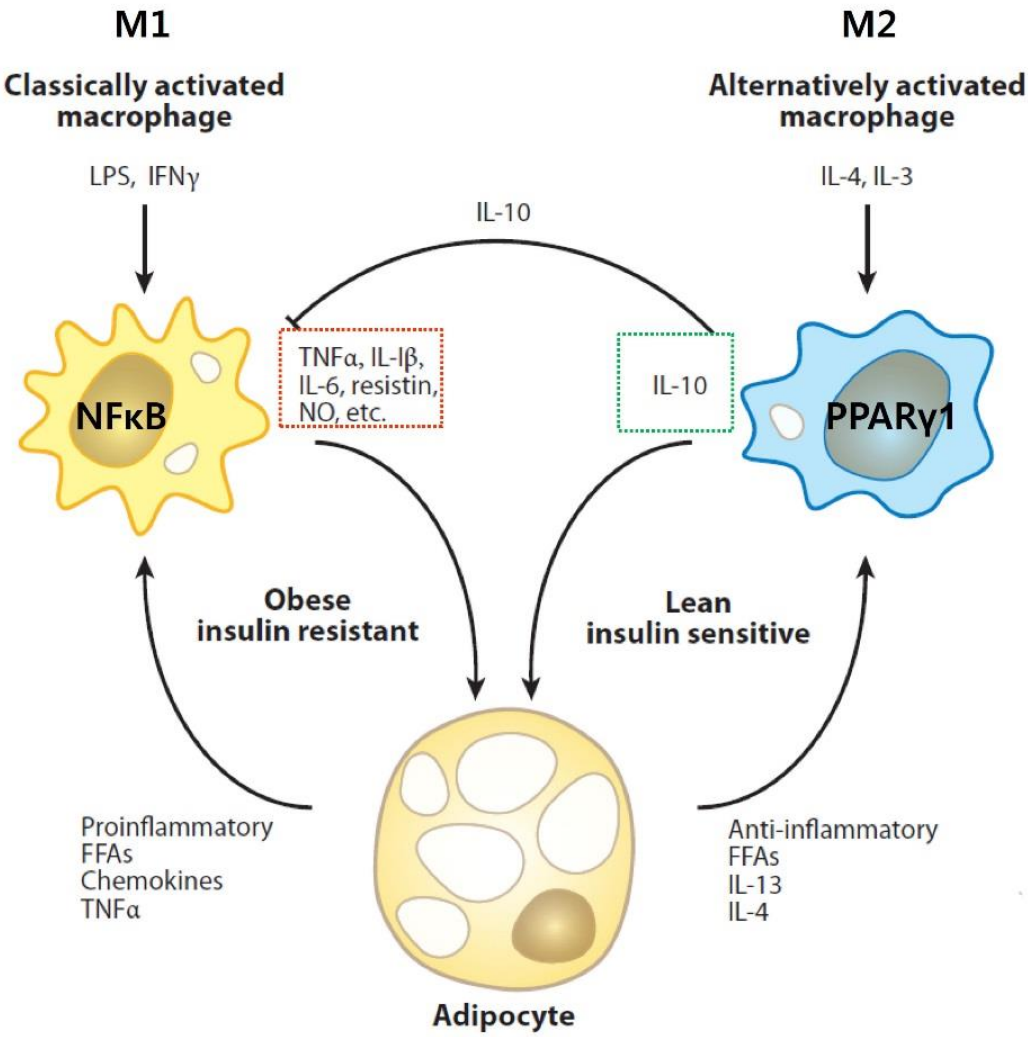

Figure 1-4. Crosstalk between macrophages and adipocytes in adipose tissue

Annu Rev Physiol 72 ; 219-246 (2010)

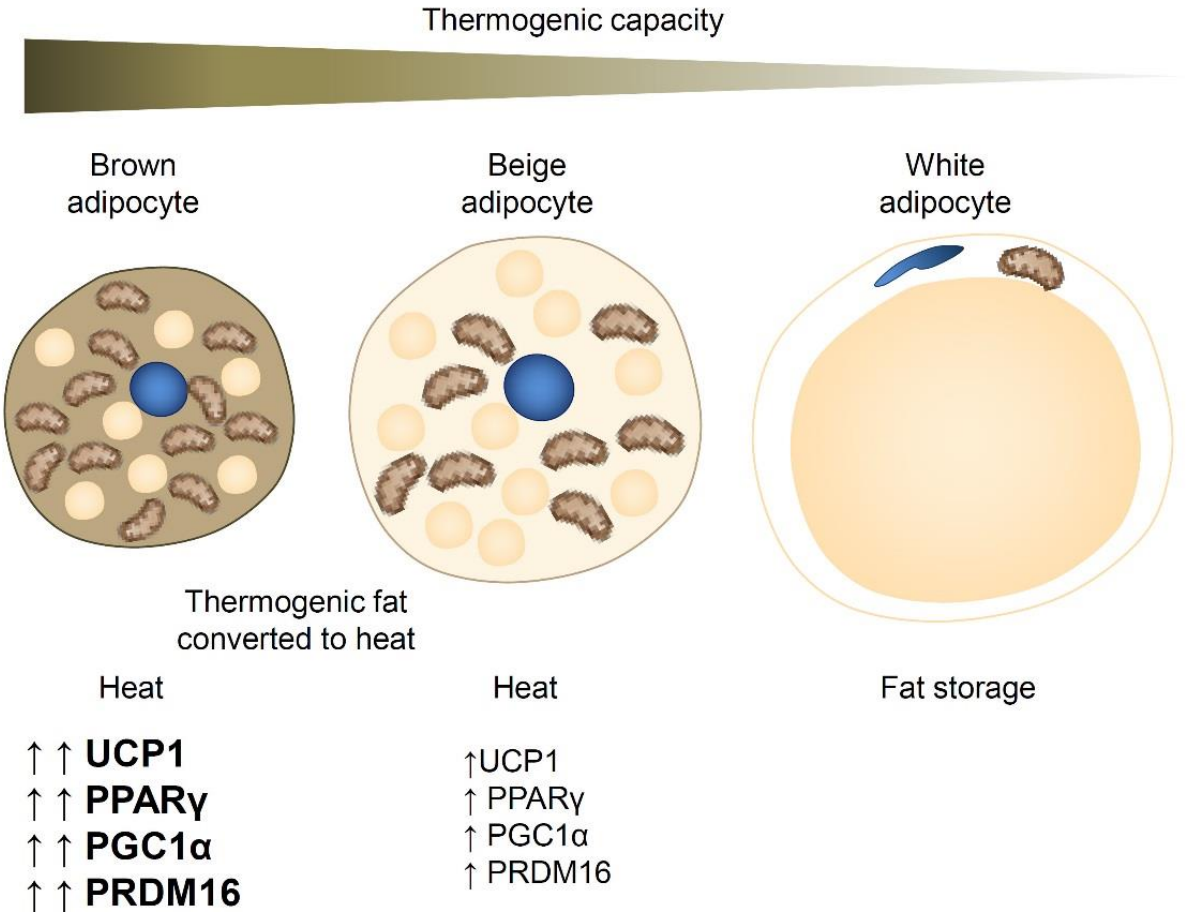

Figure 1-5. Three types of adipocytes: Brown, Beige and White adipocyte

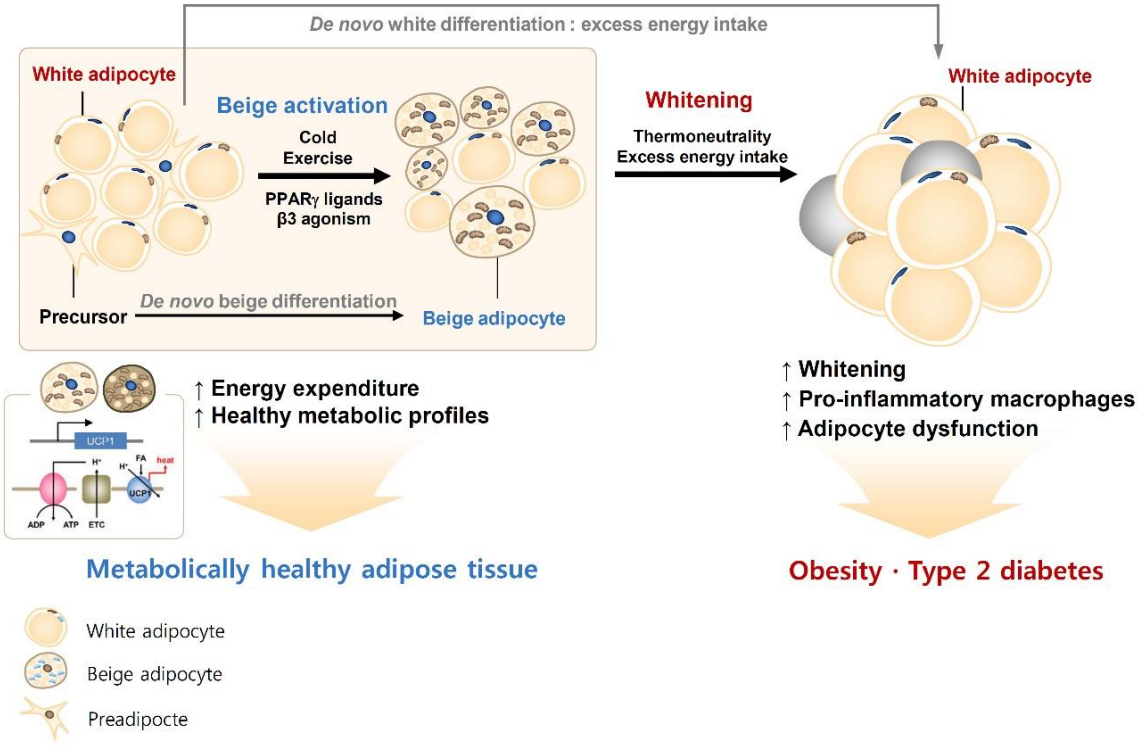

Figure 1-6. Adipose tissue beiging and metabolic health

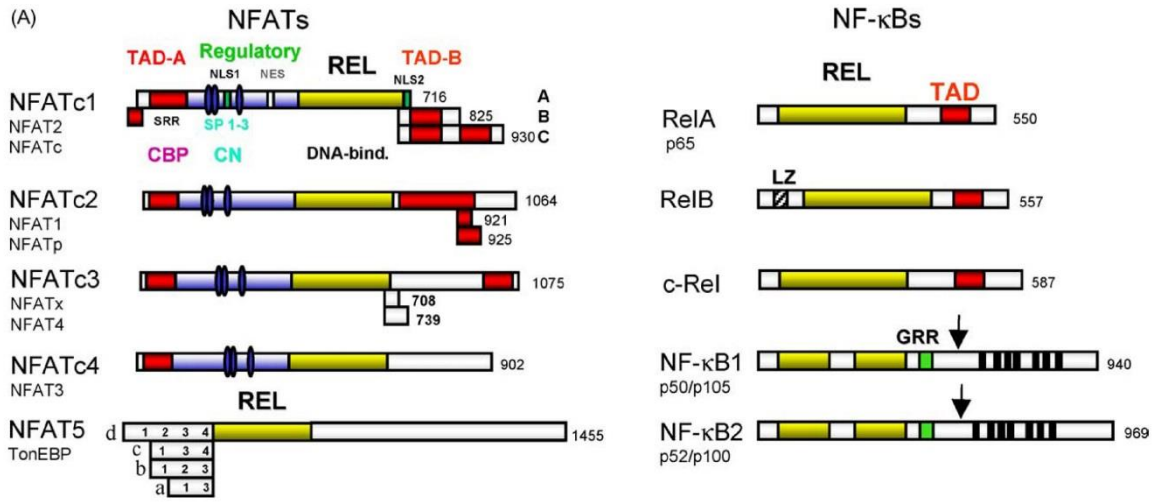

Figure 1-7. Scheme of NFATs and NFκB structure

Int J Biochem Cell Biol 36 ; 1166-1169 (2004)

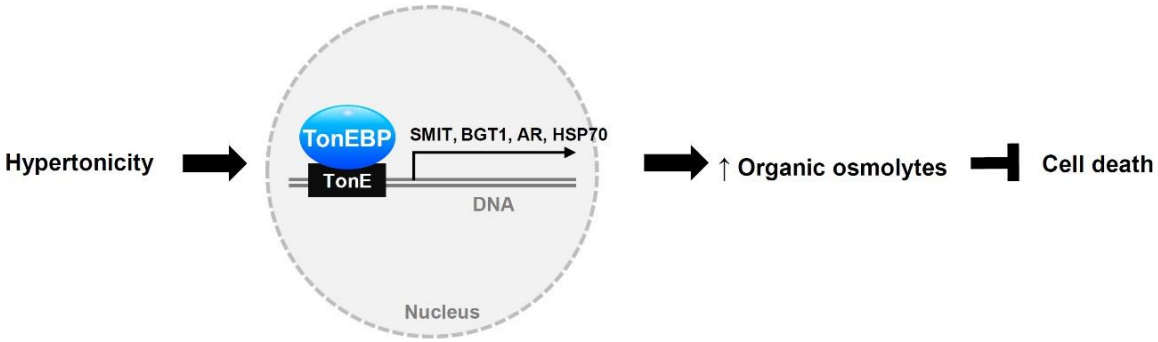

Figure 1-8. Physiology of TonEBP in hypertonic stress

Physiology 24 ; 186 (2009)

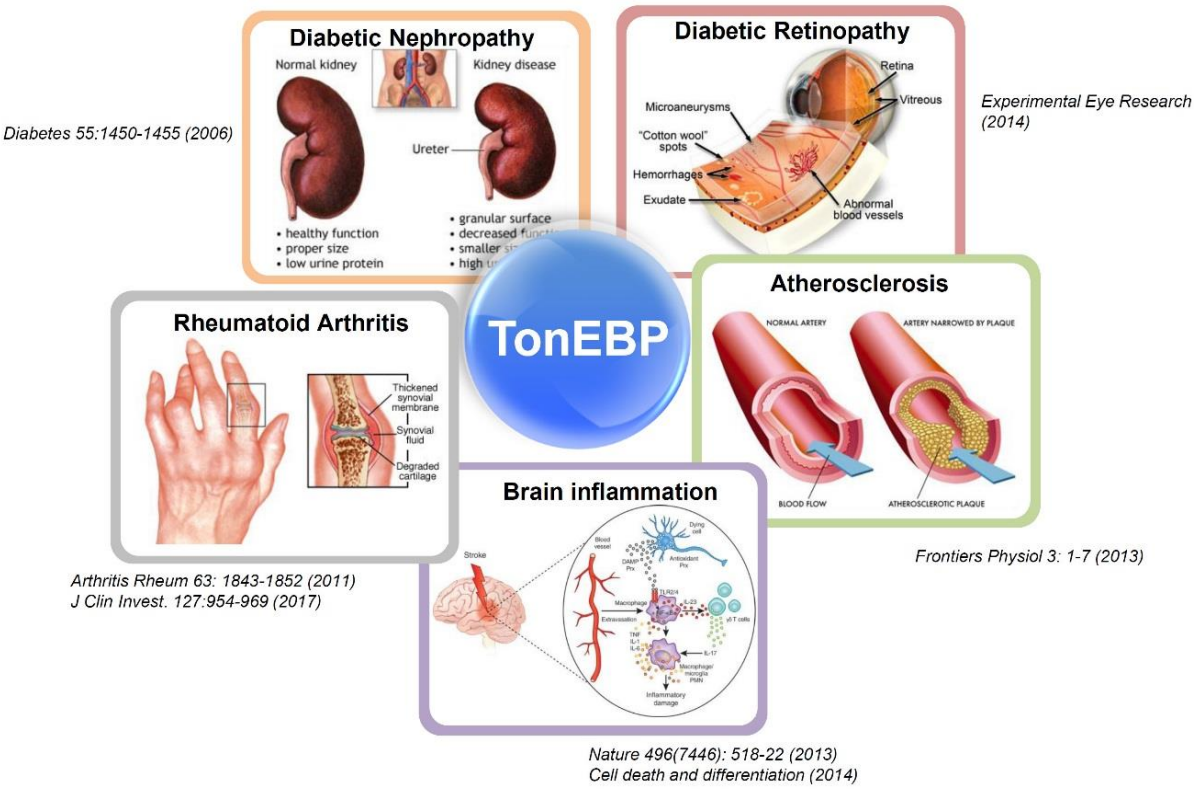

Diabetes 55:1450-1455 (2006)

Experimental Eye Research (2014)

Arthritis Rheum 63: 1843-1852 (2011)
J Clin Invest. 127:954-969 (2017)

Frontiers Physiol 3: 1-7 (2013)

Nature 496(7446): 518-22 (2013)
Cell death and differentiation (2014)

Figure 1-9. TonEBP in inflammatory diseases

1-6. Reference

1. Calle, E.E., Rodriguez, C., Walker-Thurmond, K. and Thun, M.J. 2003. Overweight, obesity, and mortality from cancer in a prospectively studied cohort of U.S. adults. *N. Engl. J. Med.* 348: 1625–1638
2. Eckel, R.H., Kahn, S.E., Ferrannini, E., Goldfine, A.B., Nathan, D.M., Schwartz, M.W., Smith, R.J. and Smith, S.R. 2011. Obesity and type 2 diabetes: what can be unified and what needs to be individualized? *J Clin Endocrinol Metab.* 96:1654-1663
3. Poirier, P., Giles, T.D., Bray, G.A., Hong, Y., Stern, J.S., Pi-Sunyer, F.X. and Eckel, R.H. 2006. Obesity and cardiovascular disease: pathophysiology, evaluation, and effect of weight loss. *Arteriosclerosis, Thrombosis, and Vascular Biology.* 26: 968–76
4. Mathers, C.D., Stevens, G.A. and Mascarenhas, M.N. 2009. GLOBAL HEALTH RISKS: Mortality and burden of disease attributable to selected major risks. *World Health Organization.*
5. Cao, Y. 2010. Adipose tissue angiogenesis as a therapeutic target for obesity and metabolic diseases. *Nat Rev Drug Discov.* 9: 107-115
6. de Luca, C and Olefsky, J.M. 2008. Inflammation and insulin resistance. *FEBS Lett.* 582; 97-105
7. Tilg, H. and Moschen, A.R. 2006. Adipocytokines: mediators linking adipose tissue, inflammation and immunity. *Nature Reviews Immunology*. 6: 772-783
8. Kusminski, C.M., Bickel, P.E. and Scherer, P.E. 2016. Targeting adipose tissue in the treatment of obesity-associated diabetes. *Nat Rev Drug Discov.* 15: 639-660
9. Fujisaka, S., Usui, I., Bukhari, A., Ikutani, M., Oya, T., Kanatani, Y., Tsuneyama, K., Nagai, Y., Takatsu, K., Urakaze, M., Kobayashi, M. and Tobe, K. 2009. Regulatory mechanisms for adipose tissue M1 and M2 macrophages in diet-induced obese mice. *Diabetes.* 58: 2574-2582
10. Olefsky, J.M. and Glass, C.K. 2010. Macrophages, inflammation, and insulin resistance. *Annu. Rev. Physiol.* 72: 219-246.
11. Peirce, V., Carobbio, S. and Vidal-Puig, A. 2014. The different shades of fat. *Nature*. 510: 76-83
12. Harms, M. and Seale, P. 2013. Brown and beige fat: development, function and therapeutic potential. *Nat Med.* 19:1252-1263
13. Nedergaard, J. and Cannon, B. 2013. How brown is brown fat? It depends where you look. *Nat Med.* 19:540-1
14. Busiello, R.A., Savarese, S. and Lombardi, A. 2015. Mitochondrial uncoupling proteins and energy metabolism. *Front Physiol.* 6: 36
15. Bartelt, A. and Heeren, J. 2014. Adipose tissue browning and metabolic health. *Nat Rev Endocrinol.* 10: 24-36
16. Miyakawa, H., Woo, S.K., Dahl, S.C., Handler, J.S. and Kwon, H. M. 1999. Tonicity-responsive

enhancer binding protein, a rel-like protein that stimulates transcription in response to hypertonicity. *Proc. Natl Acad. Sci. USA.* 96: 2538–2542

17. Lopez-Rodriguez, C., Aramburu, J., Rakeman, A.S. and Rao, A. 1994. NFAT5, a constitutively nuclear NFAT protein that does not cooperate with Fos and Jun. *Proc. Natl Acad. Sci. USA.* 96: 7214–7219
18. Aramburu, J., Drews-Elger, K., Estrada-Gelonch, A., Minguillón, J., Morancho, B., Santiago, V. and López-Rodríguez, C. 2006. Regulation of the hypertonic stress response and other cellular functions by the Rel-like transcription factor NFAT5. *Biochem. Pharmacol.* 72: 1597–1604
19. Lee, S.D., Choi, S.Y., Lim, S.W., Lamitina, S.T., Ho, S.N., Go, W.Y. and Kwon, H.M. 2007. TonEBP stimulates multiple cellular pathways for adaptation to hypertonic stress: organic osmolyte-dependent and -independent pathways. *Am. J. Physiol Renal. Physiol.* 300: F707–715
20. Go, W.Y., Liu, X., Roti, M.A., Liu, F. and Ho, S.N. 2004. NFAT5/TonEBP mutant mice define osmotic stress as a critical feature of the lymphoid microenvironment. *Proc. Natl Acad. Sci. USA.* 101: 10673–10678
21. Roth, I., Leroy, V., Kwon, H.M., Martin, P.Y., Féraille, E. and Hasler, U. 2010. Osmoprotective transcription factor NFAT5/TonEBP modulates nuclear factor-kappaB activity. *Mol Biol Cell.* 21: 3459-3474
22. Buxadé, M., Lunazzi, G., Minguillón, J., Iborra, S., Berga-Bolaños, R., Del Val, M., Aramburu, J. and López-Rodríguez, C. 2012 Gene expression induced by Toll-like receptors in macrophages requires the transcription factor NFAT5. *J. Exp.Med.* 209: 379–393
23. Yang, B., Hodgkinson, A.D., Oates, P.J., Kwon, H.M., Millward, B.A. and Demaine, A.G. Elevated activity of transcription factor nuclear factor of activated T-cells 5 (NFAT5) and diabetic nephropathy. *Diabetes.* 55: 1450-5
24. Park, J., Kim, H., Park, S.Y., Lim, S.W., Kim, Y.S., Lee, D.H., Roh, G.S., Kim, H.J., Kang, S.S., Cho, G.J., Jeong, B.Y., Kwon, H.M. and Choi, W.S. 2014. Tonicity-responsive enhancer binding protein regulates the expression of aldose reductase and protein kinase C δ in a mouse model of diabetic retinopathy. *Exp Eye Res.* 122: 13-9
25. Yoon, H.J., You, S., Yoo, S.A., Kim, N.H., Kwon, H.M., Yoon, C.H., Cho, C.S., Hwang, D. and Kim, W.U. 2011. NFAT5 is a critical regulator of inflammatory arthritis. *Arthritis Rheum.* 63: 1843–1852.
26. Halterman, J.A., Kwon, H.M., Leitinger, N. and Wamhoff, B.R. 2012. NFAT5 expression in bone marrow-derived cells enhances atherosclerosis and drives macrophage migration. *Front. Physiol.* 3: 1–7
27. Kleinewietfeld, M., Manzel, A., Titze, J., Kvakan, H., Yosef, N., Linker, R.A., Muller, D.N. and Hafler, D.A. 2013. Sodium chloride drives autoimmune disease by the induction of pathogenic

TH17 cells. *Nature*. 496: 518–522

28. Shin, H.J., Kim, H., Heo, R.W., Kim, H.J., Choi, W.S., Kwon, H.M. and Roh, G.S. 2014. Tonicity-responsive enhancer binding protein haplodeficiency attenuates seizure severity and NF-κB-mediated neuroinflammation in kainic acid-induced seizures. *Cell Death Differ.* 21: 1095-106
29. Lee, J.H., Lee, H.H., Ye, B.J., Lee-Kwon, W., Choi, S.Y., Kwon, H.M. 2015. TonEBP suppresses adipogenesis and insulin sensitivity by blocking epigenetic transition of PPARγ2. *Sci. Rep*. 5: 10937

Chapter2. Macrophage TonEBP promotes inflammation and insulin resistance by regulating M1/M2 polarization

2-1. Introduction

Type 2 diabetes is a major public health problem in worldwide with rising incidence. Type 2 diabetes characterized by hyperglycemia induces many complications including diabetic nephropathy, diabetic retinopathy, heart disease and hypertension. Obesity is a major causative factor for type 2 diabetes by inducing insulin resistance. Adipose tissue macrophages (ATMs) are critical regulators that link obesity with insulin resistance and type 2 diabetes. The number and polarization of ATMs actively cross-talk with adipocytes in adipose tissue and reflect the metabolic profiles. In lean mice, adipose tissue have alternatively activated resident macrophages comprising about 10% of stromal vascular cells (SVCs). However, M1 macrophages are infiltrated to about 50% of SVCs and ATMs are polarized from M2 type to classically activated (M1) type in obese mice [1]. The population of M1 and M2 ATMs is important to determine the level of inflammatory and metabolic states in adipose tissue of obesity. The M1 macrophages infiltrated by obesity secrete pro-inflammatory cytokines such as TNFα and promote insulin resistance in adipose tissue. M1 activation and pro-inflammatory responses are mainly promoted by transcriptional factor nuclear factor κB (NFκB). However, M2 macrophages enhances insulin sensitivity of adipocytes by secreting anti-inflammatory cytokines such as IL-10 and this polarization is enhanced by peroxisome proliferator-activated receptor γ1 (PPARγ1) [2].

NFκB transcription factor regulates the expression of several hundred cellular genes involved in a variety of cellular and physiological processes, such as immune and inflammatory responses, developmental processes, cellular growth, and apoptosis [3-4]. The key regulatory event in the activation of the p65:p50 heterodimeric NFκB is the phosphorylation of IκB proteins by the IκB kinase complex, which leads to IκB protein ubiquitination and subsequent degradation [4-5]. Removal of IκB leads to the release of cytoplasmic p65:p50 heterodimer, which then moves into the nucleus, associates with transcriptional cofactors p300 and CREB binding protein (CBP), and drives the expression of target genes. Recent studies have shown that DNA bound NFκB initiates the formation of distinct enhanceosomes in a target gene-specific manner [6-9]. NFκB is persistently active in a number of human diseases, including cancer, arthritis, chronic inflammation, asthma, neurodegenerative diseases, type2 diabetes, and heart disease [10-12], and thus, effective and safe inhibitors of NFκB would have wide-ranging therapeutic use.

Tonicity-responsive enhancer binding protein (TonEBP), also known as nuclear factor of activated T cells 5 (NFAT5), belongs to the Rel family of transcriptional factors which include NFκB and NFAT [13-14]. TonEBP was initially identified as the central regulator of cellular response to hypertonic stress

[13, 15-17]. Recent studies have demonstrated that TonEBP is involved in the M1 activation of macrophages by promoting the expression of pro-inflammatory genes in response to TLR4 activation [18-19]. TonEBP haplo-deficiency is associated with dramatically reduced inflammation and pathology in mouse models of rheumatoid arthritis [20] and atherosclerosis [21].

In order to understand molecular basis of the TonEBP function in inflammation and insulin resistance, we investigated TonEBP action in the M1 and M2 macrophage polarization. Here, we find that TonEBP is required for the recruitment of p300 to NFκB in M1 macrophage activation. In addition, we find that cerulenin is a powerful inhibitor of NFκB with minimal toxicity due to disruption of the p300 recruitment to NFκB without affecting its nuclear localization or phosphorylation. Thus, TonEBP is an essential component of the lipopolysaccharide (LPS)-induced NFκB enhanceosome critical for expression of pro-inflammatory genes. In M2 macrophage polarization, TonEBP represses M2 polarization through the suppression of PPARγ1 expression in macrophages. In myeloid specific TonEBP deficient mice fed with high fat diet (HFD), they showed improved insulin resistance without changes in body weight. Their adipose tissue has lower M1 and higher M2 macrophage population indicating lower inflammatory responses. These findings uncover the functions of macrophage TonEBP to promote insulin resistance through the regulations of NFκB activity and PPARγ1 expression.

2-2. Materials and methods

Animals

All the methods involving live mice were carried out in accordance with the approved guidelines. All experimental protocols were approved by Institutional Animal Care and Use Committee of the Ulsan National Institute of Science and Technology (UNISTACUC-12-15-A).

Mice carrying the loxP-targeted *TonEBP* gene (*TonEBP*$^{fl/fl}$) were reported previously [22]. Transgenic mice expressing Cre recombinase under the control of either the myeloid-specific lysozyme M (*LysM*) promoter were purchased from The Jackson Laboratory (Bar Harbor, ME, USA). *TonEBP*$^{fl/fl}$ and *LysM-cre* mice crossed to yield mice with specific targeted deletion of TonEBP in macrophages (*TonEBP*$^{fl/fl}$, *LysM-cre*).

For septic shock, *TonEBP*$^{fl/fl}$, *LysM-cre* mice and their *TonEBP*$^{fl/fl}$ littermates were intraperitoneally injected with D-galactosamine (700 mg/kg; Sigma Aldrich) plus LPS (150 μg/kg; Sigma Aldrich). After injection, animals were monitored for 16 h for survival.

For obese mice model, mice at 8 weeks age were fed with high fat diet (60% fat by kcal) or normal-chow diet (10% fat by kcal) during 9-16 weeks.

Cells and reagents

Macrophage cell line RAW264.7 cells, mouse embryo fibroblasts (MEFs), COS-7 cells and HEK293 cells were cultured in Dulbecco's Modified Eagle's Medium (DMEM) containing 10% fetal bovine serum (FBS; Thermo fisher scientific Inc, Waltham, MA, USA) and penicillin/streptomycin (100U/ml and 100μg/ml; GE healthcare life sciences, Logan, UT, USA). RAW264.7 cells were passaged by scraping with a rubber policeman and MEFs, COS-7 cells and HEK293 cells were passaged using trypsin/EDTA (Invitrogen, Carlsbad, CA, USA). Peritoneal macrophages derived from *TonEBP*$^{fl/fl}$ and *TonEBP*$^{fl/fl}$, *LysM-cre* mice were cultured in RPMI containing 10% fetal bovine serum, penicillin/streptomycin (100 U/ml and 100 μg/ml). Cells were maintained at 37°C in incubator with 5% CO_2. Cells were pretreated with cerulenin, BAY 11-7082 and β-lapachone (Sigma Aldrich, USA) for 1h and exposed to lipopolysaccharide (LPS; Sigma Aldrich) or Interleukin-4 (IL-4; R&D Systems, Minneapolis, MN, USA). Anti-p65, RelB, c-Rel and p52 antibodies from NFκB family sample kit (4776, Cell Signaling Technologies, Berkeley, CA, USA), anti-p50 (sc8414, SantaCruz Biotechnology, Santa Cruz, CA, USA City), ser 276 phosphorylated p65 (sc101749, SantaCruz Biotechnology), p300 (sc584, SantaCruz Biotechnology) and LaminB (sc6217, SantaCruz Biotechnology) antibodies, anti-Hsc70 (200-301-A28, Rockland, Gilbertsville, PA, USA) and anti-TonEBP antibody [13] were used for immunoblotting.

Cells were transfected with lipofectamine 2000 (Invitrogen, Carlsbad, CA, USA). All siRNA duplexes were purchased from Integrated DNA Technologies (Coralville, IA, USA) and used for siRNA-mediated knockdown. For overexpression, RAW264.7 cells were infected with the empty control virus (Ad-EV) or the adenovirus carrying the human *TONEBP* gene (Ad-TONEBP).

Isolation of the human primary monocytes and differentiation of monocyte-derived macrophages.

The study was approved by the Institutional Review Board of the Ulsan National Institute of Science and Technology (UNISTIRB-15-25-A). Human blood was provided by the Korea Gynecologic Cancer Bank through Bio & Medical Technology Development Program of the MSIP, Korea. Mononuclear cells were isolated from heparinized blood using Histopaque-1077 (Sigma-Aldrich, St. Louis, MO, USA), according to the manufacturer's instructions. Monocytes were further purified using CD14 microbead positive selection and MACS separation columns (Miltenyi Biotec, Bergisch, Germany), according to the manufacturer's instructions. The macrophages were obtained after 7 days culture of human monocytes in RPMI-1640 medium supplemented with 10% FBS, 1% sodium pyruvate, 0.1% β -mercaptoethanol and human M-CSF (20 ng/ml; Miltenyi Biotec).

Flow cytometry analysis

Stromal vascular cells (SVCs) were isolated from epididymal white adipose tissue obtained from mice fed high fat diet during 4 weeks. Epididymal white adipose tissue were minced in FACS buffer (PBS + 1% bovine serum albumin) containing 1mg/ml type II collagenase. They were incubated at 37˚C with shaking for 1 hr. After incubation, 10 ml of DMEM/F12 were added and they were centrifuged at 500g for 15 min. SVCs were incubated with 5ml of RBC lysis buffer (Sigma) for 5 min at room temperature and then they were filtered with a 40μm filter after addition of 10ml of DMEM/F12. After centrifugation at 500g for 5 min, SVCs were resuspended in FACS buffer and incubated with Fc Block (BD Biosciences) for 10 min at 4 ℃ before staining primary antibodies for 30 min at 4 ℃. PE-F4/80, PerCP-CD11b, FITC-CD11c and Alexa fluor 647-CD206 FACS antibodies are purchased from BD Biosciences. Cells were gently washed twice and resuspended in FACS buffer. After gating of F4/80 and CD11b positive cells, they were analyzed by CD11c and CD206 using a FLSRFortessa flow cytometer (BD Biosciences). Unstained and single stained cells were used for setting compensation and gates.

Metabolic analysis

Fasting blood glucose, body weight and food intake were measured weekly, Mice were given an orally injection of D-glucose (2 g/kg body weight) after overnight starvation for the glucose tolerance test (GTT) and were intra- peritoneally injected with insulin (0.75U/kg body weight) for insulin tolerance test (ITT). Serum glucose levels were determined in tail blood samples using a glucometer. Body temperatures were measured using a digital thermometer (TD-300; Shibaura Electronics, Tokyo, Japan).

Immunoblot assay

Cell were washed two times with cold PBS and lysed in RIPA buffer (0.01M Tris, pH7.4, 0.15M NaCl, 0.001M EDTA, 0.001M EGTA, 1% Triton X-100, 0.002M PMSF and protease inhibitor (roche)). After centrifugation of lysate, supernatant was used for immunoblot assay. Protein concentration was measured by BCA protein assay system (Pierce, Rockford, IL, USA). Equal amounts of protein from each sample were separated by SDS-PAGE and immunoblotted using specific primary antibodies. HRP-conjugated mouse, rabbit and goat secondary antibodies were used for detection. The antigen-antibody binding was detected by enhanced chemiluminescence Western blotting detection reagents (GE healthcare life sciences).

RNA isolation and real-time PCR

Total RNA was isolated using the TRIzol reagent (Invitrogen) according to the manufacturer's instructions. cDNA was synthesized by M-MLV reverse transcriptase (Promega, Madison, WI, USA). After reverse transcription, real time PCR was performed using SYBR Green I Master and LightCycler 480 II (Roche, Rotkreuz, Switzerland). Measured cycle threshold (Ct) values were normalized with cyclophilin A and they were expressed as fold-over control samples.

Immunohistocytochemistry

The cells were grown on glass coverslips and fixed with 4% paraformaldehyde in PBS (pH 7.4) for 20 min at 4℃. Cells were permeabilized with 0.3% Triton-X 100 in PBS for 30 min and blocked with PBS containing 3% goat serum and 1% bovine serum albumin for 1 h at room temperature. After incubation with rabbit anti-TonEBP and rabbit anti-p65 overnight at 4℃, the cells were washed with PBS and treated with goat anti-mouse or anti-rabbit Alexa Fluor 488-conjugated and Alexa Fluor 594-conjugated secondary antibodies for 1 h. Cells were washed with PBS and incubated in 0.1 μg/ml Hochest (DAPI) for 30 min. After wash with PBS, coverslips were mounted onto microscope slides. Images were recorded using an Olympus FV1000 confocal fluorescence microscope.

Immunoprecipitation assay

Cell lysates (10-500μg) were prepared using RIPA buffer in a tube on ice. Antibody (1-5μg) was added to cell lysate and they were incubated for overnight at 4℃ under rotary agitation. 40μl of protein A/G agarose beads (GE healthcare) was added and incubated for 2 hr at 4℃ under rotary agitation. The bead-antibody-antigen complex was spin downed by centrifugation at 4℃ for 1min and removed supernatant. The complex was washed for 10 min by RIPA buffer at 4℃ and it was repeated with three times. After wash, 40μl of sample buffer was added and boiled at 95℃ for 5min and centrifugated with top speed for 1min at room temperature. The samples were transferred to new tube and analyzed by immunoblotting.

Nuclear and cytoplasmic fractionation

Cells were harvested by using scrapper and centrifugation at 500 g. The cell pellet was washed by suspension with PBS. The cell nucleus and cytoplasm were separated by using Nuclear and Cytoplasmic extraction kit (Pierce) according to manufacturer's instruction. Nuclear fraction was confirmed by Lamin B.

Electromobility shift assay

Electrophoretic mobility shift assay (EMSA) was performed using Lightshift Chemiluminescent EMSA kit (Pierce). 5 μg of nuclear extracts were incubated with poly(dI:dC), binding buffer and 5' biotinylated DNA (5'- AAACAGGGGGCTTTCCCTCCTC -3' for NFκB binding site on *TNFα* promoter, N1; 5'-GCTCCGTGGAAAACTCACTTGG-3' for putative TonEBP binding site, T1; 5'-TGTCCCCAACTTTCCAAACCCT-3' for T2; 5'-ACCAAGGAAGTTTTCCGAGGGTT-3' for T3; 5'-TCATAATGGAAAATTCCATGCCA-3' for T0) at room temperature for 20 min. Samples were separated by electrophoresis for 4 h in 4% (40% 29:1 acrylamide/bis solution) gel for TonEBP and 8% gel for p65. The detection was performed according to manufacturer's instructions.

Chromatin immunoprecipitation assay

Cells were grown in 10 cm diameter culture dishes and with LPS when indicated. Fixation was performed with 1% formaldehyde at room temperature for 10 min. The fixation was stopped with 0.125 M glycine for 5 min at room temperature. After three washes with cold PBS, cells were collected and lysed in 1 ml of SDS lysis buffer (1% SDS, 10 mM EDTA and 50 mM Tris-HCl pH 8.1) for 10 min on ice. Cell lysates were sonicated (Bioruptor KRB-01, BMS, Tokyo, Japan) for six cycles of 20 s on plus 30 s off with constant frequency and maximum intensity to obtain DNA fragments between 400 and 1,000 bp. Each sample was diluted 10× in dilution buffer (0.01% SDS, 1.1 % Triton X-100, 1.2 mM EDTA, 16.7 mM Tris-HCl pH 8.1 and 167 mM NaCl) for immunoprecipitation.

Samples were pre-cleared with protein A Sepharose beads (Millipore, Bedford, MA, USA) that were previously pre-adsorbed with salmon sperm DNA for 1 h at 4℃. Specific antibodies were added after removing the pre-clearing beads: anti-p65 IgG, and normal rabbit IgG (Abcam, Cambridge, UK), anit-TonEBP serum, and normal rabbit serum (Merck millipore, Darmstadt, Germany). After adding antibodies, the lysates were incubated overnight at 4℃. Protein A Sepharose beads were then added, incubated for 2 h at 4℃, and then washed with low salt washing buffer (0.1% SDS, 1% Triton X-100, 20 mM Tris-HCl pH 8.1, 2 mM EDTA, and 10 mM NaCl), high salt washing buffer (0.1% SDS, 1% Triton X-100, 20 mM Tris-HCl pH 8.1, 2 mM EDTA and 500 mM NaCl), LiCl washing buffer (0.25 M LiCl, 1% NP-40, 1% deoxycholic acid, 1 mM EDTA and 10 mM Tris-HCl pH 8.1) and twice with final washing buffer (10 mM Tris-HCl pH 8.0 and 1 mM EDTA). To elute the DNA, beads were incubated with elution buffer (1% SDS and 100 mM NaHCO3) for 20 min at 65 ℃. To reverse the cross-linking, samples were incubated overnight at 65℃ 200 mM NaCl, 30 min at 37℃ with 50 μg/ml RNase (Pierce) and 2 hr at 45°C with 100 μg/ml proteinase K. DNA was purified using the QIAGEN PCR purification system. DNA was then subjected to RT-qPCR using primers; 5'-CCCAACTCTCAAGCTGCTCT-3' and 5'- CTTCTGAAAGCTGGGTGCAT-3' for *TNFα* promoter. Immunoprecipitated DNA from each sample was normalized to its respective chromatin input.

DNA affinity purification assay

Cells were lysed in lysis buffer (20 mM Tris-HCl pH 7.5, 150 mM NaCl and 0.5% Triton-100). 1mg of extracts were diluted with binding buffer (4 mM Tris-HCl pH 7.5, 20 mM HEPES pH 7.5, 5% glycerol, 170 mM NaCl, 0.5 mM EDTA, 1 mM MgCl2 and 0.1 % Triton X-100) and incubated overnight with 5' end biotinylated DNA probe (30 nM) containing a κB site or putative TonE site of mouse TNF-α promoter. They were mixed for 2 hr with 50 μl of streptavidin-coated agarose beads, and protease inhibitors (Roche). Beads were pelleted, washed two times with TE buffer with 100 mM NaCl, two times with binding buffer, once with PBS and then resuspended in 50 μl of Laemmli sample buffer. Precipitated proteins were separated by 7% SDS-PAGE and immunoblotted for TonEBP and p65.

Luciferase assay

Cells were transfected with either a TonE-driven Photinus luciferase plasmid or a κB-driven luciferase plasmid in pGL4.74 (hRluc/TK, Promega). The Renilla luciferase reporter plasmid (pRL-TK, Promega) was used as a control for transfection efficiency. Luciferase activity after 8 h of stimulation was measured using the Dual-Luciferase Assay System (Promega) according to the manufacturer's instructions. Luciferase activity was normalized by activity of renilla luciferase.

Cytokine production

TNFα in supernatants from LPS-stimulated cells or serum samples from D-Galactosamine (GalN)/LPS-injected mice were analyzed by ELISA using a commercial kit (R&D Systems, Minneapolis, MN, USA).

Statistical analysis

Data are presented as means + s.d. or +s.e.m Statistical significance ($p < 0.05$) was estimated by student's t-test. All statistics was performed with GraphPad Prism 5.0 software (GraphPad, San Diego, CA, USA).

2-3. Results

2-3-1. TonEBP promotes macrophage M1 activation and sepsis

Macrophage activation is a hallmark of inflammation, and NFκB is a central regulator of pro-inflammatory macrophage activation (M1 macrophage) [23]. In order to explore the role of TonEBP in macrophage activation, we obtained a line of mice with myeloid-specific deletion of the *TonEBP* gene by crossing the line in which the exon 4 of the *TonEBP* gene was flanked by lox P sequences (*TonEBP*^{fl} allele) [22] with the line expressing the cre recombinase in myeloid cells using the promoter of the lysozyme 2 gene (*LysM-cre*) [24]. Peritoneal macrophages (PECs) prepared from *TonEBP*$^{fl/fl}$, *LysM-cre* mice showed a dramatically reduced *TonEBP* mRNA expression compared to those prepared from their *TonEBP*$^{fl/fl}$ littermates (Fig. 2-1a). *TonEBP* mRNA expression in other tissues such as liver and brain was normal consistent with myeloid-specific deletion of the *TonEBP* gene (data not shown). When stimulated with LPS, PECs from the *TonEBP*$^{fl/fl}$, *LysM-cre* mice showed significantly reduced expression of NFκB-dependent pro-inflammatory genes *TNFα* and *iNOS* (Fig. 2-1a), and NO production (Fig. 2-1b) in response to LPS. In response to D-galactosamine and LPS administration, which was used to produce a mouse model of sepsis [25], the rise in serum TNFα levels were reduced by ~40% in the *TonEBP*$^{fl/fl}$, *LysM-cre* mice compared to their *TonEBP*$^{fl/fl}$ littermates (Fig. 2-1c). Furthermore, severity of sepsis measured by ensuing death was reduced in the *TonEBP*$^{fl/fl}$, *LysM-cre* animals (Fig. 2-1d). These data show that myeloid-specific deletion of the *TonEBP* gene results in blunted macrophage activation and septic shock in association with inflammatory responses.

2-3-2. TonEBP binds to the *TNFα* promoter without direct interaction with DNA

In macrophages, TonEBP is induced by Toll-like receptor engagement and activates many genes by direct binding to their promoters including that of TNFα [18]. Fig. 2-2a shows a schematic representation of 1.6 kb upstream of the mouse *TNFα* gene where three putative binding sites for TonEBP (T1, T2, and T3) and a putative NFκB binding site (N1) are located. In order to understand molecular action of TonEBP, we first examined the affinity of TonEBP and NFκB to the sites using electrophoretic mobility shift assay (EMSA) of nuclear extracts prepared from RAW264.7 macrophage cell line. The N1 probe detected several prominent bands which showed up after LPS stimulation (Fig. 2-2b). All of these bands were competed away by excess cold probe, but only the top two bands were supershifted by p65 antibody but not by TonEBP antiserum indicating that they represented p65-containing NFκB molecules. These data demonstrate that N1 is a functional κB sequence and p65-containing NFκB molecules have specific affinity to N1.

The macrophage nuclear extracts displayed specific binding to a tonicity-responsive enhancer (TonE) sequence (T0) which was enhanced by hypertonicity, supershifted by TonEBP antiserum, and competed

away by excess cold probe demonstrating that the band represented DNA-bound TonEBP molecules (Fig. 2-2c). On the other hand, none of the putative TonEBP binding sequences T1, T2, and T3 displayed binding to the band, and were unable to compete with T0 for TonEBP binding. Thus, T1, T2, and T3 are not a functional TonE and TonEBP does not have high affinity for the DNA sequence in the promoter region.

We next performed chromatin immunoprecipitation (ChIP) to investigate NFκB and TonEBP interaction to the promoter in situ. p65 bound to the N1 region in LPS-dependent manner (Fig. 2-2d) as expected from the EMSA data above. Surprisingly, TonEBP also displayed LPS-dependent binding to the region. Since TonEBP did not have affinity to the sequence in the region, we asked whether there was a protein-protein interaction between TonEBP and p65. To address this question, we performed DNA affinity purification analysis (DAPA) of the cell lysates using a biotin-labeled N1 probe. Both NFκB and TonEBP displayed LPS-dependent binding to the N1 probe (Fig. 2-2e) suggesting that there is a protein-protein interaction between them.

2-3-3. TonEBP interacts with p65 through Rel-homology domains (RHDs)

Molecular basis of the TonEBP-p65 interaction was investigated. Co-immunoprecipitation experiments revealed that both endogenous proteins (Fig. 2-3a) and over-expressed proteins (Fig. 2-3b) could be mutually pulled down by each other. In order to map sites of interaction, we produced various recombinant proteins of TONEBP and p65 (Fig. 2-4). Analyses of the recombinant proteins suggest that the RHDs are critical for both. TONEBP constructs without RHD – TONEBP ΔRHD and YC1 ΔRHD – did not show interaction with p65, while those of intact RHD such as YC1 and partial RHD such as TONEBP ΔIPT did (Fig. 2-4a). In addition, protein product of a mutant *TonEBP* allele lacking the N-terminal half of RHD did not bind p65 (see below). Likewise, p65 constructs with its RHD domain partially deleted (p65 ΔIPT and p65 ΔRHD-n) did not interact with TONEBP (Fig. 2-4b).

2-3-4. TonEBP stimulates NFκB activity independent of DNA binding

In HEK293 cells, over-expression of TONEBP resulted in a stimulation of both κB-driven and TonE-driven luciferase (Fig. 2-5a), and expression of NFκB- and TONEBP-target genes (Fig. 2-5b) as expected. On the other hand, TONEBP ΔRHD, which did not interact with p65 (Fig. 2-4a) and could not bind DNA [26], did not stimulate neither κB-driven nor TonE-driven gene expression (Fig. 2-5). TONEBP ΔIPT lacks the dimerization domain and does not bind DNA [26]. Interestingly, TONEBP ΔIPT retained its ability to interact with p65 (Fig. 2-4a) and stimulated κB-driven gene expression but not TonE-driven gene expression (Fig. 2-5). These observations demonstrate that TonEBP stimulates NFκB independent of DNA binding.

The mouse *TonEBP Δ* allele was created by deletion of exon 6 and 7 [17]. The deletion results in an

in-frame deletion of 128 amino acids in the N-terminal portion of RDH as depicted in Fig. 2-6a. Interestingly, mouse embryonic fibroblast (MEF) cells established from *TonEBPΔ/Δ* mice showed reduced κB-driven luciferase expression both in basal conditions and after LPS stimulation (Fig. 2-6b). Expression of NFκB-target genes *TNFα* and *IκBα* in response to LPS was also reduced in these cells (Fig. 2-6c) consistent with reduced NFκB activity. We investigated molecular basis for the reduced NFκB activity. The *TonEBPΔ/Δ* MEF cells expressed the TonEBP Δ protein which migrated faster than the wild type TonEBP protein (Fig. 2-6d). In these cells, expression of the NFκB subunits – p65, RelB, c-Rel, p52, and p50 – was normal. Nuclear localization of p65 and TonEBP in response to LPS looked normal (Fig. 2-6e). In addition, serine 276 phosphorylation of p65 in response to LPS was normal in the *TonEBPΔ/Δ* MEF cells (Fig. 2-6f). Finally, we asked whether reduced TonEBP expression affected DNA binding of p65. Knock-down of TonEBP did not affect DNA binding of p65 based on EMSA and DAPA (Fig. 2-7). Thus, NFκB activity was reduced in the *TonEBPΔ/Δ* MEF cells despite normal expression of NFκB subunits, nuclear translocation, phosphorylation, and DNA binding of p65 in response to LPS. The reduced NFκB activity can be explained by the inability of the mutant protein to interact with p65 (Fig. 2-8a) providing further support to the notion that TonEBP stimulates NFκB independent of DNA binding, i.e, via protein-protein interaction.

2-3-5. TonEBP is required for the recruitment co-activator p300 to NFκB: LPS-induced NFκB enhanceosome

We asked how the TonEBP-p65 interaction led to stimulation of the NFκB activity. Two possibilities were explored. One was recruitment of the large and powerful transactivation domain (TAD) of TonEBP [27]. To test this, we generated a fusion protein of p65 and the TAD. The fusion protein displayed a markedly elevated transcriptional activity which was gradually reduced as the TAD domain was serially deleted from the C-terminus (Fig. 2-9a, b) as reported earlier [27]. This observation suggests that the TAD of TonEBP enhance transactivation by p65 bound to DNA. On the other hand, over-expression of Yc1 (see Fig. 2-4a), which was expected to compete away TAD-containing TonEBP and reduce transactivation of NFκB, did not inhibit NFκB (Fig. 2-9c) suggesting that there should be other pathways of transactivation by TonEBP.

We explored the possibility that TonEBP was involved in the recruitment of transcriptional co-activators such as p300. p300 is an acetyltransferase involved in p65 acetylation which is essential in the assembly of NFκB enhanceosome [28]. When p65 was immunoprecipitated, both TonEBP and p300 were also brought down (Fig. 2-8a) suggesting that the all the three molecules were in a complex. The interaction increased in response to LPS (Fig. 2-8a) in correlation with increased nuclear localization of p65 (Fig. 2-6e). Of note, the TonEBP Δ protein did not interact with p65 and, thereby, the amount of p300 brought down with p65 was dramatically lower in the *TonEBPΔ/Δ* MEF cells (Fig. 2-8a, 2nd and

4th lane). The inability of the TonEBP Δ protein to interact with p65 and recruit p300 explains the reduced NFκB activity in the *TonEBPΔ/Δ* MEF cells (Fig. 2-6b). These data indicate that the TonEBP-p65 interaction was critical for the recruitment of p300 to p65. This was further supported by the observation that increased expression of p300 did not lead to increased κB-driven luciferase expression in the *TonEBPΔ/Δ* MEF cells (Fig. 2-8b). Thus, the inability of the TonEBP Δ protein to transactivate NFκB was due to its inability to interact with p65, i.e., inability to form the NFκB enhanceosome.

The TonEBP containing enhanceosome complex was characterized further. Knockdown of p300 led to reduced recruitment of both p300 and TonEBP to p65 (Fig. 2-10a), while knockdown of p65 did not affect the association between p300 and TonEBP (Fig. 2-10b). These observations suggest that preformed TonEBP-p300 heterodimer is recruited to p65 after its nuclear translocation in response to LPS. Knockdown of TonEBP led to reduced p300 recruitment to p65 (Fig. 2-10c), as expected. Of note, ChIP experiments revealed that the LPS-dependent assembly of NFκB enhanceosome on the promoter of the *TNFα* promoter, as measured by recruitment of p65, Sp1 and Pol II to the N1 site [29-30], was reduced after TonEBP knockdown (Fig. 2-11). Thus, TonEBP deficiency is associated with not only lower recruitment of p300 to p65 but also reduced assembly of the NFκB enhanceosome on the promoter leading to lower NFκB activity observed under these conditions.

2-3-6. Cerulenin disrupts the p65-TonEBP-p300 interaction and inhibits NFκB without toxicity

From a screening of natural compounds for inhibition of NFκB, we discovered that cerulenin, an inhibitor of fatty acid synthase [31], disrupted the p65-TonEBP-p300 interaction. Cerulenin reduced co-precipitation of TonEBP and p300 in p65 immunoprecipitation assays both under basal conditions and after LPS treatment (Fig. 2-12a).

We characterized cerulenin action in molecular detail. Cerulenin inhibited NO production in response to LPS in a dose-dependent manner without compromising cell viability (Fig. 2-12b). The lack of cytotoxicity by cerulenin contrasts with BAY11-7082, a protein kinase inhibitor: while both compounds inhibited NO production with comparative efficacy, cerulenin displayed no detectible toxicity unlike BAY11-7082 which displayed a dose-dependent decrease in viability (Fig. 2-13). The reduced NO production was associated with reduced NFκB activity based on reduced κB-driven luciferase expression (Fig. 2-12c) and reduced expression of NFκB-target genes (Fig. 2-12d) and their proteins (Fig. 2-12e). As expected, cerulenin potently inhibited systemic inflammation and septic death (Fig. 2-14). Of great interest, the reduced NFκB activity was not associated with changes in the nuclear localization, DNA binding, or phosphorylation of p65 (Fig. 2-15). Taken together, the data provide compelling evidence that cerulenin prevents inflammation by inhibiting NFκB as it specifically disrupts the p65-TonEBP-p300 interaction. As such, cerulenin displayed lower, if any, toxicity compared to BAY11-7082 blocking of the nuclear localization.

2-3-7 TonEBP suppresses M2 phenotype

Given the role of TonEBP in M1 gene expression and inflammatory diseases (see above), we explored the role of TonEBP in M2 macrophage polarization in response M1 (LPS) and M2 stimuli (IL-4). While LPS increased TonEBP expression, as previously described [18], we found that IL-4 reduced TonEBP expression (Fig. 2-16a) in mouse RAW264.7 macrophages. Time course experiments revealed that significant increase in *TonEBP* mRNA expression was reached in 3 h in response to LPS and the expression continued to rise to 12 h (Fig. 2-16b). In contrast, treatment with IL-4 caused significant and gradual reduction in *TonEBP* mRNA expression 3–12 h later (Fig. 2-16b). Thus, M2 signal reduced TonEBP expression while M1 signal promoted it. During M1 polarization of macrophages in response to LPS, anti-inflammatory M2 genes including IL-10 are induced to provide a negative feedback [32-33]. We investigated whether TonEBP knockdown using siRNA-mediated gene silencing would influence the expression of M2 phenotype in M1 polarized macrophages. TonEBP knockdown in RAW264.7 cells enhanced mRNA expression of M2 genes such as *IL-10*, arginase-1 (*Arg1*), mannose receptor (*CD206*) and IL-4 receptor α (*IL-4Rα*) both in unstimulated and LPS-stimulated cells (Fig. 2-16c). We next asked whether TonEBP regulates expression of M2 genes in M2-polarized macrophages. TonEBP knockdown increased the expression of *Arg-1, CD206* and *IL-10* genes upon IL-4 stimulation (Fig. 2-16c). Reversely, TonEBP overexpression led to reduced mRNA expression of M2 genes in both M1 and M2 polarized macrophages (Fig. 2-16d), demonstrating that TonEBP directly suppresses M2 phenotype in both M1 and M2 macrophages.

2-3-8 TonEBP suppresses IL-10 and its signaling in M1 macrophages.

Among the M2 genes suppressed by TonEBP, we were interested in IL-10 because it is an essential anti-inflammatory cytokine, capable of reducing pro-inflammatory mediators and inducing M2 phenotype in macrophages [34-36]. We found that IL-10 secretion (Fig. 2-17a) and mRNA expression (Fig. 2-16 and 2-17b) were higher in cells whose TonEBP was knocked down under basal conditions, and they increased steadily over time after stimulation with LPS. Because IL-10 leads to increase in expression of anti-inflammatory regulators such as suppressor of cytokine signaling-3 (SOCS3) [37], IL-4Rα [38] and Bcl-3 [39] through signal transducer and activator of transcription 3 (STAT3) [40], we asked whether TonEBP affected the activation of STAT3 and expression of STAT3-inducible genes in RAW264.7 cells. In line with the increased secretion of IL-10, TonEBP knockdown augmented STAT3 phosphorylation in response to LPS (Fig. 2-17c) and enhanced LPS-induced expression of SOCS3 (Fig. 2-17c) and mRNA for *IL-4Rα , SOCS3* and *Bcl-3* (Fig. 2-17d). In order to confirm the regulation of IL-10 by TonEBP in vivo, we examined peritoneal macrophages (PM) and bone marrow derived macrophages (BMDM) obtained from the *TonEBP+/Δ* mice displaying TonEBP haplodeficiency [17]. Both PM's and BMDM's from the *TonEBP+/Δ* mice showed reduced TonEBP expression, both in

unstimulated and LPS-stimulated conditions (Fig. 2-17e), and enhanced *IL-10* mRNA expression compared to those from *TonEBP*+/+ littermates (Fig. 2-17f). We asked whether the suppression of IL-10 and its signaling by TONEBP was also present in human macrophages. To answer the question, we obtained primary monocytes from three donors. Macrophages differentiated from the monocytes responded to LPS by increasing the expression of TONEBP, IL-10, and anti-inflammatory regulators like RAW264.7 cells (Fig. 2-18). In addition, expression of the IL-10 and anti-inflammatory regulators was enhanced under basal and LPS-stimulated conditions in response to TONEBP knockdown. These data demonstrate that TONEBP suppresses IL-10 expression and M2 phenotype both in human and mouse macrophages.

2-3-9. β-Lapachone, a chemotherapeutic agent, suppresses TonEBP expression and enhances IL-10 expression.

We screened a commercial library of natural compounds (BioMol, Plymouth Meeting, PA, USA) to find small molecules that suppressed TonEBP expression. Because TonEBP is essential for the expression of inducible nitric oxide synthase (iNOS) in LSP-stimulated macrophages [18], we monitored LPS-dependent nitric oxide production using the Griess reaction. Among the compounds that reduced the nitric oxide production, we found that β-lapachone, which has a variety of pharmacological effects including anti-inflammatory, anti-cancer and anti-angiogenic actions [41-43], suppressed TonEBP expression both under LPS stimulation and hypertonicity (Fig. 2-19a). As expected from the reduced TonEBP expression, β-lapachone increased the mRNA expression of *IL-10* and *CD206* whereas suppressed the mRNA levels of *COX-2* and *iNOS* in response to LPS (Fig. 2-19b). β-Lapachone also suppressed mRNA expression of tonicity-responsive TonEBP target genes such as sodium/chloride/betaine cotransporter (*BGT-1*) and sodium/myo-inositol cotransporter (*SMIT*) (Fig. 2-19c). The data provide strong evidence that the effects of β-lapachone on IL-10 expression is due to the reduction of TonEBP expression.

2-3-10. TonEBP suppresses M2 macrophage polarization through the reduction of PPARγ1 expression

We found that TonEBP regulates not only NFκB-induced M1 activation but M2 polarization. We demonstrated that M1 macrophage activation is mediated by NFκB enhanceosome consisting of NFκB, TonEBP and p300. Next, we investigated mechanism of M2 macrophage polarization by TonEBP deficiency in macrophages. M2 macrophages are polarized by several transcription factors such as C/EBPβ, PPARγ1 and STAT6 [23]. It is already published that TonEBP suppresses PPARγ expression in adipocytes leading to inhibition of adipogenesis [46]. We confirmed the increased expression of

PPARγ1 without changes in phosphorylation and expression of STAT6 and expression of C/EBPβ in TonEBP knockdowned RAW264.7 cells (Fig. 2-20a). TonEBP deficient macrophages also have enhanced *PPARγ1* and *CD36*, PPARγ target gene, mRNA expressions (Fig. 2-20b). These data demonstrated that TonEBP suppresses M2 macrophage polarization through the inhibition of PPARγ expression in macrophages.

2-3-11. Myeloid specific TonEBP deficient mice protect from obesity-induced insulin resistance in obese mice

The population of M1 and M2 ATMs is important to determine the level of inflammatory and metabolic states in adipose tissue of obesity. The M1 macrophages infiltrated by obesity secrete pro-inflammatory cytokines such as TNFα and promote insulin resistance in adipose tissue. However, M2 macrophages enhances insulin sensitivity of adipocytes by secreting anti-inflammatory cytokines such as IL-10 [2]. Inflammatory regulators such as NFkB simultaneously increase M1 and M2 activation in macrophages. Therefore, common anti-inflammatory drugs reduce M1 activation but also M2 activation. However, TonEBP increases M1 but suppresses M2, so when it is deficient, M1 activation decreases and M2 activation increases. Therefore, TonEBP inhibition might be more efficient for improvement of insulin resistance in obesity.

To examine the role of macrophage TonEBP on obesity-induced impaired glucose homeostasis, we generated myeloid-specific KO mice. WT or myeloid specific TonEBP KO mice were fed a HFD for 22 weeks. Interestingly, the myeloid specific TonEBP KO mice showed a similar weight gain compared to WT mice (Fig. 2-21a). Food intake was similar between groups (data not shown). However, the myeloid specific TonEBP KO mice protected against obesity-induced glucose intolerance and insulin resistance (Fig. 2-21b-d). Obesity causes fatty liver and it causes liver damage, but myeloid specific TonEBP KO revealed protection from liver damage showing lower AST and ALT concentration in serum (Fig. 2-21e). These phenotypes called obese but metabolically healthy were explained by reduced immune cell infiltration to eWAT, pro-inflammatory responses (M1 activation) in eWAT and liver (Fig. 2-22a-c). In this eWAT, myeloid specific TonEBP KO showed not only reduced pro-inflammatory gene but enhanced anti-inflammatory gene expression, M2 macrophage markers (*IL10*, *Ym1*, *Mgl1* and *CD206*) and transcription factor (*PPARγ1*) (Fig. 2-22d). Consistent with mRNA expression of M1 and M2 markers, we found that myeloid specific TonEBP KO mice have more M2 macrophage population ($F4/80^+$ $CD11b^+$ $CD11C^-$ $CD206^+$) with less M1 macrophages ($F4/80^+$ $CD11b^+$ $CD11C^+$ $CD206^-$) in eWAT (Fig. 2-22e-f).

To find the association of TonEBP with diabetes in humans, we isolated blood leukocytes from non-diabetic or diabetic human. In human blood monocytes, *TonEBP* mRNA expression was correlated with blood glucose (Fig. 2-22g). We conclude that macrophage TonEBP promotes insulin resistance by

suppressing M2 macrophage polarization and promoting M1 macrophage polarization. These data suggest that targeted downregulation of macrophage TonEBP may be a good therapy for alleviating inflammation-associated metabolic syndrome.

2-4. Discussion

TonEBP was originally identified based on its specific DNA binding to the tonicity-responsive enhancer (TonE) [13]. In vivo footprinting analyses revealed that DNA binding of TonEBP to the TonE sites in the promoter regions of its target genes temporally correlated with transcriptional stimulation in response to hypertonicity [44-45]. ChIP experiments have shown that the induction of TNFα in response to LPS is associated with TonEBP recruitment to its promoter (Fig. 2-2) [18]. The data presented here demonstrate that the recruitment is independent of DNA binding. Rather, TonEBP is recruited through a protein-protein interaction with NFκB. We recently reported analogous DNA binding-independent recruitment of TonEBP to the promoter of the *PPARγ* gene in association with the suppression of the promoter [46]. The histone acetyl transferase activity of p300 is critical for the formation of NFκB enhanceosome [47]: After recruitment to p65 bound to DNA, p300 acetylates histones leading to opening/remodeling of chromatin and binding of proximal factors such as Sp1 and RNA polymerase II. The data presented here are consistent with this model in that TonEBP deficiency results in not only reduced recruitment of p300 to the TNFα promoter but also other components of the NFκB enhanceosome such as Sp1 and RNA polymerase II. Thus, TonEBP-dependent recruitment of p300 is a key early step in the formation of NFκB enhanceosome.

NFκB-mediated inflammation is involved in the pathogenesis of a wide range of diseases including cancer [5], metabolic and vascular disease [11], and even viral infection [48]. Much of the anti-inflammatory activity of the widely used glucocorticoids is due to blockage of NFκB activity [49]. Genetic and pharmacological inhibition of NFκB reverses insulin resistance in animal models [50]. A recent clinical trial showed that salicylate, which inhibits NFκB, improved glycemia in patients with type 2 diabetes and decreased inflammatory mediators [51]. Effective inhibitors of NFκB with minimal side effects would be quite useful for therapeutic use against the diverse inflammatory diseases.

Obesity-associated tissue inflammation is now recognized as a major cause of insulin resistance. IL-10 and M2 macrophage can inhibit the deleterious effects of pro-inflammatory cytokines on insulin signaling [2]. Notably, loss of M2 macrophage exacerbates expression of inflammatory markers within the liver and adipose tissue [1-2] and is not always compensated by inhibition of pathologic inflammatory phenotype alone, demonstrating that the action of M2 macrophage is limited to inhibition of pro-inflammatory molecules in tissue inflammation. Thus, suppression of M1 activation in combination with promotion of M2 activation is desirable as a therapeutic strategy against inflammatory diseases. Here, myeloid specific TonEBP deficient mice have suppression of M1 activation with promotion of M2 activation in adipose tissue. This polarization of macrophages improves metabolic profiles in obese mice without changes in body weight. As such, TonEBP should be an attractive target for obesity-associated insulin resistance and inflammation.

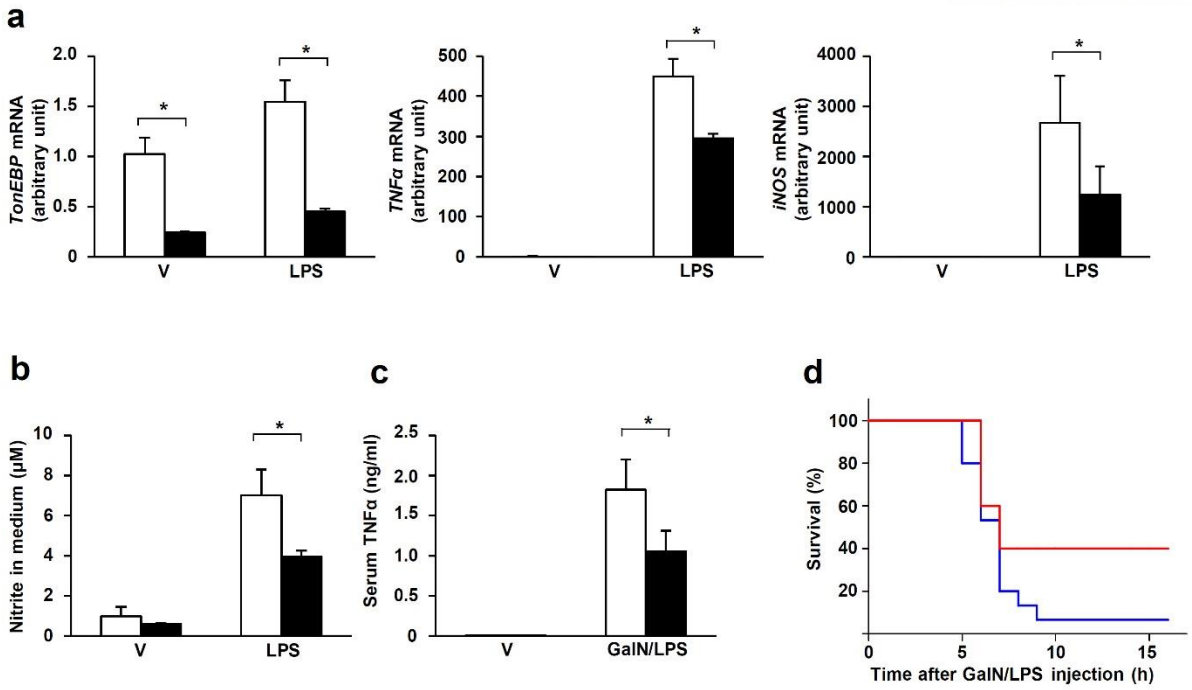

Figure 2-1. Reduced inflammation and septic death in mice with myeloid-specific deletion of the *TonEBP* gene

(a) Peritoneal macrophages (PECs) isolated from *TonEBP* $^{fl/fl}$, *LysM-cre* (solid bars) and their *TonEBP* $^{fl/fl}$ littermates (open bars) were stimulated for 6 h with LPS or vehicle (V). mRNA expression for *TonEBP, TNFα* and *iNOS* was measured by RT Q-PCR. (b) PECs were treated for 24 h with LPS or vehicle (V). Nitrite was measured using Griess reagent from the media. (c) *TonEBP* $^{fl/fl}$, *LysM-cre* mice (solid bars) and their *TonEBP* $^{fl/fl}$ littermates (open bars) were intraperitoneally injected with D-galactosamine (700 mg/kg) plus LPS (150 μg/kg) (GalN/LPS) or vehicle (V). After 1 h, TNFα was measured using ELISA from serum samples. (d) *TonEBP* $^{fl/fl}$, *LysM-cre* (red line) and their *TonEBP* $^{fl/fl}$ littermates (blue line) were intraperitoneally injected with GalN/LPS. The animals were monitored for 16 h for survival. n = 15. Data (mean + s.e.m., n = 4-5) are representative of three independent experiments. *P < 0.05 compared to *TonEBP* $^{fl/fl}$, *LysM-cre*.

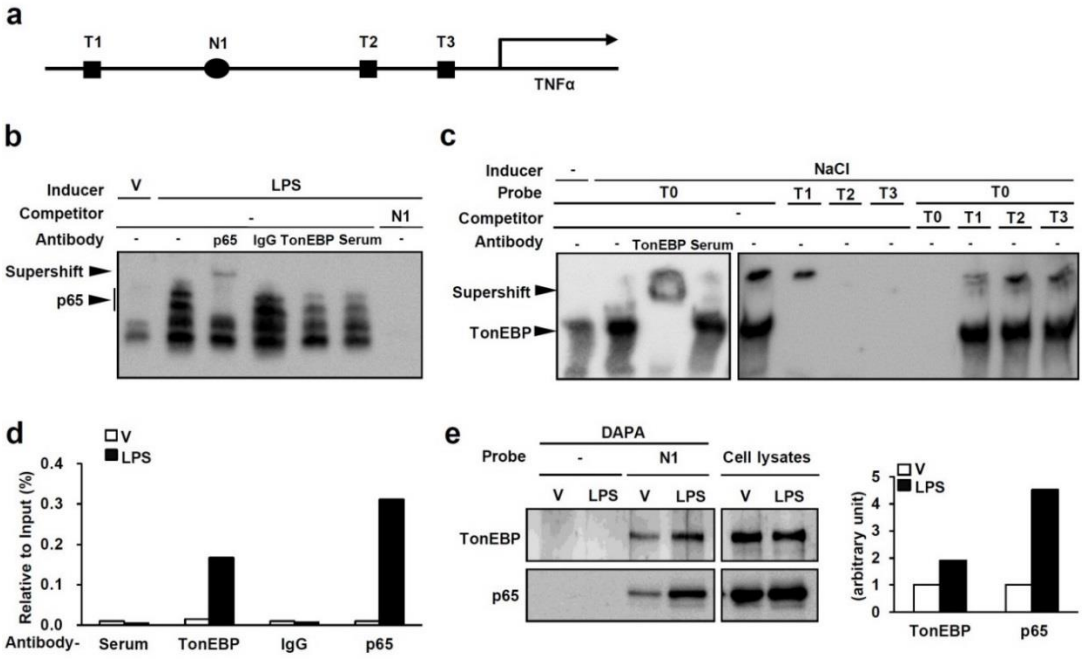

Figure 2-2. TonEBP binds to the κB site of the *TNFα* promoter without direct interaction with DNA

(a) Schematic representation of putative binding sites of TonEBP (T1, T2, T3) and NFκB (N1) in the *TNFα* promoter region. The DNA sequences for putative binding sites were described in electromobility shift assay in Methods. (b) Nuclear extracts were prepared from RAW264.7 cells stimulated for 1 h with LPS (100ng/ml) or vehicle (V). EMSA was performed using the nuclear extracts and biotin-labeled N1 probe. Where indicated, anti-p65 IgG (p65) or normal IgG (IgG) was added to supershift p65-DNA complex; and-TonEBP serum (TonEBP) or normal rabbit serum (Serum) to supershift TonEBP-DNA complex. In the last lane, 50 times concentration of unlabeled N1 was added for competition. (c) Nuclear extracts were prepared from RAW264.7 cells cultured for 24 h in hypertonic medium containing extra 75 mM NaCl (NaCl) or control, isotonic medium (-). EMSA was performed using the nuclear extracts and biotin-labeled probes: T0 (positive control for TonEBP binding), T1, T2, and T3. Anti-TonEBP antibody and normal rabbit serum were used to supershift TonEBP-DNA complex. In the last 4 lanes, 50 times concentration of unlabeled probe was added for competition. (d) RAW264.7 cells were treated for 1 h with LPS or vehicle (V). ChIP was performed using normal rabbit serum, anti-TonEBP serum, normal IgG, and anti-p65 IgG. The precipitates were quantified for the N1 region using Q-PCR. A representative set of four independent sets of experiments is shown. (e) Cell extracts were prepared from RAW264.7 cells treated for 1 h with LPS or vehicle (V). Biotin-labeled N1 probe was used to perform DAPA. DAPA samples and cell lysates were immunoblotted for TonEBP and p65. Images of immunoblots are shown on the left, and intensity ratios of TonEBP and p65 in DAPA/cell lysate are plotted on the right. A representative set of four independent sets of experiments is shown.

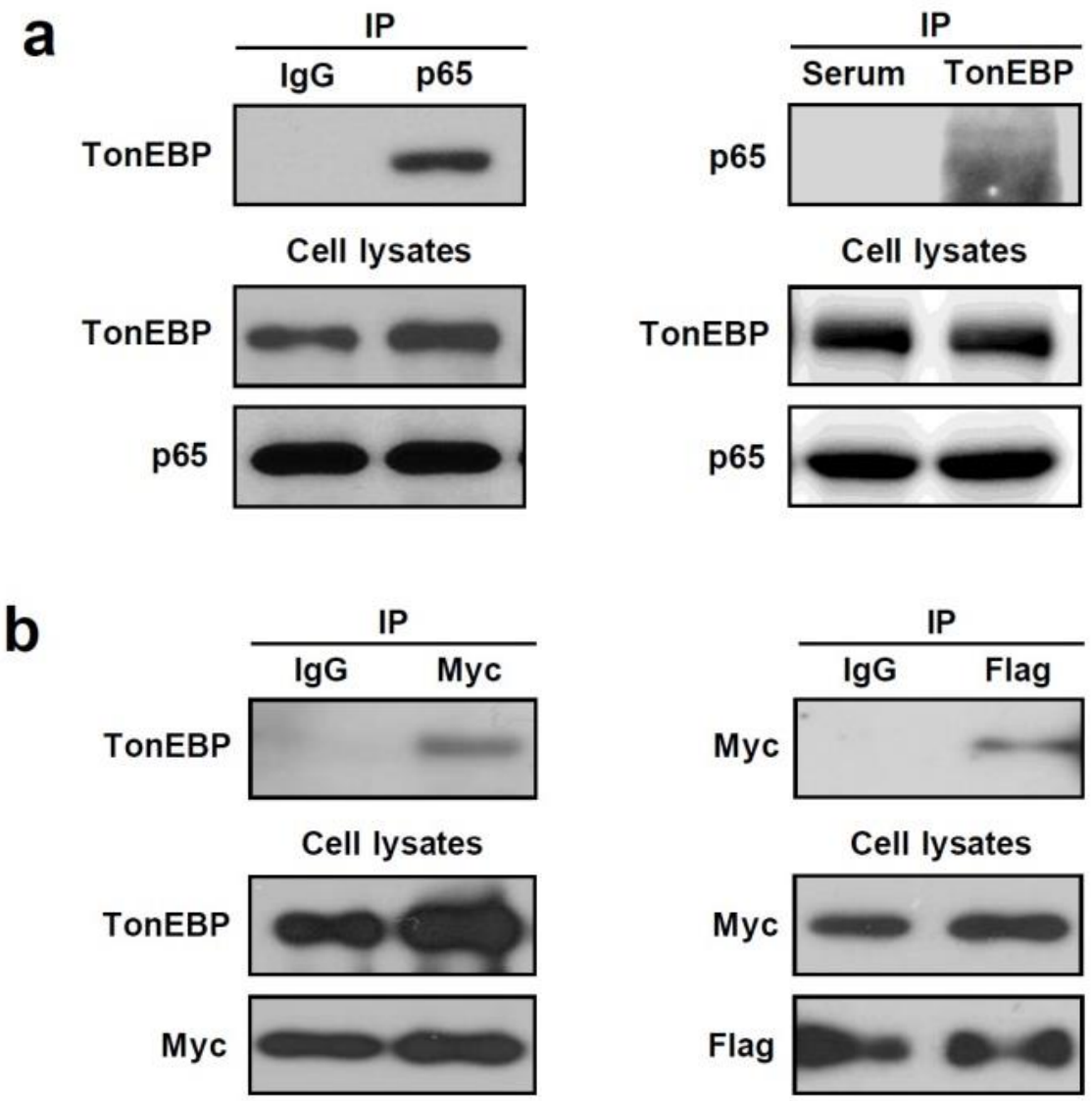

Figure 2-3. TonEBP interacts with p65

(a) MEF cell lysates were immunoprecipitated (IP) with normal IgG or anti-p65 IgG (left), or normal serum or anti-TonEBP serum (right). The immunoprecipitates and cell lysates were immunoblotted for TonEBP and p65 as indicated. (b) COS-7 cells were co-transfected with Myc-p65 and Flag-TonEBP. Cell lysates were immunoprecipitated with normal IgG or anti-Myc IgG (left), or anti-Flag IgG (right). The immunoprecipitates and cell lysates were immunoblotted for TonEBP, Myc, or Flag as indicated. A representative set of three independent sets of experiments is shown.

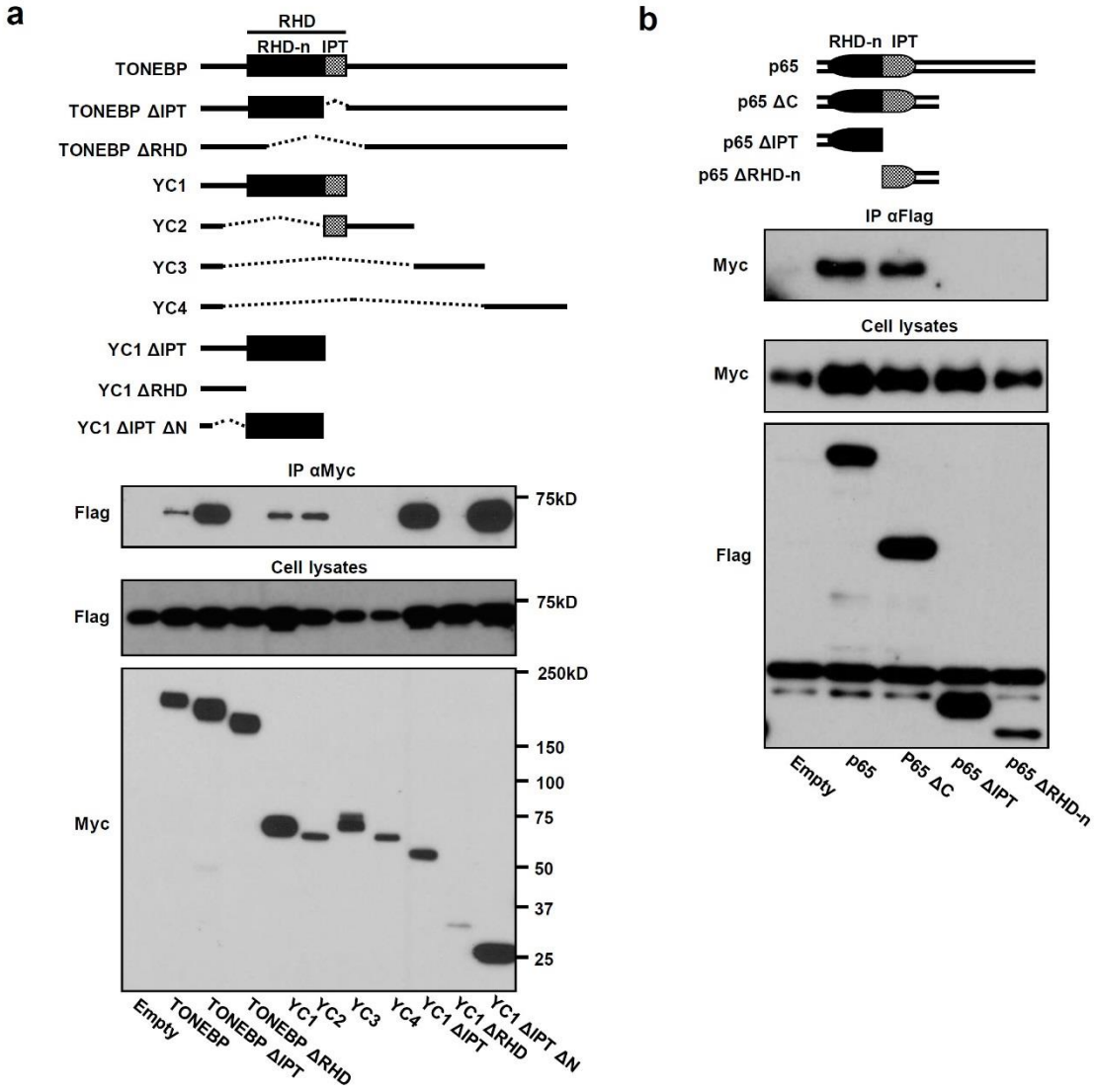

Figure 2-4. TonEBP interacts with p65 via respective RHDs.

(a) Schematic representation of human TONEBP and its recombinant fragments. RHD, Rel-homology domain; RHD-n, N-terminal subdomain of RHD involved in DNA contact; IPT, Ig-like, plexins, transcription factors domain with an immunoglobin-like fold involved in dimer formation. COS-7 cells were cotransfected for 24 h with Flag-p65 plus Myc-tagged TONEBP or one of the recombinant TONEBP fragments shown. Cell lysates were immunoprecipitated (IP) with anti-Myc antibody.

(b) Schematic representation of p65 and its fragments. COS-7 cells were cotransfected for 24 h with Myc-YC1 plus Flag-tagged p65 or one of its fragments shown. Cell lysates were immunoprecipitated with anti-Flag antibody. A representative set of two independent sets of experiments is shown.

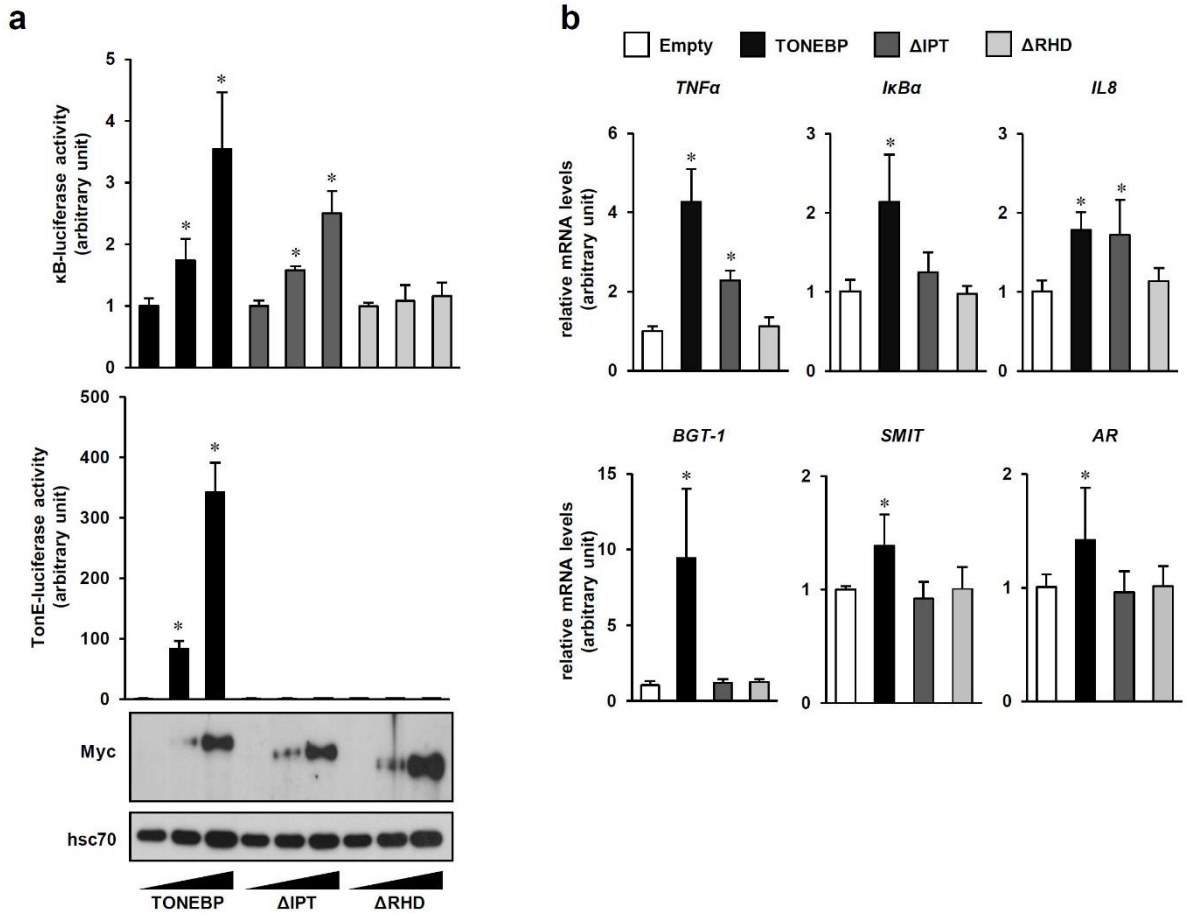

Figure 2-5. Stimulation of NFκB by TonEBP requires the TonEBP-p65 interaction

(a) COS-7 cells were transfected with increasing amount of Myc-tagged TONEBP, TONEBPΔIPT (ΔIPT) or TONEBPΔRHD (ΔRHD) along with κB-luciferase or TonE-luciferase reporter construct. Cells were stimulated for 6 hours with LPS (100 ng/ml) before measuring luciferase activity. The activity of luciferase is shown relative to those cells transfected with empty expression vector. Expression of TONEBP, TONEBPΔIPT and TONEBPΔRHD protein were examined by immunoblotting with anti-Myc antibody. (b) HEK293 cells were transfected with the constructs indicated at the top. mRNA expression was examined by RT Q-PCR for NFκB-target genes *TNFα, IκBα,* and *IL8,* and TonEBP-target genes *BGT-1, SMIT,* and *AR.* Data are normalized to those transfected with empty vector. Data (mean + s.d., n = 5-6) are representative of three independent experiments. *P < 0.05 compared to empty.

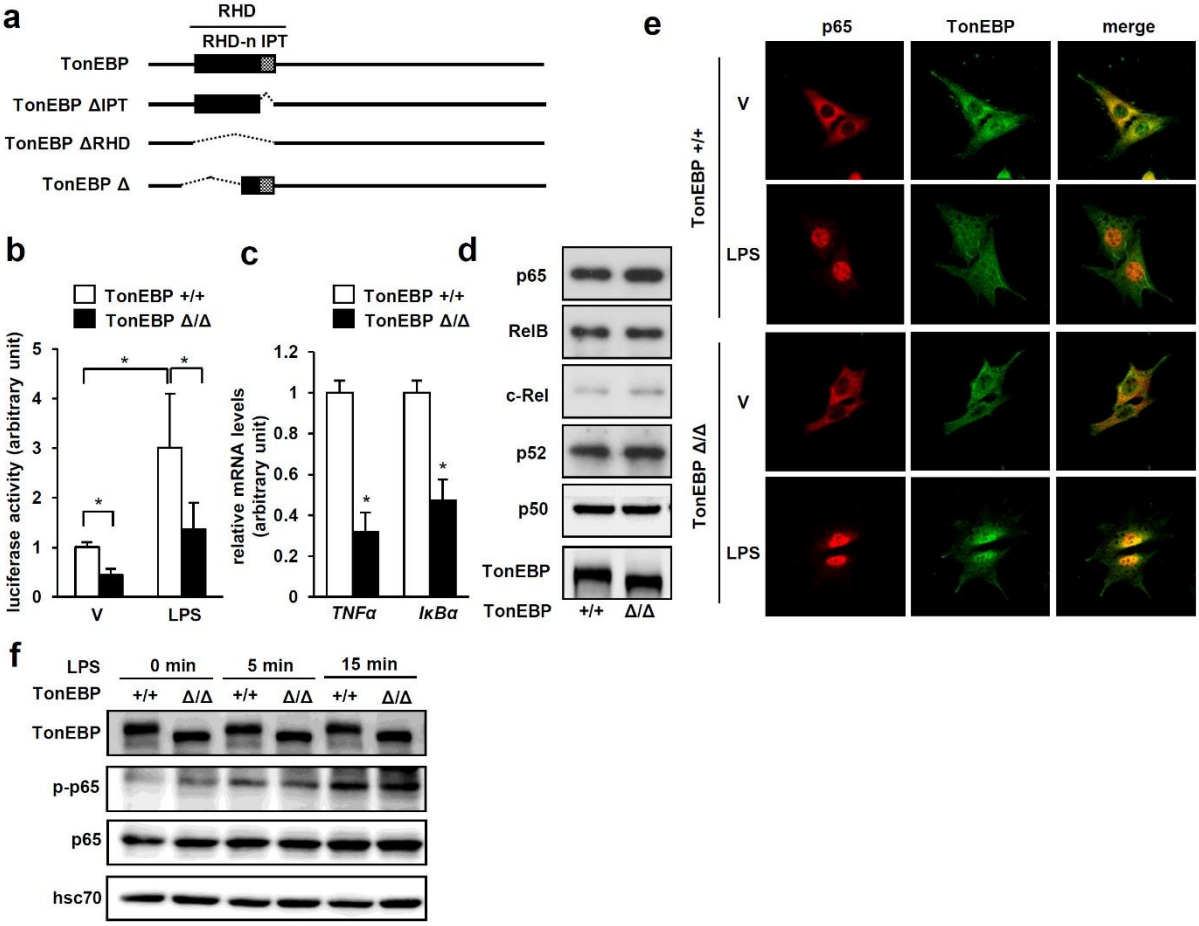

Figure 2-6. Reduced NFκB activity in *TonEBPΔ/Δ* MEF cells despite normal expression and regulation of NFκB

(a) Schematic representations of TonEBP, TonEBP ΔIPT, TonEBP ΔRHD (see Fig. 3), and protein product of the *TonEBPΔ* allele which lacks exon 6 and 7 leading to an in-frame deletion of a portion of RHD-n as indicated. (b) *TonEBP*+/+ or *TonEBPΔ/Δ* MEF cells were transfected with the κB-luciferase construct. Cells were treated with LPS (100 ng/ml) or vehicle (V) for 6 hours before measuring luciferase activity. (c) Cells were treated with LPS for 6 hours. *TNFα* and *IκBα* mRNA were quantified by RT Q-PCR. (d) Cells were immunoblotted for p65, RelB, c-Rel, p52, p50 and TonEBP. (e) Cells grown on coverslips were treated with LPS or vehicle (V), and immunostained for p65 (red) and TonEBP (green). Co-localization is shown in orange in merged images. (f) Cells were treated with LPS for 0, 5, and 15 min as indicated, and immunoblotted for TonEBP, serine 276 phosphorylated p65 (p-p65), p65, and hsc70. Data (mean + s.d., n = 4) are representative of two or three independent experiments. *P < 0.05 compared to corresponding *TonEBP* +/+.

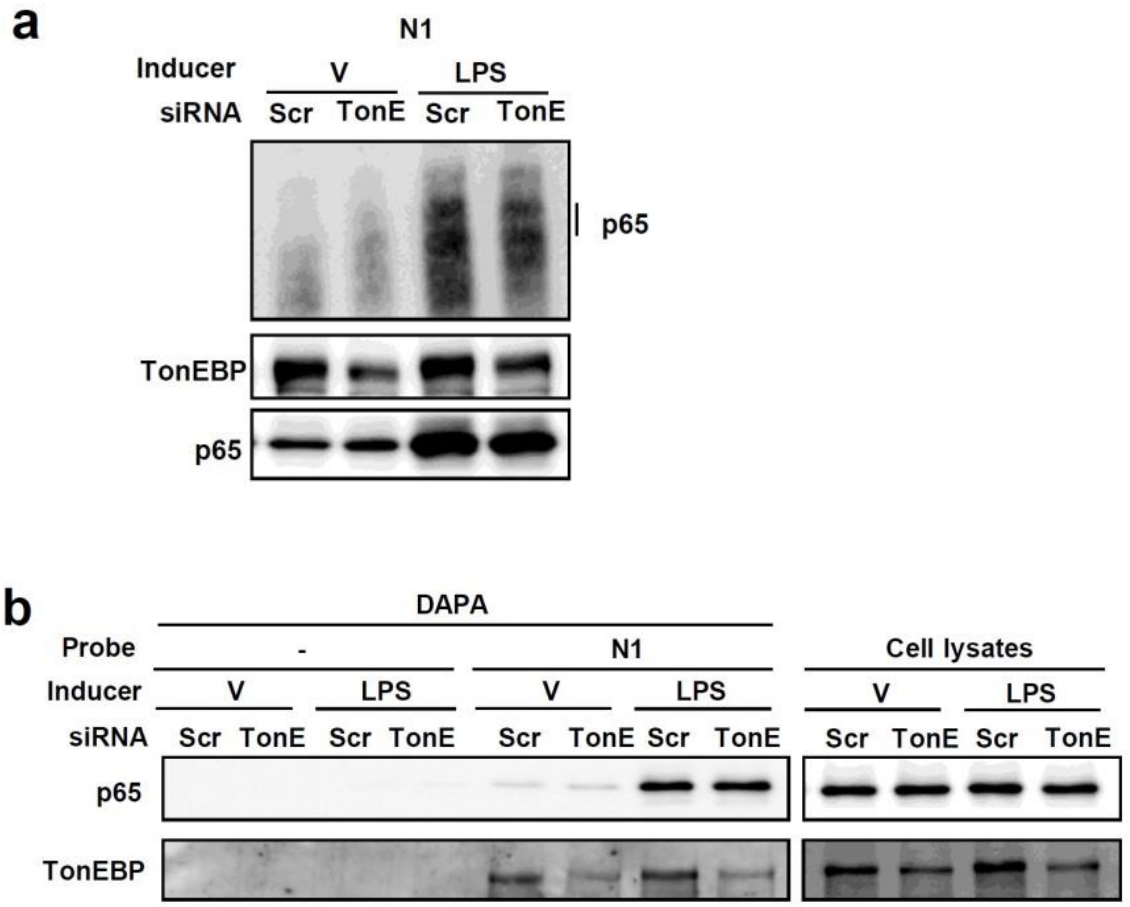

Figure 2-7. TonEBP knockdown does not affect DNA binding of p65

(a) RAW264.7 cells were transfected with TonEBP-targeting siRNA (TonE) or scrambled siRNA (Scr) followed by treatment with LPS or vehicle (V). Nuclear extracts were prepared and EMSA was performed with the N1 probe as in Fig. 2-1b (top). The nuclear extracts were immunblotted for TonEBP and p65 (bottom). (b) DAPA was performed with the N1 probe as in Fig. 2-1e. Data are representative of two independent experiments.

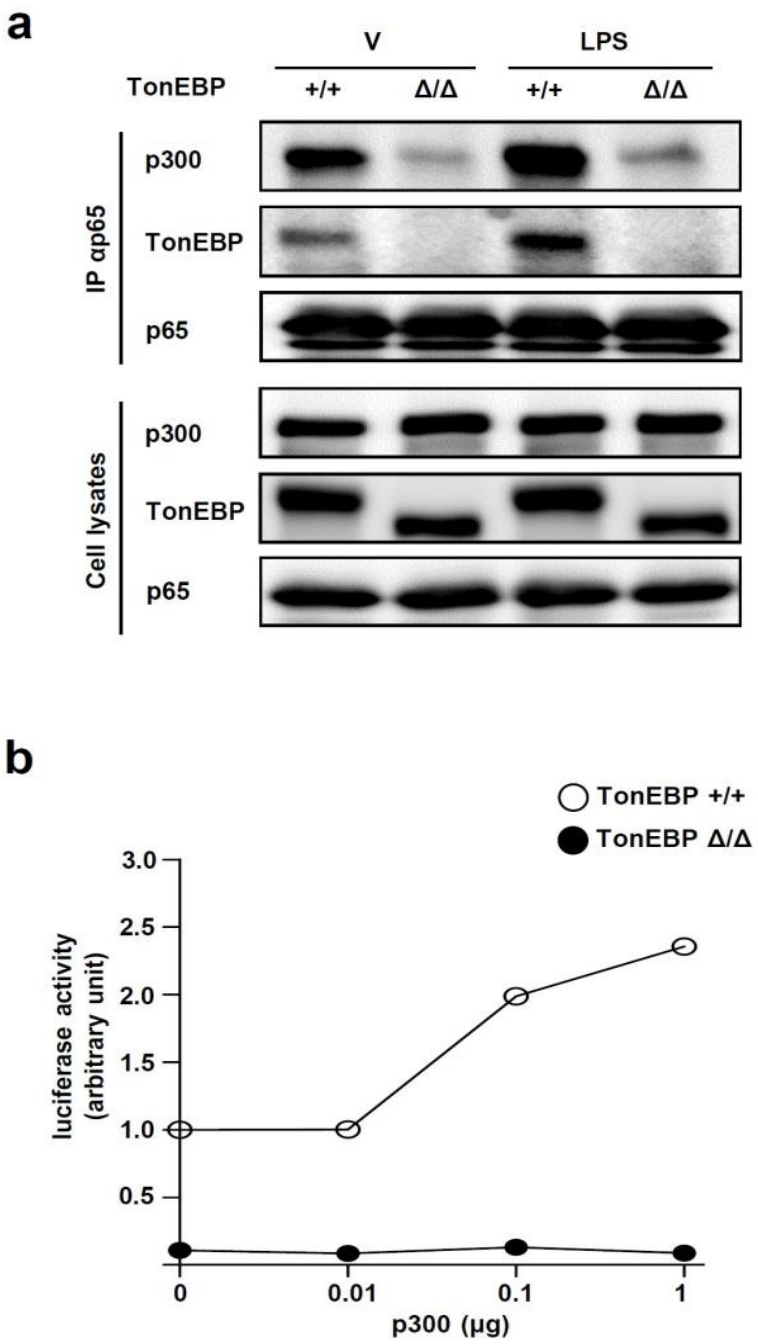

Figure 2-8. The TonEBPΔ protein is unable to recruit p300 co-activator to p65

(a) *TonEBP+/+* or *TonEBPΔ/Δ* MEF cells were treated with LPS or vehicle (V). Lysates of *TonEBP+/+* or *TonEBPΔ/Δ* MEF cells were immunoprecipitated (IP) using anti-p65 antibody followed by immunoblotting for p300, TonEBP and p65. (b) Cells were transfected with increasing amount of a p300 expression plasmid along with the κB-luciferase reporter. After 6 h treatment with LPS, luciferase was measured. A representative of three independent experiments is shown.

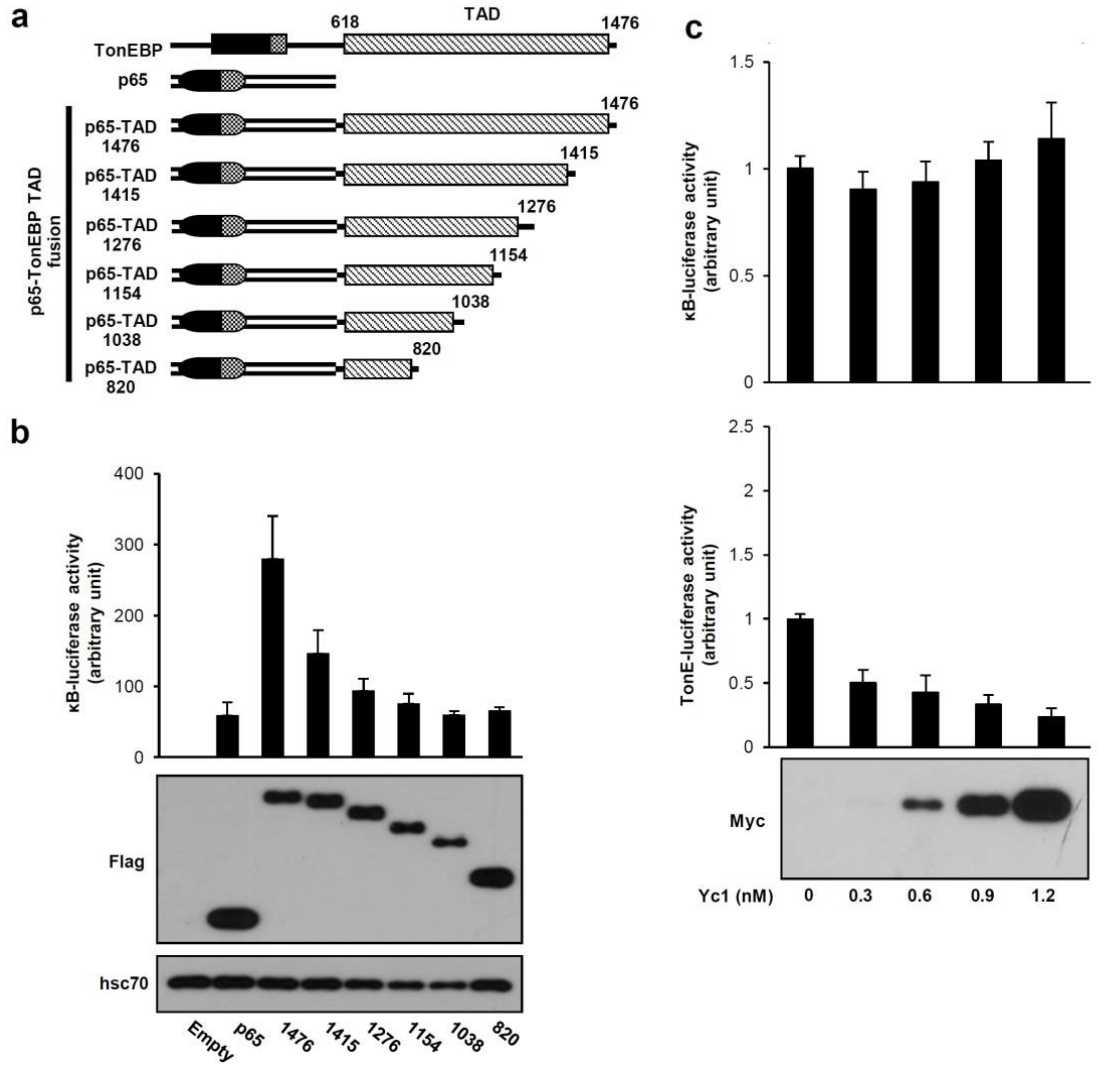

Figure 2-9. The transactivation domain of TonEBP mediates the NFκB activation

(a) Schematic representation of the p65-TonEBP fusion constructs. Transactivation domain (TAD) of TonEBP (amino acids 618-1476) and its serial deletions were fused to p65 as shown. (b) COS-7 cells were transfected with Flag-tagged p65 or various p65-TonEBP fusion constructs along with a κB-luciferase reporter construct driven. Cells were stimulated for 6 hours with LPS before measuring luciferase activity. Expression of the p65-TonEBP fusion proteins was examined by immunoblotting for Flag. (c) COS7 cells were transfected with Myc-Yc1 along with a luciferase reporter construct driven by κB or TonE. Cells were stimulated for 6 hours with LPS before measuring κB luciferase activity or stimulated for 6 hours with hypertonicity before measuring TonE luciferase activity. Data (mean + s.d., n = 5-6) are representative of three independent experiments.

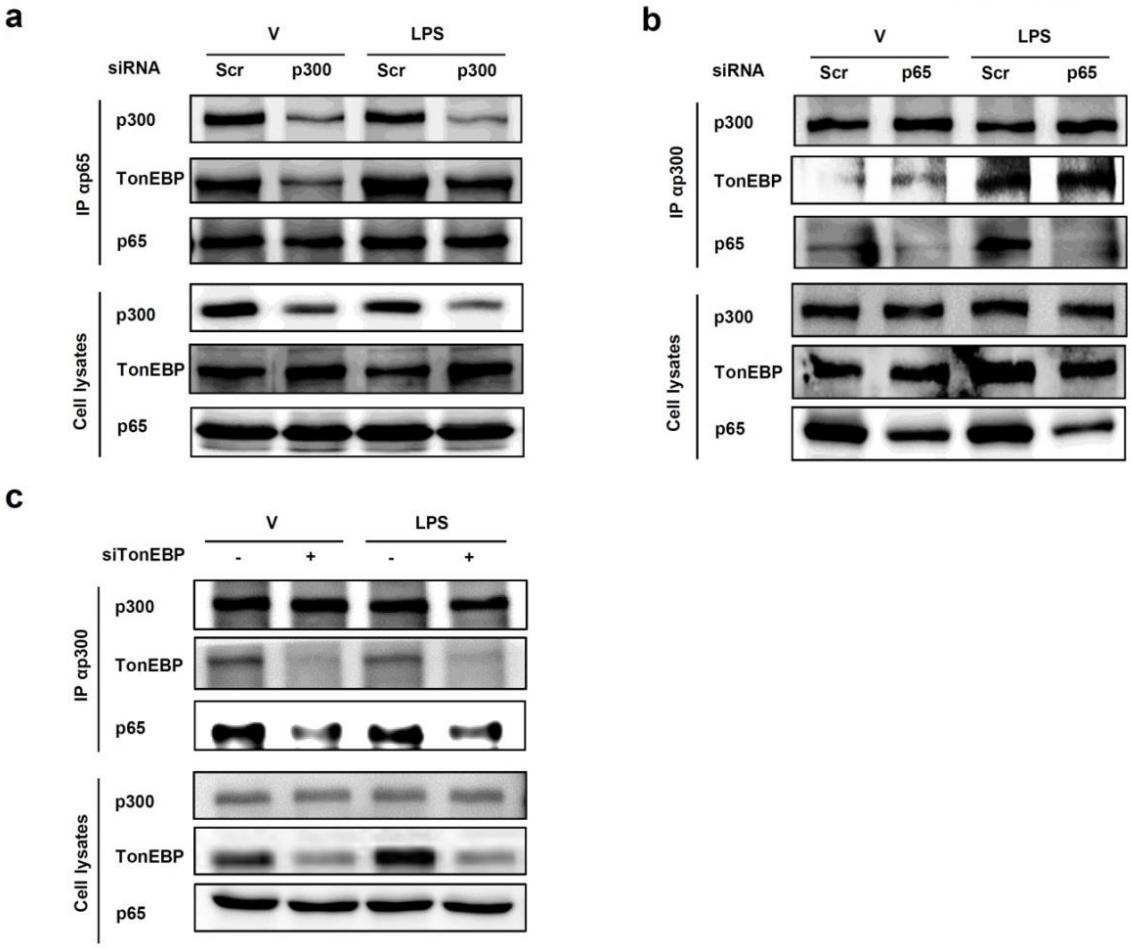

Figure 2-10. TonEBP-p300 interaction is independent of p65

(a) MEF cells were transfected with p300-targeted siRNA or scrambled (Scr) siRNA followed by stimulation with LPS or vehicle (V). Cell lysates were immunoprecipitated (IP) using anti-p65 antibody and immunoblotted for p300, TonEBP and p65. (b) MEF cells transfected with p65-targeted siRNA or scrambled (Scr) siRNA were treated as above. Cell lysates were immunoprecipitated using anti-p300 antibody. (c) MEF cells transfected with TonEBP-targeted siRNA or scrambled (Scr) siRNA were treated as above. Cell lysates were immunoprecipitated using anti-p300 antibody. Data are representative of two independent experiments.

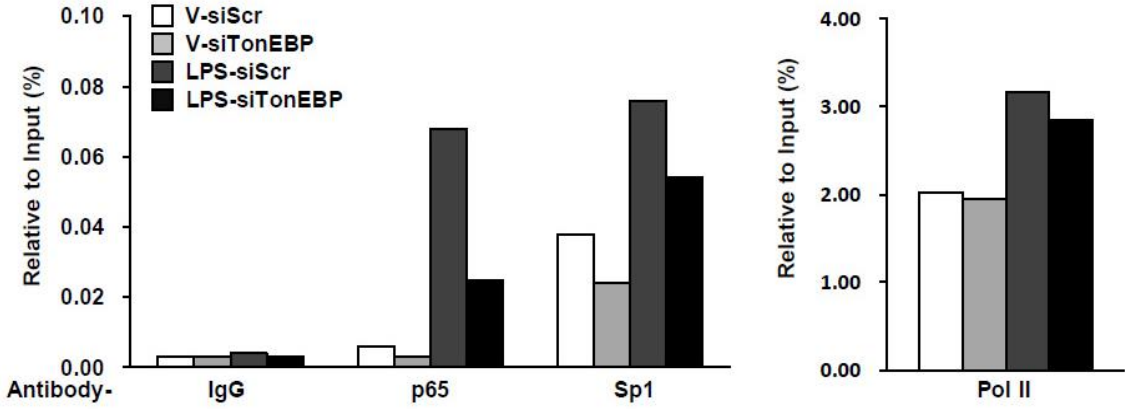

Figure 2-11. TonEBP deficiency breaks down the LPS-induced NFκB enhanceosome assembly on *TNFα* promoter

RAW264.7 cells were transfected with TonEBP-targeted siRNA or scrambled (Scr) siRNA followed by stimulation with LPS or vehicle (V) for 1h. ChIP was performed using normal rabbit IgG, anti-p65 IgG, anti-Sp1 IgG, and anti-Pol II IgG. The precipitates were quantified for the N1 region using Q-PCR. A representative set of three independent experiments is shown. Data are representative of three independent experiments.

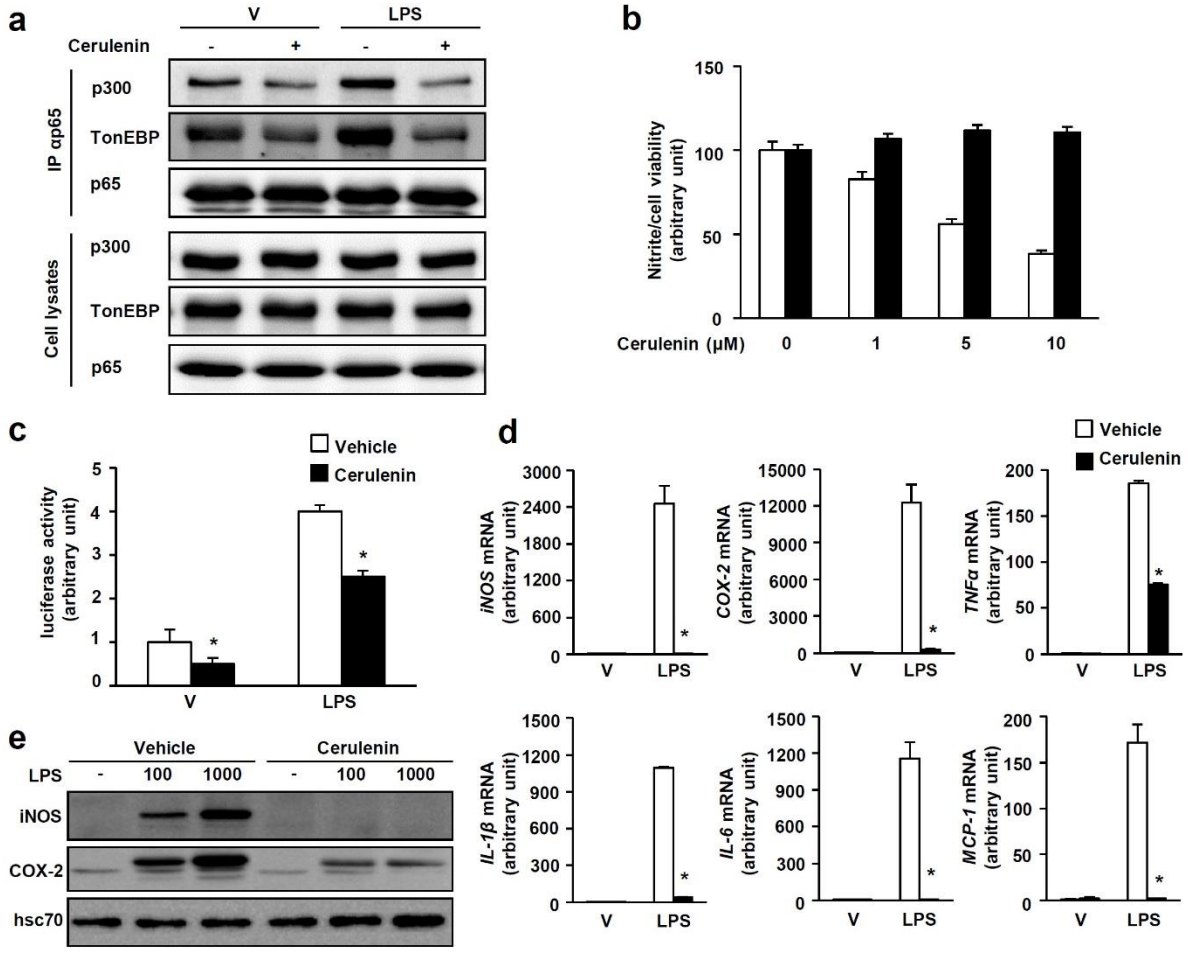

Figure 2-12. Cerulenin breaks up the TonEBP-p300-p65 interaction and reduces inflammation

(a) MEF cells were treated without or with cerulenin (10 μM) for 1 h followed by vehicle (V) or LPS (100 ng/ml) for an additional 1 h. Cell lysates were immunoprecipitated (IP) using anti-p65 antibody. The immunoprecipitates and cell lysates were immunoblotted for p300, TonEBP and p65. (b) PECs were treated with 0 to 10 μM cerulenin as indicated for 1 h, followed by LPS for 24 h. Nitrite in the medium (open bars) and cell viability based on reduction of MTT (solid bars) were measured. (c) PECs transfected with the κB-luciferase construct were treated with vehicle or cerulenin (10 μM) for 1 h, followed by vehicle (V) or LPS for an additional 6 h. Luciferase activity was measured from cell lysates. (d) PECs were treated as in (c) and mRNA expression for *iNOS*, *COX-2, TNFα, IL-1β, IL-6* and *MCP-1* was measured by RT Q-PCR. (e) PECs pre-treated for 1 h with vehicle or cerulenin (10 μM) were stimulated for 24 h with 0, 100, and 1,000 ng/ml of LPS. Expression of iNOS and COX-2 was visualized by immunoblotting. Data (mean + s.d., n = 4-5) are representative of three independent experiments. *P < 0.05 compared to vehicle.

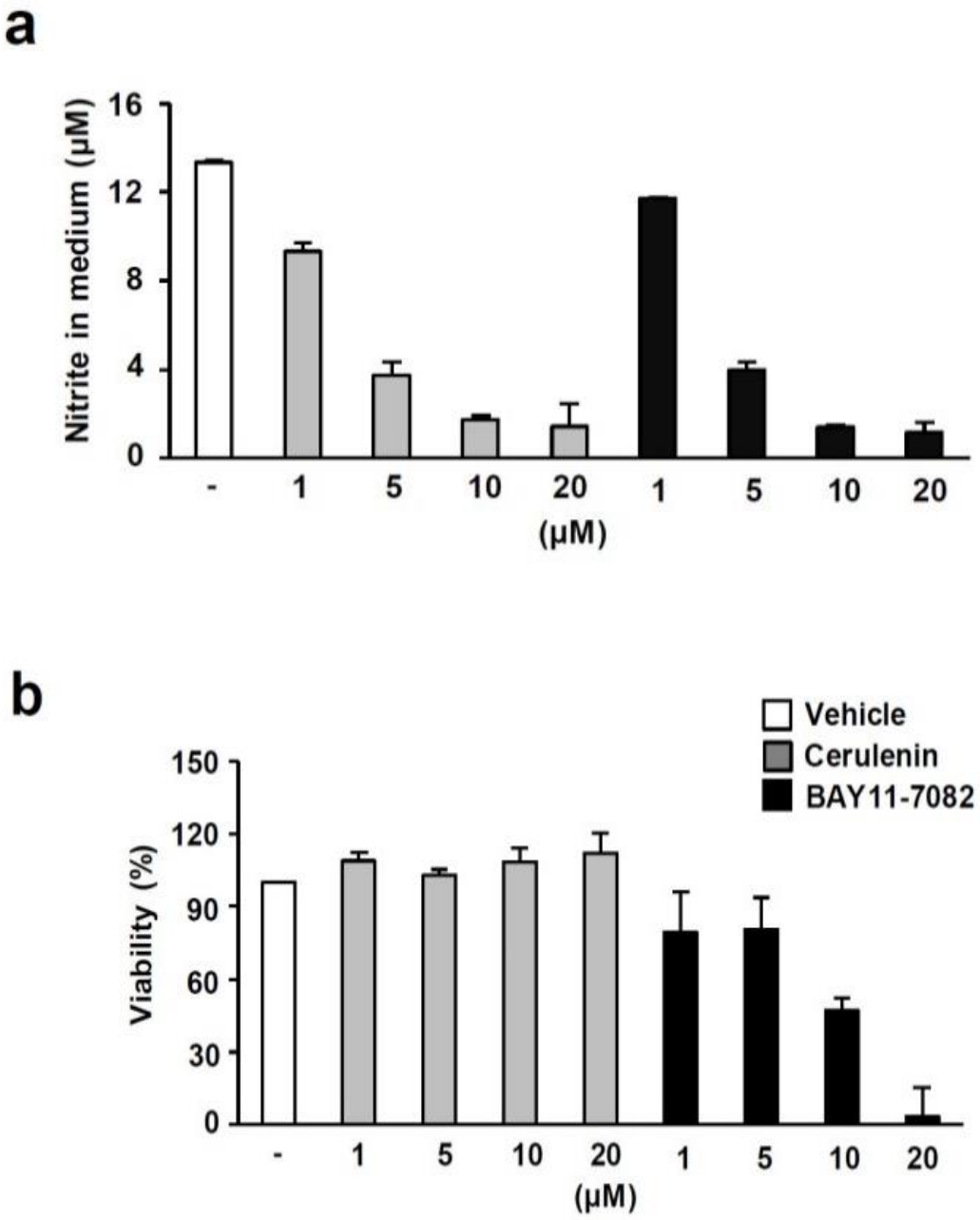

Figure 2-13. Cerulenin reduces inflammation without cytotoxicity

(a) RAW264.7 cells were treated for 1 h with vehicle, or 1 to 20 μM of cerulenin or BAY11-7082 as indicated. The cells were then treated for 24 h with LPS. Nitrite in the media (a) and cell viability (b) were measured. Data (mean + s.d., n = 5) are representative of four independent experiments.

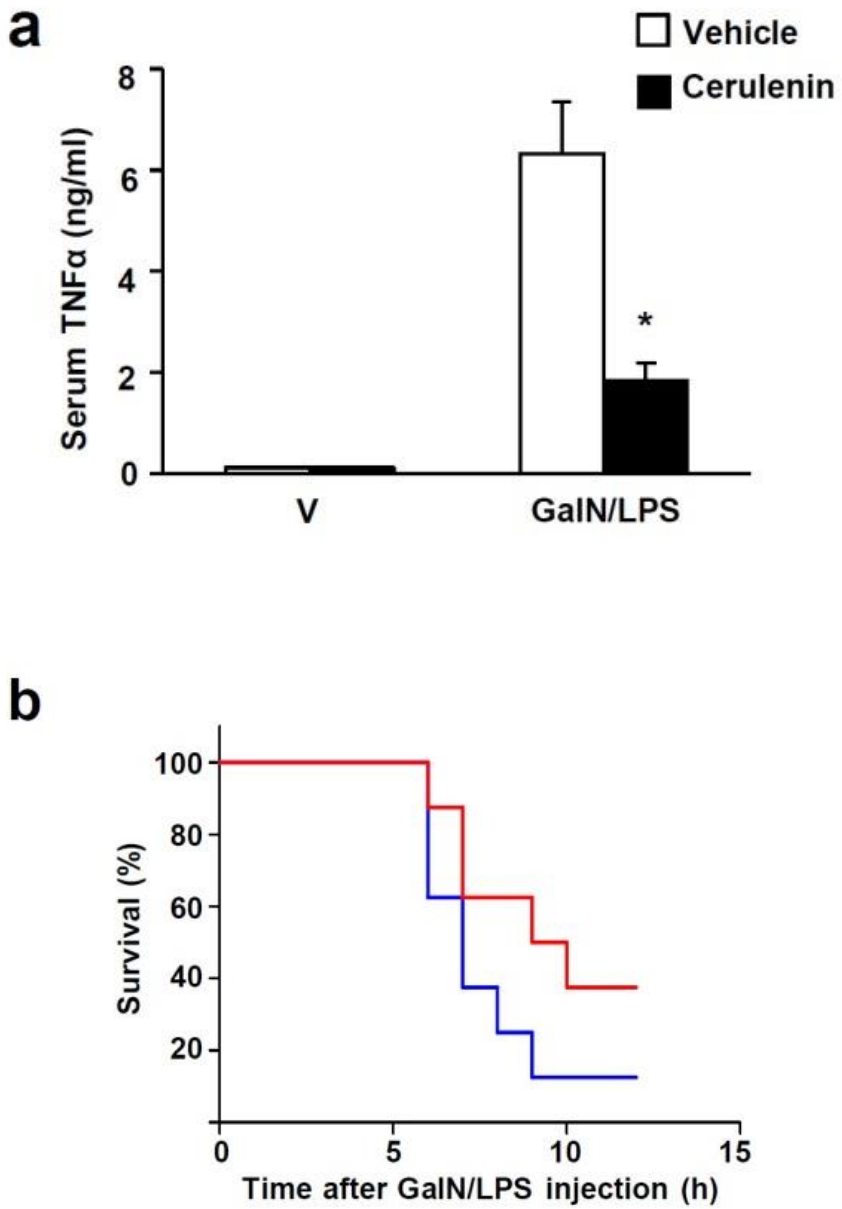

Figure 2-14. Cerulenin reduces inflammation and septic death in mice

(a) Mice were intraperitoneally injected with vehicle or cerlenin (60 mg/kg body weight). After 1 h, vehicle or GalN/LPS was administered as in Fig. 7. After another hour, TNFα was measured from serum samples. Data (mean + s.d., n = 5) are representative of three independent experiments. *P < 0.05 compared to vehicle. (b) Animals pre-treated with vehicle (blue line) or cerulenin (red line) were administered with GalN/LPS as in (a). The animals were monitored for survival. n = 8.

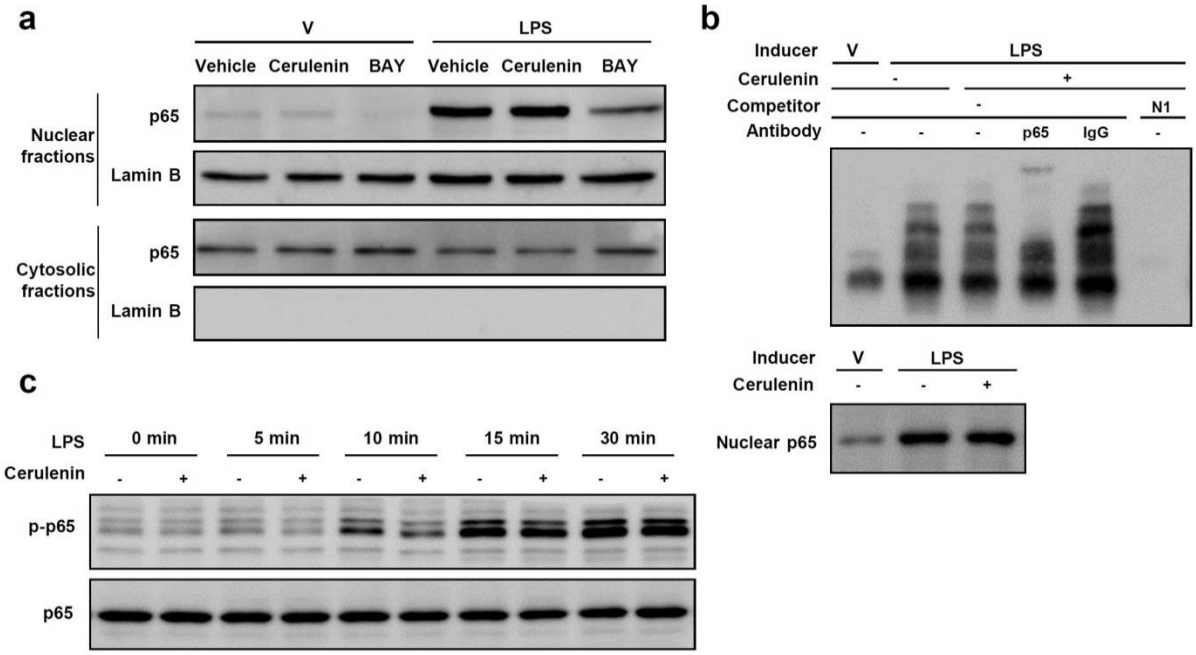

Figure 2-15. Cerulenin does not affect nuclear localization, DNA binding, and phosphorylation of p65

(a) RAW264.7 cells were treated for 1 h with vehicle, cerulenin, or BAY 11-7082 (BAY) followed by 1 h treatment with vehicle (V) or LPS. Nuclear and cytoplasmic fractions were separated and immunoblotted for p65, and lamin B. (b) Cells were pretreated with cerulenin and then LPS as above. EMSA was performed using nuclear extracts and biotin-labeled N1 probe. Where indicated, anti-p65 IgG (p65) or control IgG (IgG) was added to supershift p65-DNA complex. In the last lane, 50 times concentration of unlabeled (cold) N1 was added for competition. Bottom panel shows p65 immunoblot of the nuclear extracts. (c) Vehicle (-) or cerulenin treated cells were incubated with LPS for 0 to 30 min as indicated, and immunoblotted for serine 276 phosphorylated p65 (p-p65) and p65. Data are representative of three independent experiments.

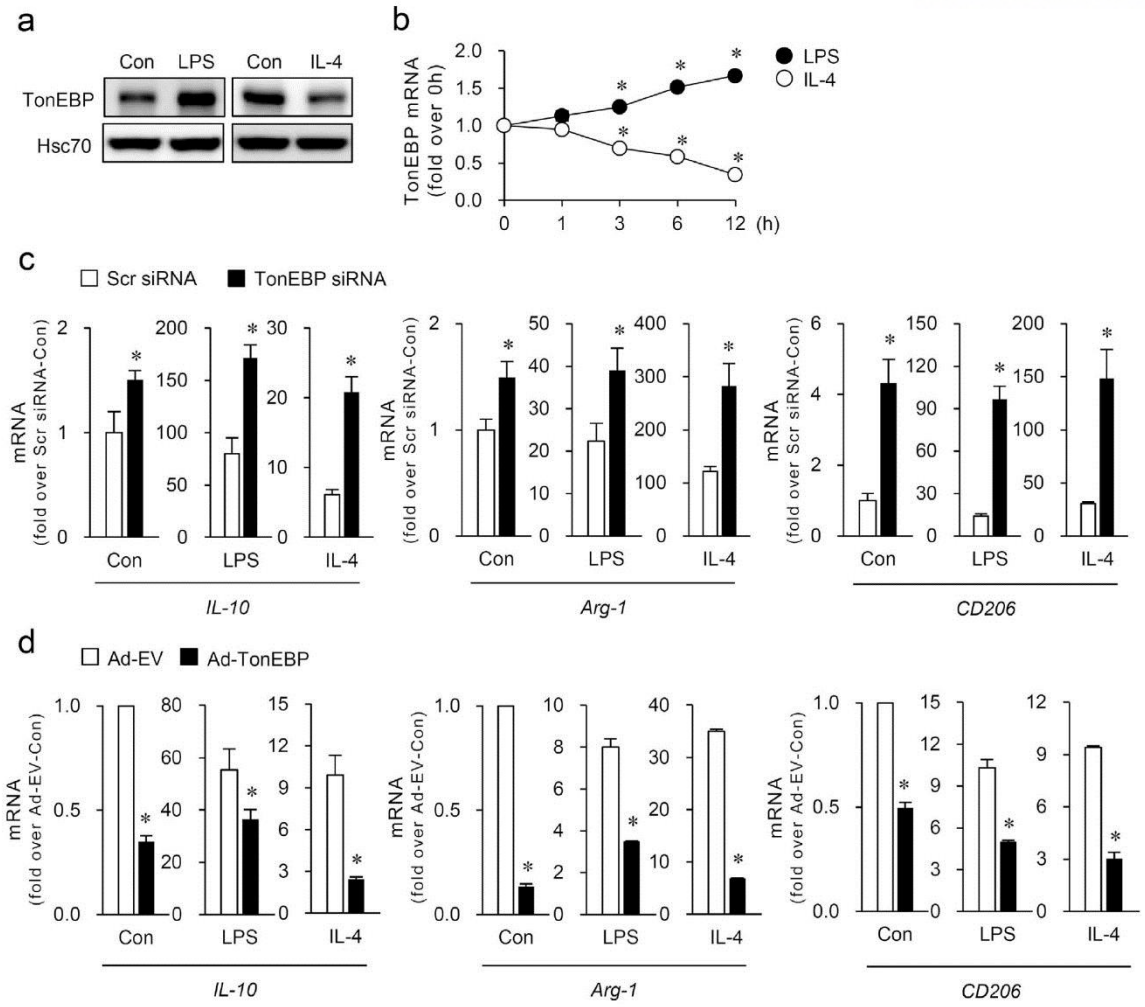

Figure 2-16. IL-4 diminishes the expression of TonEBP which reduces the expression of M2 genes in macrophages

(a) RAW264.7 cells were treated for 24 h with vehicle (Con), LPS (100 ng/ml), or IL-4 (10 ng/ml) and immunoblotted for TonEBP and Hsc70. (b) Cells were treated with LPS or IL-4 up to 12 h as indicated. Quantitative RT-PCR was performed for *TonEBP* mRNA and expressed in fold over 0h. s.d. bars are smaller than the circles (n = 3). *P < 0.05 compared to 0 h. (c) Cells transfected with scrambled (Scr) or TonEBP targeted siRNA were treated for 6 h with vehicle (Con), LPS, or IL-4. Quantitative RT-PCR was performed for mRNA for *IL-10*, *Arg-1* and *CD206*, and expressed in fold over Scr siRNA and Con. (d) Cells infected with adenovirus expressing TonEBP (Ad-TonEBP) or with empty vector (Ad-EV) were treated with LPS or IL-4. Data (mean + s.d., n = 3) are representative of three independent experiments. *P < 0.05 compared to corresponding scrambled siRNA or Ad-EV.

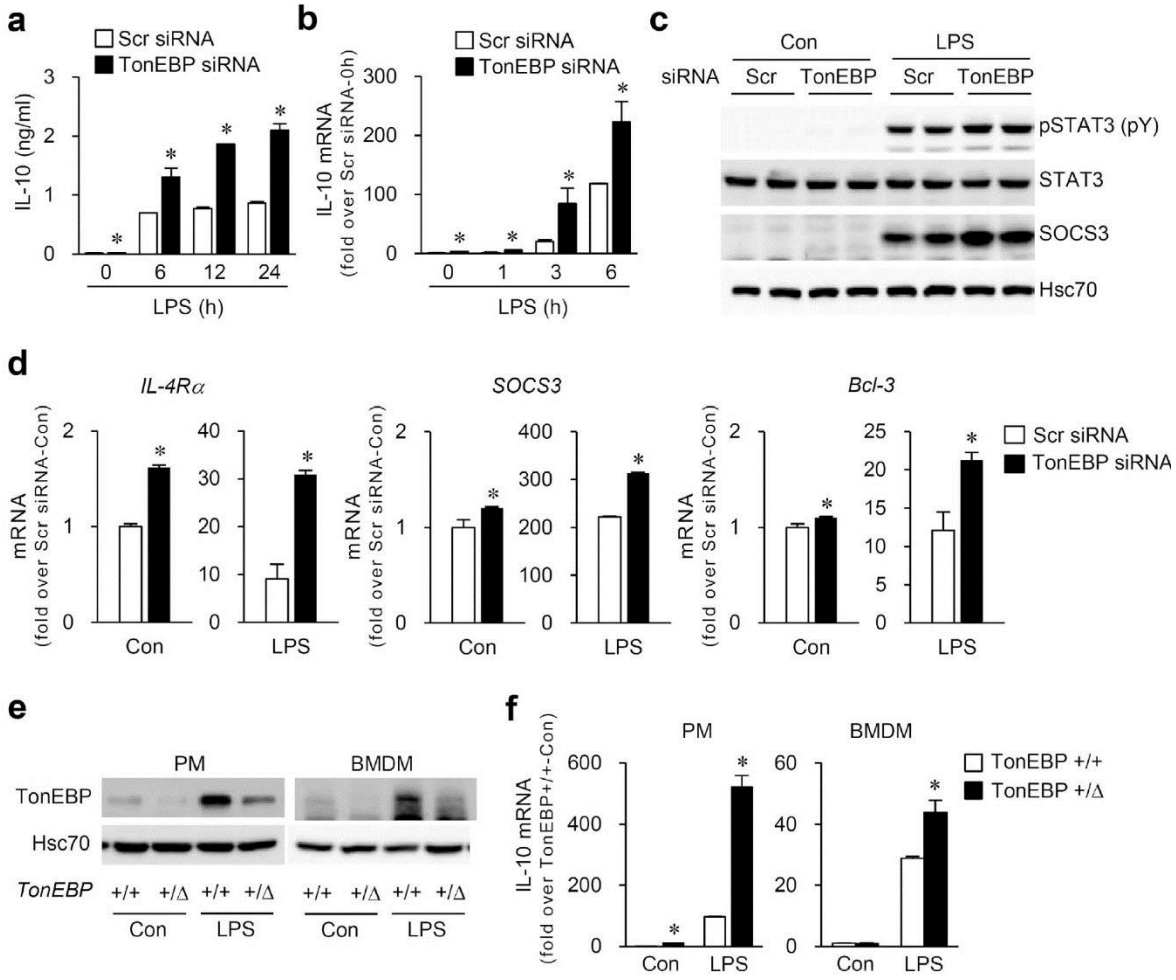

Figure 2-17. TonEBP deficiency enhances the expression and signaling of IL-10 in M1 macrophages

(a–d) RAW264.7 cells transfected with scrambled (Scr) or TonEBP-targeted siRNA and treated with LPS (100 ng/ml) for up to 24 h as indicated (a,b), 18 h (c) or 6 h (d). IL-10 concentration in the medium was measured by ELISA (a) and *IL-10* mRNA abundance by quantitative RT-PCR (b). In (c), immunoblotting was performed for SOCS3, STAT3, phospho-STAT (p-STAT3), and Hsc70. In (d), mRNA for *IL-4Rα* , *SOCS3* and *Bcl-3* was measured. (e,f) Thioglycollate-elicited peritoneal macrophages (PM) or bone marrow-derived macrophages (BMDM) obtained from *TonEBP +/Δ* mice and their *TonEBP* +/+ littermates were treated with vehicle (Con) or LPS (100 ng/ml) for 18 h (e) or 6 h (f). Immunoblotting for TonEBP and Hsc70 (e) and quantitative RT-PCR for *IL-10* mRNA (f) were performed. Data (mean + s.d., n = 3) are representative of three independent experiments.

*P < 0.05 compared to corresponding scrambled siRNA or *TonEBP +/Δ* mice.

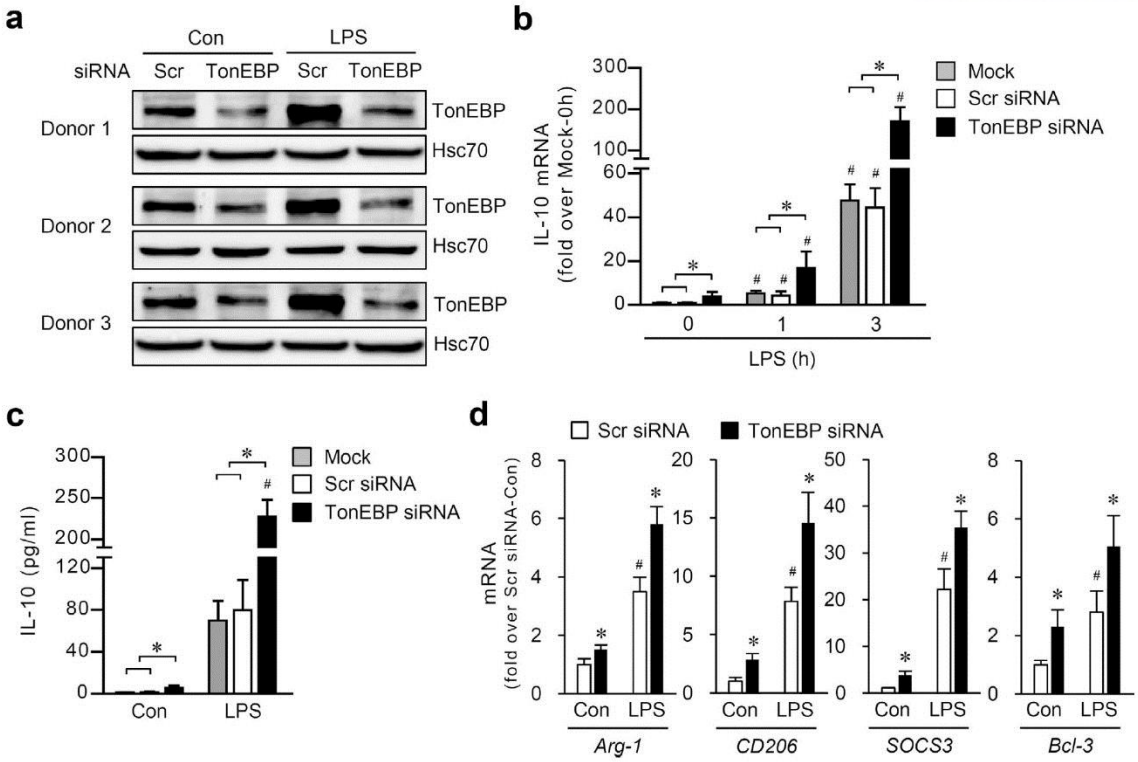

Figure 2-18. TONEBP deficiency enhances the expression of IL-10 in primary human macrophages obtained from 3 donors

The human macrophages were transfected with scrambled (Scr) or TONEBP-targeted siRNA. 48 h later, the cells were treated with vehicle (Con) or LPS (100 ng/ml) for 6 h (a,d), 1 and 3 h (b), or 6 h (c). Immunoblotting was performed for TONEBP and HSC70 (a). In (b), *IL-10* mRNA abundance was measured by quantitative RT-PCR. In (c), IL-10 concentration in the medium was measured by ELISA. In (d), mRNA for *ARG-1, CD206, SOCS3*, and *BCL-3* was measured. Mean + s.d., n = 3. *P < 0.05 compared to corresponding scrambled siRNA.

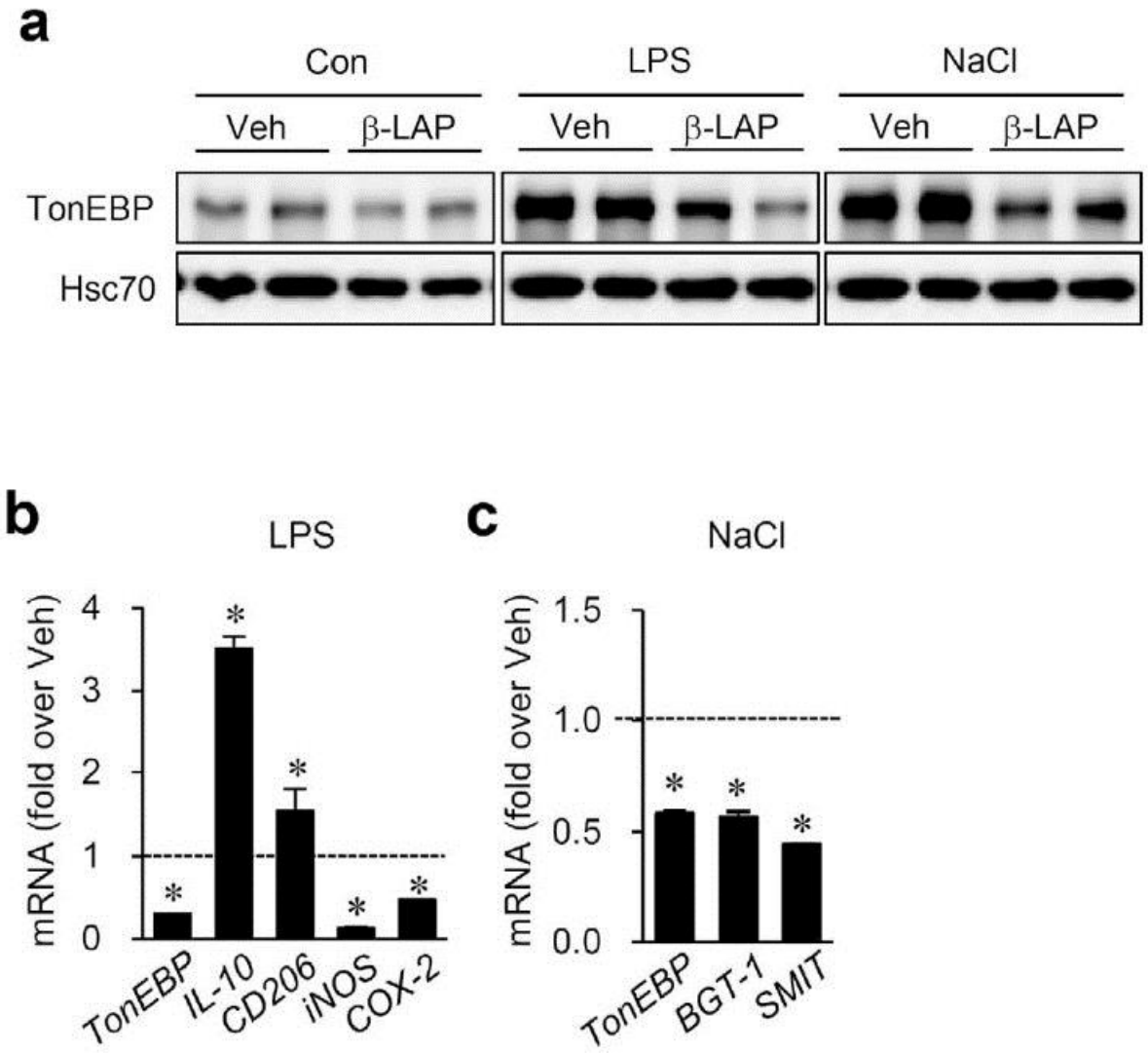

Figure 2-19. β-lapachone reduces TonEBP expression and enhances IL-10 expression

RAW264.7 cells were treated for 1 h with vehicle (Veh) or 10 μ M β -lapachone (β -LAP), followed by a 6 h treatment with vehicle (Con), 100 ng/ml LPS, or additional 75 mM NaCl. (a) Immunoblotting was performed for TonEBP and Hsc70. (b,c) From the LPS and NaCl treated cells, mRNA for the genes indicated was measured by quantitative RT-PCR. mRNA abundance in β -LAP over that of Veh is shown. Data (mean + s.d.; n = 3 to 5) are representative of three independent experiments. *P < 0.05 compared to vehicle.

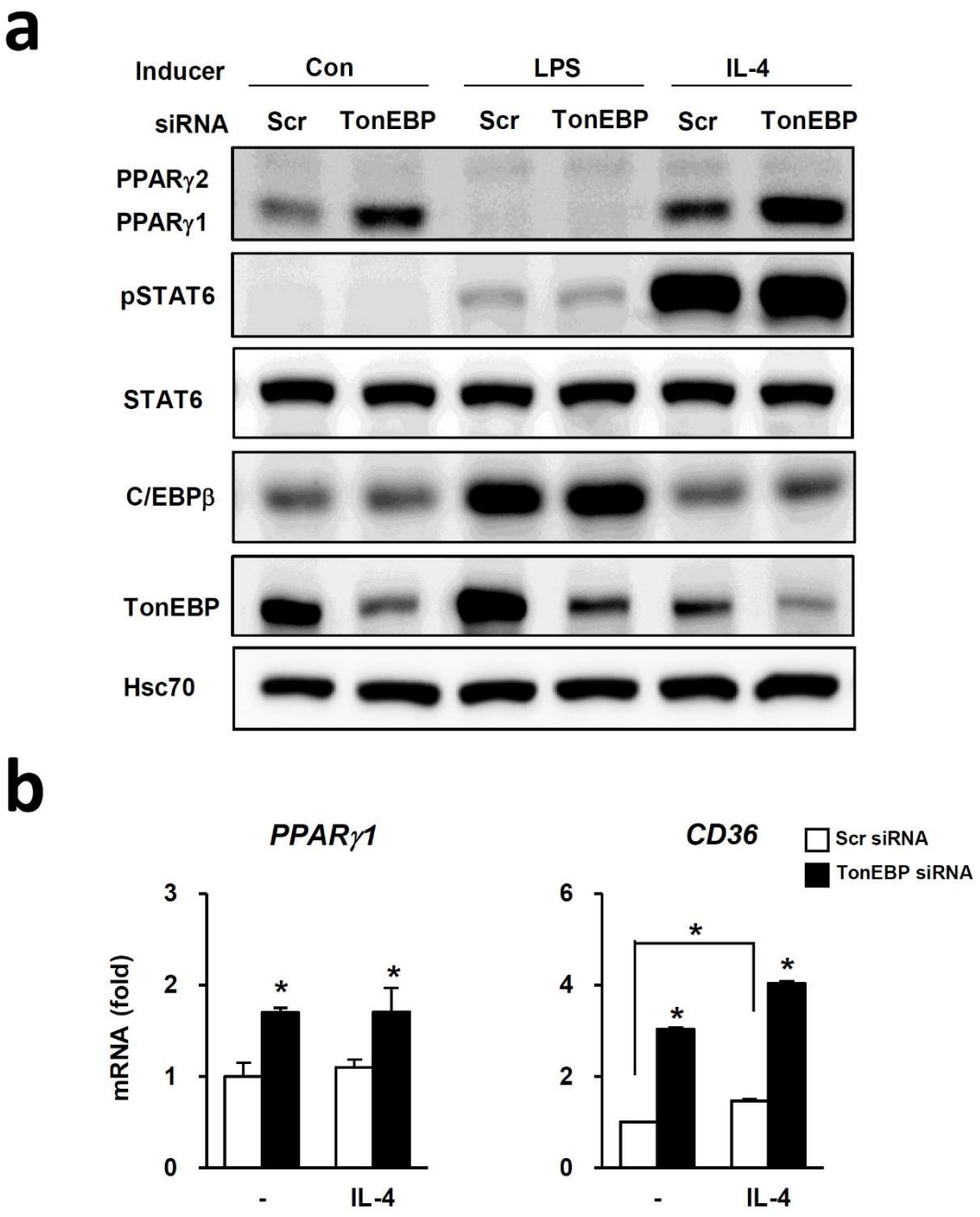

Figure 2-20. TonEBP deficiency increases PPARγ1 expression in RAW264.7 cells

(a) Scr siRNA or TonEBP siRNA transfected RAW264.7 cells were treated for 24 h with vehicle (Con), LPS (100 ng/ml), or IL-4 (10 ng/ml) and immunoblotted for PPARγ, pSTAT6, STAT6, C/EBPβ, TonEBP and Hsc70. (b) Scr siRNA or TonEBP siRNA transfected cells were treated with IL-4 for 12 h. Quantitative RT-PCR was performed for *PPARγ1* and *CD36* mRNA and expressed in fold over 0h, Scr siRNA. Data (mean + s.d., n = 3) are representative of four independent experiments. *P < 0.05 compared to scrambled siRNA.

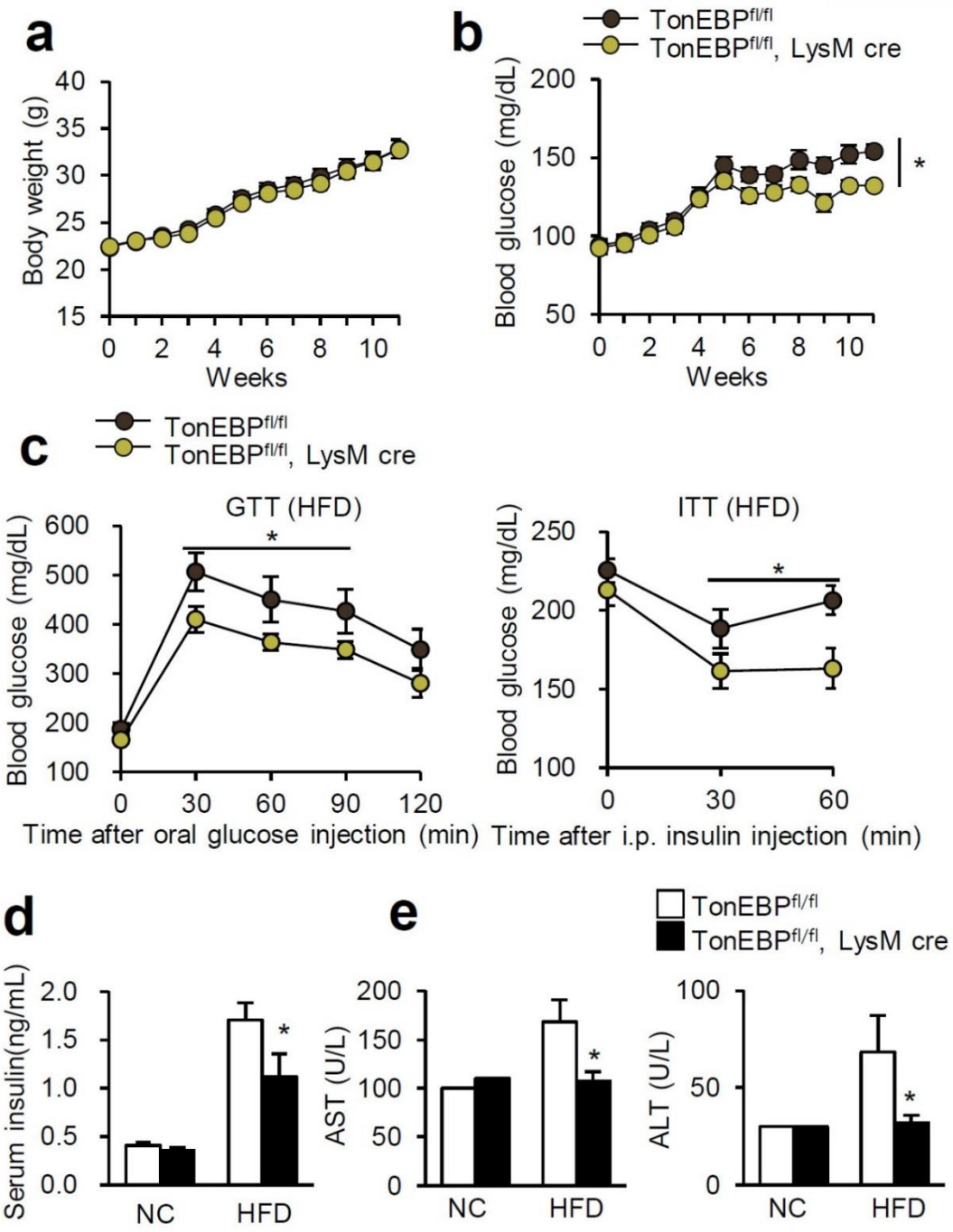

Figure 2-21. Myeloid specific TonEBP deficiency improves metabolic profiles in obesity

(a) Body weights and (b) fasting blood glucose level (c) GTT and ITT (d) serum insulin (e) serum AST and ALT concentration of male WT (*TonEBP* $^{fl/fl}$) and myeloid specific TonEBP deficient mice (*TonEBP* $^{fl/fl}$, *LysM cre*) on a C57BL/6 background, fed either a NC or a HFD (n = 7–10 mice per group). Data (mean + s.e.m.) are representative of four independent experiments. *P < 0.05 compared to WT (*TonEBP* $^{fl/fl}$).

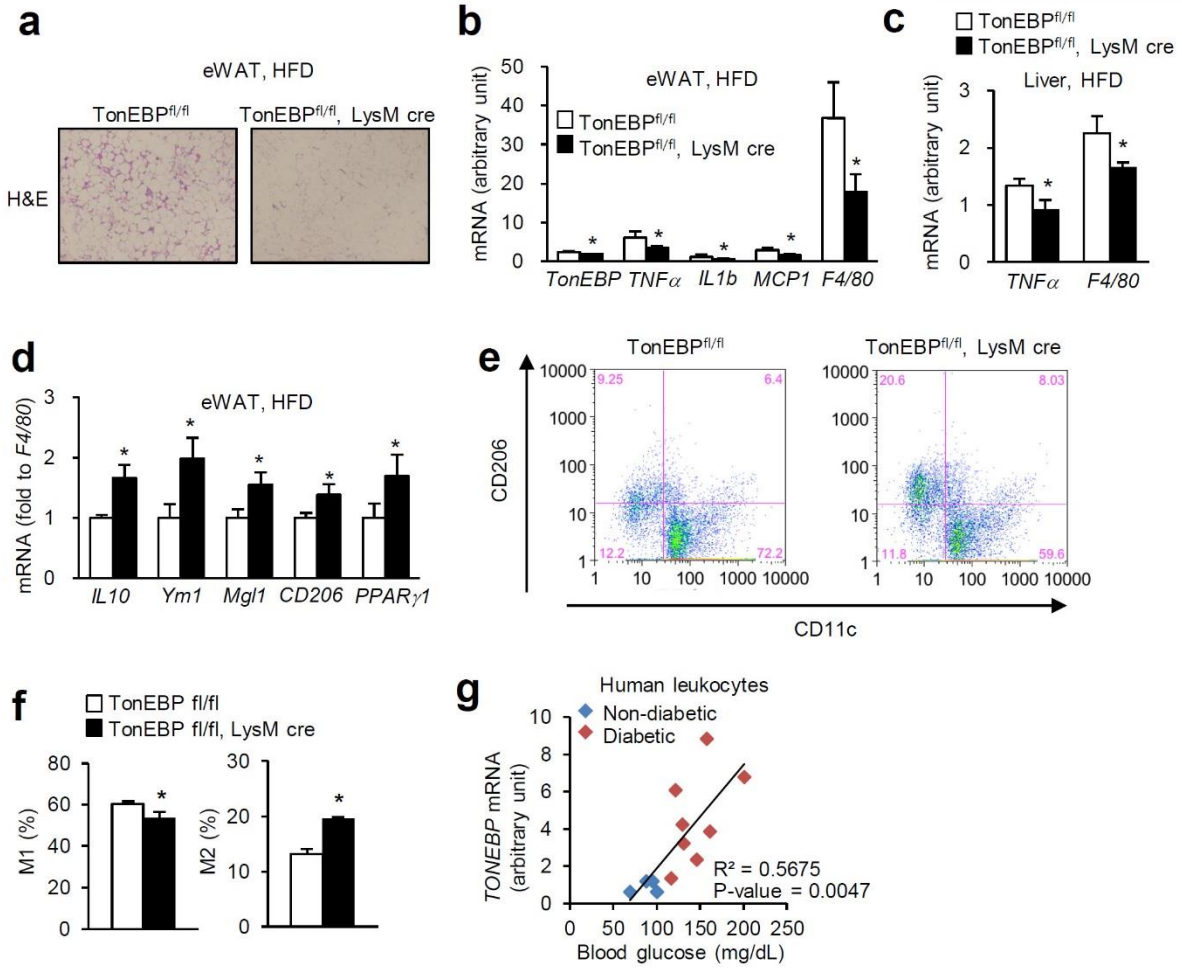

Figure 2-22. Myeloid specific TonEBP deficiency reduces adipose tissue inflammation by regulating macrophage polarization

(a) Representative images of H&E stained sections of from WT (*TonEBP* $^{fl/fl}$) and myeloid specific TonEBP deficient mice (*TonEBP* $^{fl/fl}$, *LysM Cre*) fed with HFD. (b) pro-inflammatory gene (*TNFα, IL1b, MCP1 and F4/80*) and (c) anti-inflammatory and M2 genes (*IL10, Ym1, Mgl1, CD206 and PPARγ1*) mRNA levels in eWAT from WT (*TonEBP* $^{fl/fl}$) and myeloid specific TonEBP deficient mice (*TonEBP* $^{fl/fl}$, *LysM Cre*) fed with HFD (n = 7–10). (d) pro-inflammatory gene (*TNFα and F4/80*) mRNA levels in liver. (e) Representative FACS analysis plots and (f) average percentages for M1 ($F4/80^+$ $CD11b^+$ $CD11C^+$ $CD206^-$) and M2 ($F4/80^+$ $CD11b^+$ $CD11C^-$ $CD206^+$) macrophage population in eWAT from WT (*TonEBP* $^{fl/fl}$) and myeloid specific TonEBP deficient mice (*TonEBP* $^{fl/fl}$, *LysM Cre*) fed with HFD (n = 5). (g) Human leukocyte *TONEBP* mRNA in blood from non-diabetic and diabetic human (n=12 total individuals). Data (mean + s.e.m., n = 7-10) are representative of three independent experiments. *P < 0.05 compared to *TonEBP* $^{fl/fl}$.

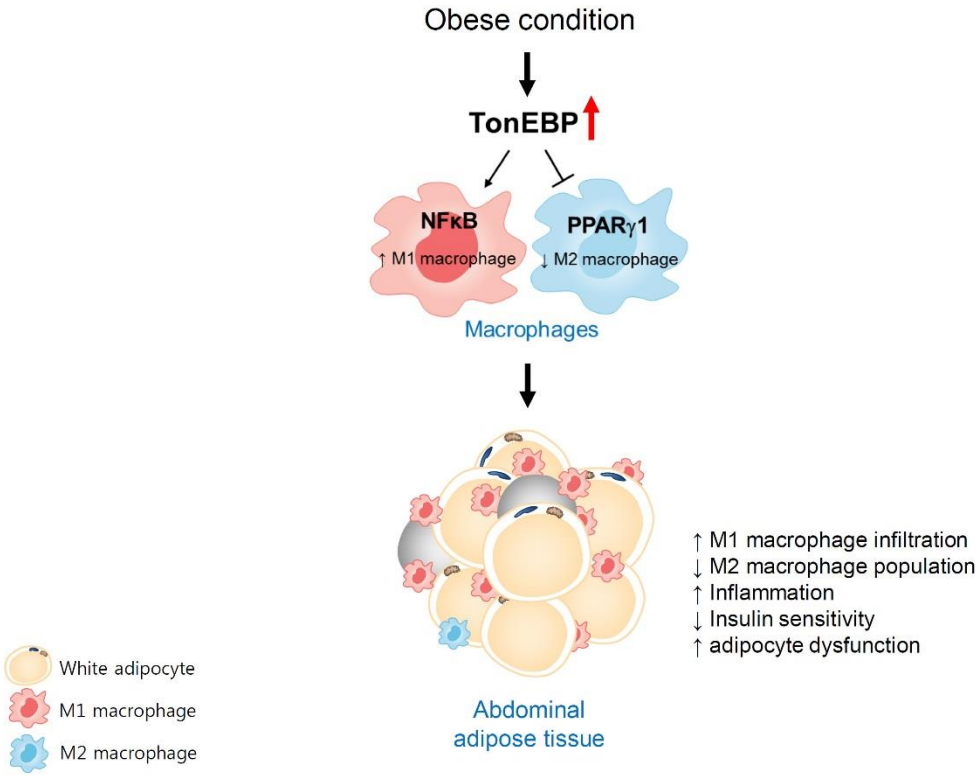

Figure 2-23. Schematic model for the role of TonEBP in obesity-induced insulin resistance

2-5. References

1. Fujisaka, S., Usui, I., Bukhari, A., Ikutani, M., Oya, T., Kanatani, Y., Tsuneyama, K., Nagai, Y., Takatsu, K., Urakaze, M., Kobayashi, M. and Tobe, K. 2009. Regulatory mechanisms for adipose tissue M1 and M2 macrophages in diet-induced obese mice. *Diabetes.* 58: 2574-2582
2. Olefsky, J.M. and Glass, C.K. 2010. Macrophages, inflammation, and insulin resistance. *Annu. Rev. Physiol.* 72: 219-246.
3. Karin, M. and Lin, A. 2002. NF-κB at the crossroads of life and death. Nat. Immunol. 3: 221-227
4. Oeckinghaus, A., Hayden, M.S. and Ghosh, S. 2011. Crosstalk in NF-κB signaling pathways. *Nat. Immunol*. 12: 695-708
5. Karin, M. and Greten, F.R. 2005. NF-κB: linking inflammation and immunity to cancer development and progression. *Nat. Rev. Immunol*. 5: 749-759
6. Richmond, A. 2002. NF-κB, chemokine gene transcription and tumour growth. *Nat. Rev. Immunol*. 2: 664-674
7. Chen, L.F. and Greene, W.C. 2004. Shaping the nuclear action of NF-κB. *Nat. Rev. Mol. Cell Biol*. 5: 392-401
8. Wan, F. and Lenardo, M.J. 2010. The nuclear signaling of NF-κB: current knowledge, new insights, and future perspectives. *Cell Res.* 20: 24-33
9. Tartey, S. and Takeuchi, O. 2015. Chromatin remodeling and transcriptional control in innate immunity: emergence of Akirin2 as a novel player. *Biomolecules.* 5: 1618-1633
10. Okamoto, T. 2006. NF-κB and rheumatic diseases. Endocr. Metab. Immune. *Disord. Drug Targets.* 6: 359-372
11. Hansson, G.K. and Hermansson, A. 2011. The immune system in atherosclerosis. *Nat. Immunol*. 12: 204-212
12. Gilmore, T.D. and Garbati, M.R. 2011. Inhibition of NF-κB signaling as a strategy in disease therapy. *Curr. Top Microbiol. Immunol.* 349: 245-263
13. Miyakawa, H., Woo, S.K., Dahl, S.C., Handler, J.S. and Kwon, H.M. 1999. Tonicity-responsive enhancer binding protein, a rel-like protein that stimulates transcription in response to hypertonicity. *Proc. Natl Acad. Sci. USA.* 96: 2538–2542
14. Lopez-Rodriguez, C., Aramburu, J., Rakeman, A.S. and Rao, A. 1999. NFAT5, a constitutively nuclear NFAT protein that does not cooperate with Fos and Jun. *Proc. Natl. Acad. Sci. USA.* 96: 7214–7219
15. Aramburu, J., Drews-Elger, K., Estrada-Gelonch, A., Minguillón, J., Morancho, B., Santiago, V. and López-Rodríguez, C. 2006. Regulation of the hypertonic stress response and other cellular functions by the Rel-like transcription factor NFAT5. *Biochem. Pharmacol*. 72: 1597–1604

16. Lee, S.D., Choi, S.Y., Lim, S.W., Lamitina, S.T., Ho, S.N., Go, W.Y. and Kwon, H.M. 2007. TonEBP stimulates multiple cellular pathways for adaptation to hypertonic stress: organic osmolyte-dependent and -independent pathways. *Am. J. Physiol Renal. Physiol.* 300: F707–715
17. Go, W.Y., Liu, X., Roti, M.A., Liu, F. and Ho, S.N. 2004. NFAT5/TonEBP mutant mice define osmotic stress as a critical feature of the lymphoid microenvironment. *Proc. Natl Acad. Sci. USA.* 101: 10673–10678
18. Buxadé, M., Lunazzi, G., Minguillón, J., Iborra, S., Berga-Bolaños, R., Del, Val. M., Aramburu, J., López-Rodríguez, C. 2012. Gene expression induced by Toll-like receptors in macrophages requires the transcription factor NFAT5. *J. Exp. Med.* 209: 379–393
19. Kim, N.H., Choi, S., Han, E.J., Hong, B.K., Choi, S.Y., Kwon, H.M., Hwang, S.Y., Cho, C.S. and Kim, W.U. 2014. The xanthine oxidase-NFAT5 pathway regulates macrophage activation and TLR-induced inflammatory arthritis. *Eur J Immunol*. 44: 2721-2736
20. Yoon, H.J., You, S., Yoo, S.A., Kim, N.H., Kwon, H.M., Yoon, C.H., Cho, C.S., Hwang, D. and Kim, W.U. 2011. NFAT5 is a critical regulator of inflammatory arthritis. *Arthritis Rheum.* 63: 1843–1852
21. Halterman, J.A., Kwon, H.M., Leitinger, N. and Wamhoff, B.R. 2012. NFAT5 expression in bone marrow-derived cells enhances atherosclerosis and drives macrophage migration. *Front. Physiol*. 3: 1–7
22. Küper, C., Beck, F.X. and Neuhofer, W. 2015. Generation of a conditional knockout allele for the NFAT5 gene in mice. *Front Physiol*. 5: 507
23. Lawrence, T. and Natoli, G. 2011. Transcriptional regulation of macrophage polarization: enabling diversity with identity. *Nat Rev Immunol*. 11: 750-761
24. Clausen, B.E., Burkhardt, C., Reith, W., Renkawitz, R. and Förster, I. 1999. Conditional gene targeting in macrophages and granulocytes using LysMcre mice. *Transgenic Res.* 8: 265-277
25. Buras, J.A., Holzmann, B. and Sitkovsky, M. 2005. Animal models of sepsis: setting the stage. *Nat Rev Drug Discov.* 4: 854-865
26. Lee, S.D., Woo, S.K. and Kwon, H.M. 2002. Dimerization is required for phosphorylation and DNA binding of TonEBP/NFAT5. *Biochem Biophys Res Commun.* 294: 967-975
27. Lee, S.D., Colla, E., Sheen, M.R., Na, K.Y. & Kwon, H.M. 2003. Multiple domains of TonEBP cooperate to stimulate transcription in response to hypertonicity. *J Biol Chem.* 278: 47571-47577
28. Hoberg, J.E., Popko, A.E., Ramsey, C.S. and Mayo, M.W. 2006. IkappaB kinase alpha-mediated derepression of SMRT potentiates acetylation of RelA/p65 by p300. *Mol Cell Biol.* 26: 457-471
29. Shakhov, A.N., Collart, M.A., Vassalli, P., Nedospasov, S.A. and Jongeneel, C.V. 1990. Kappa B-type enhancers are involved in lipopolysaccharide-mediated transcriptional activation of the tumor necrosis factor alpha gene in primary macrophages. *J Exp Med.* 171: 35-47

30. Tsai, E.Y., Falvo, J.V., Tsytsykova, A.V., Barczak, A.K., Reimold, A.M., Glimcher, L.H., Fenton, M.J., Gordon, D.C., Dunn, I.F. and Goldfeld, A.E. 2000. A lipopolysaccharide-specific enhancer complex involving Ets, Elk-1, Sp1, and CREB binding protein and p300 is recruited to the tumor necrosis factor alpha promoter in vivo. *Mol Cell Biol.* 20: 6084-6094
31. Funabashi, H., Kawaguchi, A., Tomoda, H., Omura, S., Okuda, S. and Iwasaki, S. 1989. Binding site of cerulenin in fatty acid synthetase. *J Biochem*. 105: 751-755
32. Stout, R.D., Jiang, C., Matta, B., Tietzel, I., Watkins, S.K. and Suttles, J. 2005. Macrophages sequentially change their functional phenotype in response to changes in microenvironmental influences. *J. Immunol*. 175: 342–349
33. Novak, M.L. and Koh, T.J. 2013. Macrophage phenotypes during tissue repair. *J. Leukoc. Biol*. 93: 875–881
34. Gordon, S. 2003. Alternative activation of macrophages. *Nat. Rev. Immunol*. 3: 23–35
35. Martinez, F.O., Helming, L. and Gordon, S. 2009. Alternative activation of macrophages: an immunologic functional perspective. *Annu.Rev. Immunol.* 27: 451–483
36. Mosser, D.M. and Edwards, J.P. 2008. Exploring the full spectrum of macrophage activation. *Nat. Rev. Immunol.* 8: 958–969
37. Berlato, C., Cassatella, M.A., Kinjyo, I., Gatto, L., Yoshimura, A. and Bazzoni, F. 2002. Involvement of suppressor of cytokine signaling-3 as a mediator of the inhibitory effects of IL-10 on lipopolysaccharide-induced macrophage activation. *J. Immunol.* 168: 6404–6411
38. Biswas, A., Bhattacharya, A., Kar, S. and Das, P.K. 2011. Expression of IL-10-triggered STAT3-dependent IL-4Rα is required for induction of arginase 1 in visceral leishmaniasis. *Eur. J. Immunol.* 41: 992–1003
39. Kuwata, H., Watanabe, Y., Miyoshi, H., Yamamoto, M., Kaisho, T., Takeda, K. and Akira, S. 2003. IL-10-inducible Bcl-3 negatively regulates LPS-induced TNF-alpha production in macrophages. *Blood.* 102: 4123–4129
40. Williams, L., Bradley, L., Smith, A. and Foxwell, B. 2004. Signal transducer and activator of transcription 3 is the dominant mediator of the anti-inflammatory effects of IL-10 in human macrophages. *J. Immunol.* 172: 567–576
41. de Castro, S.L., Emery, F.S. and da Silva Junior, E.N. 2013. Synthesis of quinoidal molecules: strategies towards bioactive compounds with an emphasis of lapachones. *Eur. J. Med. Chem.* 69: 678–700
42. Kung, H.N., Lu, K.S. and Chau, Y.P. 2013. The chemotherapeutic effects of lapacho tree extract: β -lapachone. *Chemotherapy.* 3: 2
43. Reinicke, K.E., Bey, E.A., Bentle, M.S., Pink, J.J., Ingalls, S.T., Hoppel, C.L., Misico, R.I., Arzac, G.M., Burton, G., Bornmann, W.G., Sutton, D., Gao, J. and Boothman, D.A. 2005. Development

of beta-lapachone prodrugs for therapy against human cancer cells with elevated NAD(P)H:quinone oxidoreductase 1 levels. *Clin. Cancer Res*. 11: 3055–3064

44. Rim, J.S., Atta, M.G., Dahl, S.C., Berry, G.T., Handler, J.S. and Kwon, H.M. 1998. Transcription of the sodium/myo-inositol cotransporter gene is regulated by multiple tonicity-responsive enhancers spread over 50 kilobase pairs in the 5'-flanking region. *J Biol Chem*. 273: 20615-20621
45. Miyakawa, H., Woo, S.K., Chen, C.P., Dahl, S.C., Handler, J.S. and Kwon, H.M. 1998. Cis- and trans-acting factors regulating transcription of the BGT1 gene in response to hypertonicity. *Am J Physiol*. 274: F753-761
46. Lee, J.H., Lee, H.H., Ye, B.J., Lee-Kwon, W., Choi, S.Y. and Kwon, H.M. 2015. TonEBP suppresses adipogenesis and insulin sensitivity by blocking epigenetic transition of PPARγ2. *Sci Rep*. 5: 10937
47. Teferedegne, B., Green, M.R., Guo, Z. and Boss, J.M. 2006. Mechanism of action of a distal NF-kappaB-dependent enhancer. *Mol Cell Biol*. 26: 5759-5770
48. Rahman, M.M. and McFadden, G. 2011 Modulation of NF-κB signalling by microbial pathogens. *Nat Rev Microbiol*. 9: 291-306
49. Glass, C.K. and Saijo, K. 2010. Nuclear receptor transrepression pathways that regulate inflammation in macrophages and T cells. *Nat Rev Immunol*. 10: 365-376
50. Yuan, M., Konstantopoulos, N., Lee, J., Hansen, L., Li, Z.W., Karin, M. and Shoelson, S.E. 2001. Reversal of obesity- and diet-induced insulin resistance with salicylates or targeted disruption of Ikkbeta. *Science*. 293: 1673-1677
51. Goldfine, A.B., Fonseca, V., Jablonski, K.A., Chen, Y.D., Tipton, L., Staten, M.A. and Shoelson, S.E. 2013. Salicylate (salsalate) in patients with type 2 diabetes: a randomized trial. *Ann Intern Med*. 159: 1-12

Chapter3. Adipocyte TonEBP promotes obesity through the suppression of WAT beiging

3-1. Introduction

The single most important variable in the pathogenesis of metabolic disease is energy balance. If energy consumption exceeds energy expenditure, weight gain and ultimately obesity result. Excess energy is stored as lipids in adipose tissue, but the unfettered expansion of adipose tissue can result in a pathological condition characterized by hypoxia and leading to insulin resistance, impaired thermogenic activity, and chronic inflammation [1-2]. Adipose tissue is also capable of transforming chemical energy into heat, thus inhibiting excessive fat accumulation, through the activity of specialized thermogenic adipocytes. In addition to the classical brown adipocytes that largely comprise brown adipose tissue, and which constitutively express thermogenic genes, 'brown-like' adipocytes, known as beige cells, are also present in white adipose tissue, and thermogenesis can be induced in these cells in response to a variety of activators [3]. Activation of the thermogenic gene program in brown or beige adipocytes increases systemic energy expenditure and can ameliorate or prevent the development of obesity-associated metabolic disorders as a result. Thus, efforts aimed at gaining a deeper understanding of the regulation of energy storage, mobilization, and use by adipocytes may lead to the identification of potential future therapies for metabolic disease [4].

TonEBP, also known as nuclear factor of activated T cells 5 (NFAT5), belongs to the Rel family of transcriptional factors including nuclear factor κB (NFκB) and NFAT1-4 [15, 6]. TonEBP has a variety of molecular and physiological functions. TonEBP was initially identified as the central DNA binding transcription factor of cellular response to hypertonic stress by regulating genes such as *BGT1, SMIT, AR* and *HSP70* [5, 7-9]. Recent studies have revealed that TonEBP act as a transcriptional co-activator in activation of NFκB and it promotes the M1 activation of macrophages and pro-inflammatory responses [10]. Consequently, TonEBP haplo-deficiency is associated with reduced inflammation leading to prevention of inflammatory and autoimmune diseases including rheumatoid arthritis [11], atherosclerosis [12] and encephalomyelitis [13] in mouse models. The more recent study showed that TonEBP inhibits adipogenesis through the suppression of PPARγ2 expression, suggesting that TonEBP is one of the key transcription factors that control adipogenesis [29]. In this regulation, TonEBP is a transcriptional co-suppressor in PPARγ2 transcription by recruiting histone methyltransferase to the promoter. These studies demonstrated that TonEBP has pleiotropic functions including DNA binding transcription factor, transcriptional co-activator and transcriptional co-repressor in inflammation and adipocyte differentiation. Inflammation and adipocyte differentiation is critical for obesity and type 2 diabetes development. However, the role of TonEBP in obesity was uncovered.

Here, we report that the expression of TonEBP in adipose tissues is required for the development of obesity and insulin resistance in mice, whereas its ablation enhances adipocyte thermogenesis and beiging, and prevents ectopic deposition of triglyceride. The substantial expression of TonEBP in the adipose tissue of obese mice and its significant association with indices of metabolic dysfunction suggest that TonEBP represents a novel target for the treatment of obesity, type 2 diabetes, and its complications.

3-2. Materials and methods

Animals

All the methods involving live mice were carried out in accordance with the approved guidelines. All experimental protocols were approved by Institutional Animal Care and Use Committee of the Ulsan National Institute of Science and Technology (UNISTACUC-12-15-A).
TonEBP haplo-deficient mice (*TonEBP+/Δ*) were described previously [5].

Mice carrying the loxP-targeted *TonEBP* gene (*TonEBP*$^{fl/fl}$) were reported previously. Transgenic mice expressing Cre recombinase under the control of *Adiponectin* (*AQ*) promoter were purchased from The Jackson Laboratory (Bar Harbor, ME, USA). *TonEBP*$^{fl/fl}$ and *LysMcre* or *AQcre* mice crossed to yield mice with specific targeted deletion of TonEBP in macrophages or adipocytes (*TonEBP*$^{fl/fl}$*, LysMcre, TonEBP* $^{fl/fl}$*, AQcre*).

For obese mice model, mice at 8 weeks age were fed with high fat diet (60% fat by kcal) or normal-chow diet (10% fat by kcal) during 16 weeks. Mice were intraperitoneally injected with RG108 (Cayman, 12 mg/kg every 2 days) before feeding with high fat diet.

Cells and reagents

Pre-adipocyte cell line 3T3-L1 cells and macrophage cell line RAW264.7 cells were cultured in Dulbecco's Modified Eagle's Medium (DMEM) containing 10% fetal bovine serum (FBS; Thermo fisher scientific Inc, Waltham, MA, USA) and penicillin/streptomycin (100U/ml and 100μg/ml; GE healthcare life sciences, Logan, UT, USA). For induction of adipocyte differentiation, adipogenesis inducing medium (AIM) including 1μM dexamethasone, 0.5 mM isobutylmethylxanthine, and 1μM insulin, 125 μM indomethacin and 1 nM Triiodothyronine (T3) was used as described [14]. Cells were maintained at 37℃ in incubator with 5% CO_2. Cells were treated with isoproterenol (Sigma Aldrich, USA) for 4h after adipocyte differentiation. Anti-Adrb3 (Abcam, Cambridge, UK), anti-Hsc70 (Rockland, Gilbertsville, PA, USA) and anti-TonEBP antibody [5] were used for immunoblotting.

Human adipocytes samples

Adipocyte RNA of subcutaneous abdominal adipose tissue from 15 Saudi Arabian subjects were obtained from the Obesity Research Center at the College of Medicine of King Saud University, Riyadh, Saudi Arabia. The experiments were approved by the College of Medicine Ethics Committee, King Saud University. Total RNA was isolated using the TRIzol reagent (Invitrogen, Carlsbad, CA, USA) according to the manufacturer's instructions. cDNA was synthesized by M-MLV reverse transcriptase (Promega, Madison, WI, USA). After reverse transcription, real time PCR was performed using SYBR Green I Master and LightCycler 480 II (Roche, Rotkreuz, Switzerland).

Measured cycle threshold (Ct) values were normalized with 36B4 and they were expressed as fold-over control samples.

Transfection

When the cells grow at the 70% of confluence, cells were transfected for 48 h with TonEBP siRNA or control scrambled siRNA (10nM) and miR-negative control, miR-30b or miR-30c (100nM) using lipofectamine RNAiMAX (Invitrogen, Carlsbad, CA) following the manufacturer's instructions.

Isolation and differentiation of preadipocytes

Preadipocytes were isolated from inguinal white adipose tissue obtained from 4-weeks-old animals. Inguinal white adipose tissue were minced in DMEM/F12 medium and digested with 10 ml HEPES buffer containing 1mg/ml type II collagenase. They were incubated at 37˚C with gentle shaking for 1 hr. After incubation, 10 ml of DMEM/F12 were added and they were centrifuged at 500g for 15 min. Stromal vascular cells (SVCs) were incubated with 5ml of RBC lysis buffer (Sigma) for 5 min at room temperature and then they were filtered with a 40μm filter after addition of 10ml of DMEM/F12. After centrifugation at 500g for 5 min, SVCs were differentiated to adipocyte with AIM.

Immunoblot assay

Cell were washed two times with cold PBS and lysed in RIPA buffer (0.01M Tris, pH7.4, 0.15M NaCl, 0.001M EDTA, 0.001M EGTA, 1% Triton X-100, 0.002M PMSF and protease inhibitor (roche)). After centrifugation of lysate, supernatant was used for immunoblot assay. Protein concentration was measured by BCA protein assay system (Pierce, Rockford, IL, USA). Equal amounts of protein from each sample were separated by SDS-PAGE and immunoblotted using specific primary antibodies. HRP-conjugated mouse, rabbit and goat secondary antibodies were used for detection. The antigen-antibody binding was detected by enhanced chemiluminescence Western blotting detection reagents (GE healthcare life sciences).

RNA isolation and real-time PCR

Total RNA was isolated using the TRIzol reagent (Invitrogen, Carlsbad, CA, USA) according to the manufacturer's instructions. cDNA was synthesized by M-MLV reverse transcriptase (Promega, Madison, WI, USA). After reverse transcription, real time PCR was performed using SYBR Green I Master and LightCycler 480 II (Roche, Rotkreuz, Switzerland). Measured cycle threshold (Ct) values were normalized with cyclophilin A or 36B4 and they were expressed as fold-over control samples.

Metabolic analysis

Fasting blood glucose, body weight and food intake were measured weekly, and body composition was measured using a quantitative nuclear magnetic resonance system (EchoMRI100V; Echo Medical Systems, Houston, TX, USA). Oxygen consumption, carbon dioxide production, heat production and locomotor activity were monitored using Comprehensive Lab Animal Monitoring System (CLAMS; Columbus Instruments, Columbus, OH, USA). Mice were given an orally injection of D-glucose (2 g/kg body weight) after overnight starvation for the glucose tolerance test (GTT) and were intra-peritoneally injected with insulin (0.75U/kg body weight) for insulin tolerance test (ITT). Serum glucose levels were determined in tail blood samples using a glucometer. Body temperatures were measured using a digital thermometer (TD-300; Shibaura Electronics, Tokyo, Japan)

Nuclear and cytoplasmic fractionation

Cells were harvested by using scrapper and centrifugation at 500 g. The cell pellet was washed by suspension with PBS. The cell nucleus and cytoplasm were separated by using Nuclear and Cytoplasmic extraction kit (Pierce) according to manufacturer's instruction. Nuclear fraction was confirmed by Lamin B.

Electromobility shift assay

EMSA assay were performed using Lightshift Chemiluminescent EMSA kit (Pierce). 5 μg of nuclear extracts were incubated with poly(dI:dC), binding buffer and 5' biotinylated DNA (5'-CAATTTGGAAAAATTTTGACT -3' for TonEBP binding site on *Adrb3* promoter) at room temperature for 20 min. Samples were separated by electrophoresis for 4 h in 4% (40% 29:1 acrylamide/bis solution) gel for TonEBP. The detection was performed according to manufacturer's instructions.

Immunoprecipitation assay

Cell lysates (10-500μg) were prepared using RIPA buffer in a tube on ice. Antibody (1-5μg) was added to cell lysate and they were incubated for overnight at 4℃ under rotary agitation. 40μl of protein A/G agarose beads (GE healthcare) was added and incubated for 2 hr at 4℃ under rotary agitation. The bead-antibody-antigen complex was spin downed by centrifugation at 4℃ for 1min and removed supernatant. The complex was washed for 10 min by RIPA buffer at 4℃ and it was repeated with three times. After wash, 40μl of sample buffer was added and boiled at 95℃ for 5min and centrifugated with top speed for 1min at room temperature. The samples were transferred to new tube and analyzed by immunoblotting.

Chromatin immunoprecipitation assay

Cells were grown in 10 cm diameter culture dishes and with LPS when indicated. Fixation was performed with 1% formaldehyde at room temperature for 10 min. The fixation was stopped with 0.125 M glycine for 5 min at room temperature. After three washes with cold PBS, cells were collected and lysed in 1 ml of SDS lysis buffer (1% SDS, 10 mM EDTA and 50 mM Tris-HCl pH 8.1) for 10 min on ice. Cell lysates were sonicated (Bioruptor KRB-01, BMS, Tokyo, Japan) for six cycles of 20 s on plus 30 s off with constant frequency and maximum intensity to obtain DNA fragments between 400 and 1,000 bp. Each sample was diluted 10× in dilution buffer (0.01% SDS, 1.1 % Triton X-100, 1.2 mM EDTA, 16.7 mM Tris-HCl pH 8.1 and 167 mM NaCl) for immunoprecipitation. Samples were pre-cleared with protein A Sepharose beads (Millipore, Bedford, MA, USA) that were previously pre-adsorbed with salmon sperm DNA for 1 h at 4℃. Specific antibodies were added after removing the pre-clearing beads: anti-PolII IgG (Pierce), and normal rabbit IgG (Abcam, Cambridge, UK), anit-TonEBP serum, and normal rabbit serum (Merck millipore, Darmstadt, Germany). After adding antibodies, the lysates were incubated overnight at 4℃. Protein A Sepharose beads were then added, incubated for 2 h at 4℃, and then washed with low salt washing buffer (0.1% SDS, 1% Triton X-100, 20 mM Tris-HCl pH 8.1, 2 mM EDTA, and 10 mM NaCl), high salt washing buffer (0.1% SDS, 1% Triton X-100, 20 mM Tris-HCl pH 8.1, 2 mM EDTA and 500 mM NaCl), LiCl washing buffer (0.25 M LiCl, 1% NP-40, 1% deoxycholic acid, 1 mM EDTA and 10 mM Tris-HCl pH 8.1) and twice with final washing buffer (10 mM Tris-HCl pH 8.0 and 1 mM EDTA). To elute the DNA, beads were incubated with elution buffer (1% SDS and 100 mM NaHCO3) for 20 min at 65 ℃. To reverse the cross-linking, samples were incubated overnight at 65℃ 200 mM NaCl, 30 min at 37℃ with 50 μg/ml RNase (Pierce) and 2 hr at 45°C with 100 μg/ml proteinase K. DNA was purified using the QIAGEN PCR purification system. DNA was then subjected to RT-qPCR using primers; 5'-GACAACTCATGGAGCAGTCTT -3' and 5'- CTTACTTACTGTGCCATCTCCC -3' for *Adrb3* promoter. Immunoprecipitated DNA from each sample was normalized to its respective chromatin input.

Luciferase assay

Cells were transfected with either a TonE-driven Photinus luciferase plasmid or an adrb3 promoter 6kb-driven luciferase plasmid in pGL4.74 (hRluc/TK, Promega). The Renilla luciferase reporter plasmid (pRL-TK, Promega) was used as a control for transfection efficiency. Luciferase activity was measured using the Dual-Luciferase Assay System (Promega) according to the manufacturer's instructions. Luciferase activity was normalized by activity of renilla luciferase.

ELISA

Leptin and adiponectin in serum from mice were analyzed by ELISA using a commercial kit (R&D Systems*). Insulin was analyzed by ELISA using a commercial kit (Alpco, Salem, N*H, USA).

Lipid analysis

Triacylglycerol (TG), free fatty acid (FFA) and cholesterol level in serum was measured using TG, FFA or cholesterol quantification kit (Abcam) according to manufacturer's instructions.

MNase accessibility assay by qPCR

MNase accessibility assay by q-PCR was performed using micrococcal nuclease (MNase) described as previously with minor modification50. Washed cells were lysed in cold NP-40 lysis buffer (10 mM Tris-HCl (pH 7.4), 10 mM NaCl, 3 mM MgCl2, 0.5% NP-40, 0.15mM spermine (Sigma), 0.5 mM spermidine(Sigma)), followed by incubation on ice for 5 min. Nuclei were pelleted by centrifuge at 5000 rpm for 3 min at 4˚C and resuspended with MNase digestion buffer without CaCl2 (10 mM Tris-HCl (pH 7.4), 15 mM NaCl, 60 mM KCl, 0.15 mM spermine, 0.5 mM spermidine). After centrifugation, the nuclei were resuspended with MNase digestion buffer supplemented with CaCl2. Then, half of the each sample was treated MNase with 5 unit/sample and the other half of that was treated digestion buffer, and samples were incubated at 37˚C for 1 min. The digestion reaction was stopped by addition of stop solution (100mM EDTA/10mM EGTA (pH 8.1) in 10 mM Tris-HCl (pH 7.4)). RNaseA (10μg/sample) and proteinase K (100μg/sample) were added and samples were incubated at 37˚C overnight. DNA, purified by Phenol/chloroform/isoamyl alcohol extraction, was analyzed by q-PCR using primer pairs covering near -1.8kb region of the *Adrb3* promoter. Chromatin accessibility was calculated from (amount of PCR product in undigested sample) / (amount of PCR product in digested sample).

DNA methylation analysis using bisulfite sequencing

DNA was purified by DNA purification kit (Qiagen). Bisulfite conversion was performed using EpiTect Bisulfite Kit (Qiagen). After conversion, *Adrb3* promoter region was amplified by PCR using primers designed by Methprimer software (www.urogene.org/methprimer/index1.html). Amplified DNA was cloned into bacteria by TOPO TA cloning kit (Invitrogen). Plasmid from each clone was sequenced by Macrogen commercial services.

Statistical analysis

Data are presented as means + s.d. or + s.e.m. Statistical significance ($p < 0.05$) was estimated by student's t-test. All statistics was performed with GraphPad Prism 5.0 software (GraphPad, San Diego, CA, USA).

3-3. Results

3-3-1. Adipose TonEBP expression increases in obesity

It was previously reported that TonEBP is expressed in many tissues. However, we found that TonEBP expression in inguinal white adipose tissue (iWAT) is very low in lean mice (Fig. 3-1). Interestingly, TonEBP mRNA and protein expression was significantly upregulated in iWAT and epididymal white adipose tissue (eWAT) of male mice fed a high fat diet (HFD; 60% energy as fat) for 16 weeks, compared with control mice fed a normal chow diet (NC; 10% energy as fat) (Fig. 3-2a and b). Similarly, TonEBP mRNA expression was higher in iWAT from 16-week-old leptin receptor mutant db/db ($Lepr^{db/db}$) obese mice (Fig. 3-2c). In addition, HFD-fed mice exhibited lower mRNA expression of the thermogenic genes *PPARGC1A* (encoding PPARγ coactivator 1α (PGC1-α)), *Dio2*, *CPT1α, Cidea, PPARα*, and *Adrb3*, and of markers of beiging (*UCP-1*, *CD137*, and *TMEM26*), in iWAT (Fig. 3-2d and e). Subcutaneous adipose *TONEBP* mRNA expression also correlated with the body mass index (BMI) of a group of subjects from Saudi Arabia (Fig. 3-2f). Together, these data suggest that adipose TonEBP expression is associated with obesity-induced metabolic dysfunction, including impaired thermogenic function.

3-3-2. TonEBP haplo-deficient mice are resistant to the development of diet-induced obesity

To study the physiological role of TonEBP, TonEBP haplo-deficient mice and wild-type (WT) littermates were fed either a NC or HFD for up to 15 weeks, starting at 8 weeks of age. The homozygous TonEBP-deficient mice died soon after birth. The haplo-deficient mice on the NC showed a similar weight gain to WT mice (Fig. 3-3a) but those on the HFD were resistant to weight gain (Fig. 3-3a and b). Food intake was similar between the groups (Fig. 3-3c). To further assess the body composition changes accompanying this decrease in body mass, a whole body echo MRI analysis was performed. The lower body mass of TonEBP haplo-deficient mice after 8 weeks on a HFD was accounted for a reduction in fat mass, without an alteration in body length or lean body mass (Fig. 3-3d). Accordingly, the haplo-deficient mice exhibited lower masses of inguinal, epididymal, and dorsal fat pads (Fig. 3-3e), indicating resistance to diet-induced obesity. We also observed that TonEBP haplo-deficient mice on a $Lepr^{db/db}$ background were relatively protected against weight gain and adiposity compared with WT mice (Fig. 3-4a and b).

3-3-3. Adipocyte TonEBP suppresses thermogenesis and beiging of WAT

A reduction of adipose tissue weight without an alteration in food intake (Fig. 3-3e) suggested a potential increased energy expenditure by TonEBP haplo-deficient mice. The measurement of oxygen consumption (VO_2) and carbon dioxide production (VCO_2) over 72 h (including both light and dark phases) showed higher consumption rates in the haplo-deficient mice (Fig. 3-5a and b). Consistent

with the higher VO_2, the haplo-deficient mice generated more heat (Fig. 3-5c) and had a ~0.6℃ higher body temperature (Fig. 3-5d). In addition, their body temperature remained higher even in a cold environment (4℃) for up to 6 h (Fig. 3-5e), suggesting enhanced adaptive thermogenesis and energy expenditure.

Reduced thermogenesis is a characteristic feature of obesity in humans and mice [20]. We examined whether TonEBP affects adipose thermogenic and beige marker gene expression. As expected, we found an upregulation of thermogenic genes, such as *PGC1-α, Dio2*, and *Cidea* (Fig. 3-6a), and beige marker genes, such as uncoupling protein-1 (*UCP-1*), *CD137*, and *TMEM26*, in iWAT (Fig. 3-6b) from TonEBP haplo-deficient mice. Furthermore, assay of iWAT from haplo-deficient mice exposed to a cold environment revealed a significant upregulated the expression of these genes, and of UCP-1 protein (Fig. 3-6c), consistent with the observations made under ambient conditions. Histological and immunohistochemical analysis of iWAT revealed features of beiging WAT, including multilocular lipid droplets and higher expression of UCP-1 by adipocytes (Fig. 3-6d).

Consistent with the in vivo data, enhanced basal and β3 adrenergic agonist (isoproterenol)-stimulated expression of thermogenic genes and hormone-sensitive lipase (HSL) was observed in TonEBP haplo-deficient primary adipocytes differentiated from the stromal vascular fraction and in 3T3-L1 cells transfected with small interfering RNA (siRNA) targeting TonEBP (Fig. 3-6e and 3-7a). In addition, after adipocyte differentiation, adenovirus-mediated overexpression of TonEBP reduced basal and isoproterenol-stimulated expression of these genes (Fig. 3-7b). These findings indicate that TonEBP deficiency promotes energy expenditure through the activation of thermogenesis and beiging of WAT in adipocytes.

3-3-4. TonEBP haplo-deficient mice resist obesity-induced insulin resistance and metabolic dysfunction

We next assessed glucose homeostasis and insulin sensitivity in HFD-fed WT and haplo-deficient mice. TonEBP haplo-deficient mice maintained lower fasting glucose levels than WT mice between weeks 1 and 15 of HFD feeding (Fig. 3-8a) and showed improved glucose tolerance and insulin sensitivity in glucose (GTT) and insulin (ITT) tolerance tests (Fig. 3-8b). After 15 weeks of HFD feeding, the haplo-deficient mice showed lower serum fasting glucose and insulin concentrations than WT controls (Fig. 3-8c). Furthermore, TonEBP haplo-deficient $Lepr^{db/db}$ obese mice had lower blood glucose levels than WT mice (Fig. 3-8d). To confirm the effect of TonEBP deficiency on insulin sensitivity, we injected HFD-fed mice with insulin and found that Akt activation was significantly enhanced in the eWAT and liver of haplo-deficient mice (Fig. 3-8e).

In addition to its role in lipid storage, adipose tissue also functions as an endocrine organ, secreting a large number of polypeptide hormones, termed adipokines, which can modify systemic glucose

homeostasis and insulin sensitivity. We measured serum adipokine levels in the haplo-deficient mice and showed that levels of the anti-diabetic adipokine adiponectin [15] were significantly higher in haplo-deficient mice on the HFD (Fig. 3-9a, left). Consistent with this, *adiponectin* mRNA expression was higher in HFD-fed haplo-deficient mice than in WT mice (Fig. 3-9a, right). Levels of serum leptin, a pro-diabetic adipokine, are positively correlated with increasing adiposity [16]. Serum leptin level remained low in the HFD-fed haplo-deficient mice (Fig. 3-9b, left), while *leptin* mRNA levels were lower in HFD haplo-deficient mice than in WT mice (Fig. 3-9b, right). These data indicate that TonEBP deficiency led to an adipokine profile favoring maintenance of insulin sensitivity. Histological analysis revealed significantly lower lipid accumulation in brown adipose tissue and smaller adipocyte size in iWAT from HFD-fed haplo-deficient mice (Fig. 3-9c), indicating that TonEBP deficiency leads to healthier adipocyte morphology as a result of lower triglyceride accumulation, possibly due to an increased rate of lipolysis. In addition, eWAT contained significantly fewer crown-like structures, lower macrophage infiltration, and lower expression of the inflammatory cytokine tumor necrosis factor α (TNFα) in HFD-fed haplo-deficient mice (Fig. 3-9d and e). In eWAT, obesity-induced inflammatory responses resulted in adipocyte dysfunction, characterized by lower expression of genes involved in lipid metabolism (Fig. 3-9f), but expression of these genes was restored in TonEBP haplo-deficient mice (Fig. 3-9g).

Chronic exposure of mice to a HFD causes fatty liver (steatosis) and increased liver mass [19]. Both C57/BL6 and $Lepr^{db/db}$ mice haplo-deficient for TonEBP had lower liver mass than WT mice (Fig 3-10a and 3-10b). TonEBP haplo-deficient mice also had smaller lipid droplets in their hepatocytes and a lower serum alanine aminotransferase (ALT) concentration than WT mice (Fig. 3-10c and d).

HFD-fed haplo-deficient mice did not show high fasting serum cholesterol (total and low density lipoprotein (LDL)) levels, and these were thus lower than those of WT mice (Fig. 3-11). Consistent with increased expression of the key lipolytic enzyme, *HSL*, in haplo-deficient mice (discussed below), serum triglyceride concentration was lower, but there was no difference from controls in serum free fatty acid (FFA) concentration (Fig. 3-11).

These data suggest that TonEBP is a critical factor that mediates the detrimental effects of HFD-induced obesity, such as altered serum adipokine secretion, deleterious plasma lipid profile, hepatic steatosis and insulin resistance.

3-3-5. TonEBP suppresses *Adrb3* gene expression in isolated adipocytes

Stimulation of β3-adrenergic receptor (Adrb3) signaling increases thermogenesis and HSL-mediated lipolysis, leading to reduced fat mass [21]. Interestingly, we found that the HFD-mediated reduction in expression of *Adrb3* is restored in the iWAT of TonEBP haplo-deficient mice (Fig. 3-12a). Furthermore, there was a trend towards higher expression of Adrb3 in the iWAT of haplo-deficient mice exposed to a cold environment (Fig. 3-12b). Consistent with the in vivo study, *Adrb3* expression was increased in primary adipocytes isolated from the haplo-deficient mice (Fig. 3-12c). Its expression was also higher in both basal and isoproterenol-stimulated TonEBP-silenced 3T3-L1 cells (Fig. 3-12d) and lower in 3T3-L1 cells overexpressing TonEBP (Fig. 3-12e). These data demonstrate that TonEBP downregulates Adrb3 expression in adipocytes.

We next investigated the molecular basis of this TonEBP-mediated *Adrb3* gene suppression. First, we constructed a pGL3 luciferase reporter vector by inserting a 5.9 kb promoter sequence from the mouse *Adrb3* gene (Fig. 3-13a). TonEBP knockdown stimulated *Adrb3* promoter-driven luciferase expression in 3T3-L1 adipocytes (Fig. 3-13b). Next, because the mouse Adrb3 promoter contains one putative TonEBP consensus binding sequence (Fig. 3-13a), we investigated whether TonEBP bound to this putative binding site in 3T3-L1 cells using an electrophoretic mobility shift assay, and found that it did (Fig. 3-13c). To confirm this interaction, we performed chromatin immunoprecipitation in WT and TonEBP-silenced 3T3-L1 cells. Fragments of the *Adrb3* promoter containing the TonEBP binding sites were precipitated using a TonEBP antibody, and this was reduced by TonEBP knockdown (Fig. 3-13d).

Next, we evaluated the chromatin accessibility in the promoter region by analyzing sensitivity to micrococcal nuclease. Chromatin accessibility was enhanced by TonEBP knockdown at both the TonEBP binding region (region A in the *Adrb3* promoter) and the transcription start site (TSS) region (the B and C region of the *Adrb3* promoter) (Fig. 3-14a).

We further confirmed TonEBP-mediated transcriptional inhibition at the Adrb3 promoter by showing higher RNA polymerase II binding at the Adrb3 promoter in TonEBP knockdown adipocytes (Fig. 3-14b). A recent study reported that DNA methylation is associated with insulin resistance and thermogenic gene regulation. TonEBP deficiency in iWAT and 3T3-L1 reduced DNA methylation in the B and C region of the *Adrb3* promoter, demonstrated using bisulfite sequencing (Fig. 3-14c and d). Among the DNA methyltransferases, we found that DNA methyltransferase 1 (DNMT1) was recruited to the Adrb3 promoter through its interaction with TonEBP (Fig. 3-15a and b). Taken together, these findings suggest that TonEBP is recruited to the *Adrb3* promoter as a transcriptional repressor.

3-3-6. DNMT inhibition enhances Adrb3 expression and beiging of WAT

To elucidate the potential role of DNA methylation in WAT beiging, we used RG108, which is a DNMT inhibitor. When mice were intraperitoneally injected with RG108 (12 mg/kg every 2 days), they resisted HFD-induced gains in body mass (Fig. 3-16a and b), fat mass (Fig. 3-16b and c), and fasting glucose (Fig. 3-16d). Consistent with the in vitro data, RG108-injected mice demonstrated higher energy expenditure (Fig. 3-17a-c), resistance to the cold (Fig. 3-17d), and enhanced beiging of WAT (Fig. 3-71e and f). Treatment of adipocytes with RG108 enhanced *UCP-1* and *Adrb3* expression in a dose-dependent manner, without affecting expression of TonEBP (Fig. 3-17g). Since RG108 inhibits all of the DNMTs, we examined whether DNMT1 specifically regulated the expression of *UCP-1* and *Adrb3* and *Adrb3* promoter activity by silencing DNMT1 expression using siRNA in adipocytes. The protein and mRNA expression of *UCP-1* and *Adrb3*, and *Adrb3* promoter activity, were reduced by DNMT1 knockdown (Fig. 3-18a and b). These data show that DNMT1-induced DNA methylation suppresses the beiging of WAT and its effects on energy expenditure.

3-3-7. miR-30 promotes thermogenesis in adipocytes by targeting TonEBP

miRs inhibit translation or induce target mRNA degradation by base-pairing to recognition sites [24, 25]. The microRNA-30 (miR-30) family are potent regulators of thermogenesis in adipocytes [22], and miR-30 is downregulated in obese mice [23]. Using prediction program in TargetScan Mouse 6.2 (www.targetscan.org), we found that *TonEBP* is a potential target gene for miR-30, possessing two binding sites for miR-30b and miR-30c in its 3' UTR (Fig. 3-19a). *TonEBP* mRNA and protein expression was significantly reduced in 3T3-L1 adipocytes transfected with miR-30b and miR-30c mimics (Fig. 3-19b). Consistent with this, miR-30b and miR-30c mimic administration enhanced mRNA expression of thermogenic genes (Fig. 3-19c). These data suggest that miR-30b and miR-30c would suppress TonEBP expression in lean mice, while in obese mice TonEBP expression would increase as a result of the lower levels of miR-30b and miR-30c, resulting in lower expression of thermogenic genes.

3-3-8. Adipocyte-specific TonEBP knockout mice have a similar phenotype to TonEBP haplo-deficient mice

To further investigate the specific role of adipocyte TonEBP in thermogenesis and in the development of obesity in response to HFD feeding, we generated adipocyte-specific knockout mice (AKO) using the Cre-lox system (*TonEBP* $^{fl/fl}$*; adiponectin* promoter driven-Cre). As controls, floxed TonEBP mice that did not express Cre recombinase were used (*TonEBP* $^{fl/fl}$; WT). Both WT and AKO mice were fed a HFD for up to 12 weeks, starting at 8 weeks of age. The AKO mice were resistant to the development of obesity and showed lower fasting glucose levels than WT mice, with no difference

in food intake (Fig. 3-20a). In addition, the AKO mice demonstrated higher O_2 consumption and CO_2 production rates (Fig. 3-20b and c) and generated more heat (Fig. 3-20d), also illustrated by having a higher body temperature than controls (Fig. 3-20e), suggesting enhanced energy expenditure. These mice also showed higher mRNA expression of *Adrb3* and thermogenic genes, such as *UCP-1*, in iWAT, similar to the expression profile identified in the haplo-deficient mice, when either HFD-fed (Fig. 3-20f) or cold-exposed (Fig. 3-20g). These data further confirm that an absence of TonEBP in adipocytes enhances thermogenic activity and beiging of WAT.

3-4. Discussion

Adipose tissues have received a lot of attention since as it has become clear that adipocytes and macrophages in them are important integrators of diverse physiological pathways regulating systemic insulin sensitivity and energy homeostasis [26]. It is therefore urgently necessary to identify regulatory convergence points that can be therapeutic targets to improve insulin resistance and impaired energy homeostasis in obesity.

Here, we report for the first time that TonEBP is a critical suppressor of thermogenesis and beiging in WAT. TonEBP expression is specifically increased in iWAT in response to HFD feeding. Moreover, genetic TonEBP deficiency increased expression of beige adipocyte markers and genes involved in thermogenesis in this tissue. In addition, TonEBP haplo-deficient mice were resistant to cold exposure, establishing TonEBP as a central regulator of WAT thermogenesis.

Understanding the molecular basis of the functional plasticity of adipocytes in obesity is essential to identify novel biomarkers and therapeutic targets for the development of anti-obesity and anti-diabetic drugs. Although altered DNA methylation patterns are associated with adipocyte differentiation and obesity, the significance and exact molecular mechanisms involved in these have not been identified. Our findings show that the effect of TonEBP deficiency on the beiging of white adipocytes is mediated in part through suppression of Adrb3 expression by DNMT1-induced DNA methylation. TonEBP deficiency promotes chromatin opening and recruitment of RNA polymerase II through a reduction in DNA methylation in the *Adrb3* promoter region. There is growing evidence for an involvement of epigenetic mechanisms in the development of complex diseases like obesity and type 2 diabetes [30, 31]. Thus, elucidating the role and mechanisms involved in DNA methylation is important to enhance understanding of obesity, considering the crucial role of the former in gene expression and chromatin architecture. In particular, DNA methylation provides a tissue-specific gene regulatory system, capable of controlling transcription factor accessibility and the recruitment of co-repressors or co-activators to chromatin. Indeed, a previous study demonstrated that TonEBP acts as a transcriptional repressor of adipocyte differentiation by blocking epigenetic transition [14].

miRNAs showed regulatory roles in many biological processes including fat metabolism, adipocyte differentiation and insulin action associated with obesity and type 2 diabetes [27, 28]. Recent studies show that miRNA expression is dysregulated in obese adipose tissue [29]. The miR-30 family are potent regulators of thermogenesis and beiging of WAT [22]. Interestingly, we found that independently reducing expression of miR-30b and miR-30c increased the expression of TonEBP, indicating that TonEBP is a target of both miR-30b and miR-30c. Our data suggest that suppression of TonEBP is an important mechanism whereby miR-30b and miR-30c regulate thermogenic gene expression.

In summary, we identified a new transcriptional regulator, TonEBP, which is capable of simultaneously regulating multiple processes including inflammation and thermogenesis, and thus regulating adiposity and energy homeostasis. The importance of this mechanism is further highlighted by the extremely low expression of TonEBP in WAT from lean mice and the higher TonEBP expression in obese mice, implying a central role for TonEBP in the promotion of insulin resistance and obesity (Fig. 3-14). The phenotypes generated by ablation of TonEBP suggest that TonEBP has a potent cell-autonomous effect to inhibit WAT beiging and insulin resistance. Our findings imply that TonEBP is an excellent candidate drug target for the stimulation of beiging in WAT during obesity, and may therefore be utilized to design future therapeutics for the treatment of obesity, type 2 diabetes, and other diseases characterized by insulin resistance.

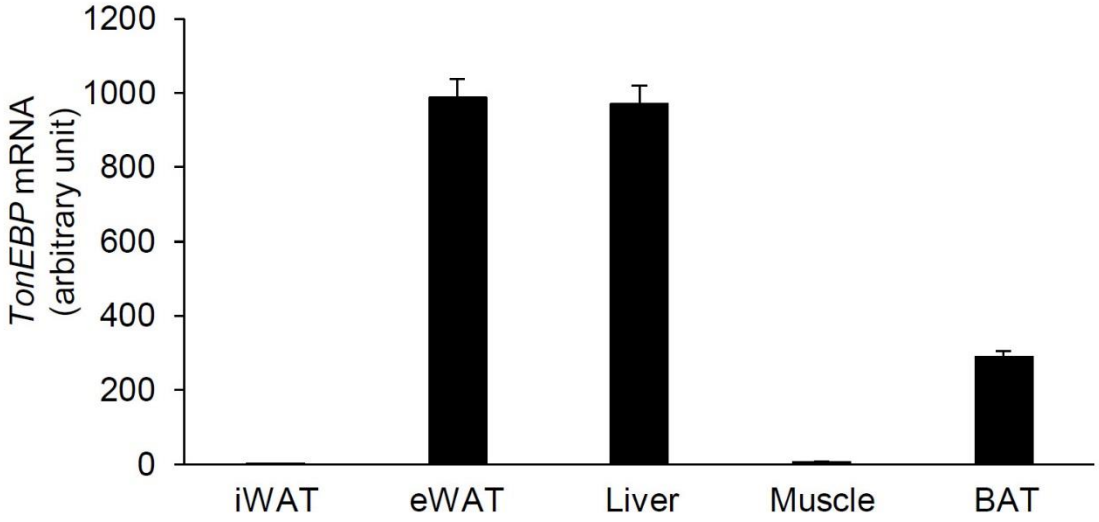

Figure 3-1. *TonEBP* mRNA expression in metabolic tissues.

TonEBP mRNA levels in eWAT, iWAT, BAT, muscle, and liver from C57BL/6J mice (n = 5–7 mice per group). Data (mean + s.e.m.) are representative of three independent experiments.

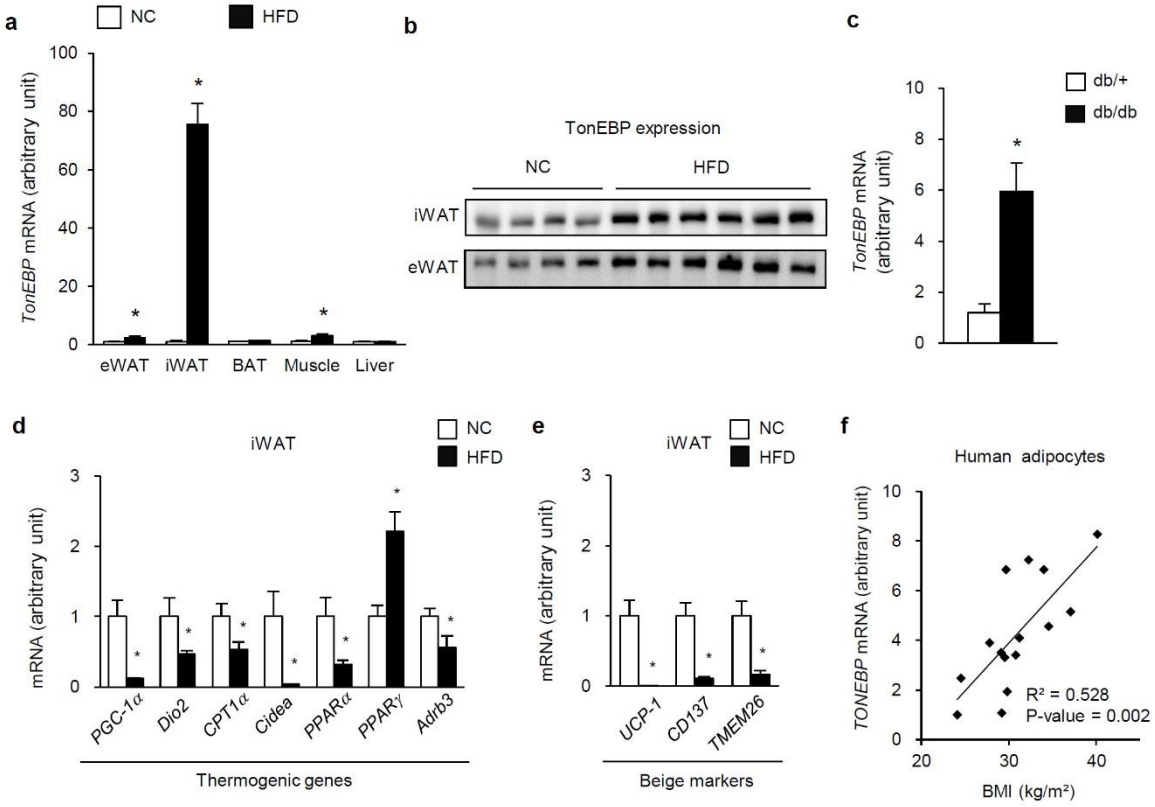

Figure 3-2. Adipocyte TonEBP expression was induced in obesity

(a) *TonEBP* mRNA levels in eWAT, iWAT, BAT, muscle, and liver from C57BL/6J mice fed a NC or a HFD (n = 5–7 mice per group). (b) TonEBP protein level in iWAT and eWAT. (c) *TonEBP* mRNA levels in iWAT from C57BL/6J mice on *+/db* or *db/db* (n = 5–7 mice per group). (d) Thermogenic genes and (e) beige marker genes mRNA level in iWAT from C57BL/6J mice fed a NC or a HFD (n = 5–7 mice per group). (f) Correlation of human adipocyte *TONEBP* mRNA level in subcutaneous fat from Saudi Arabian people with a range of BMIs (n = 15). All data are representative of four independent experiments and presented as mean + s.e.m. * $p < 0.05$ vs. HFD or *db/db* determined using Student's t test.

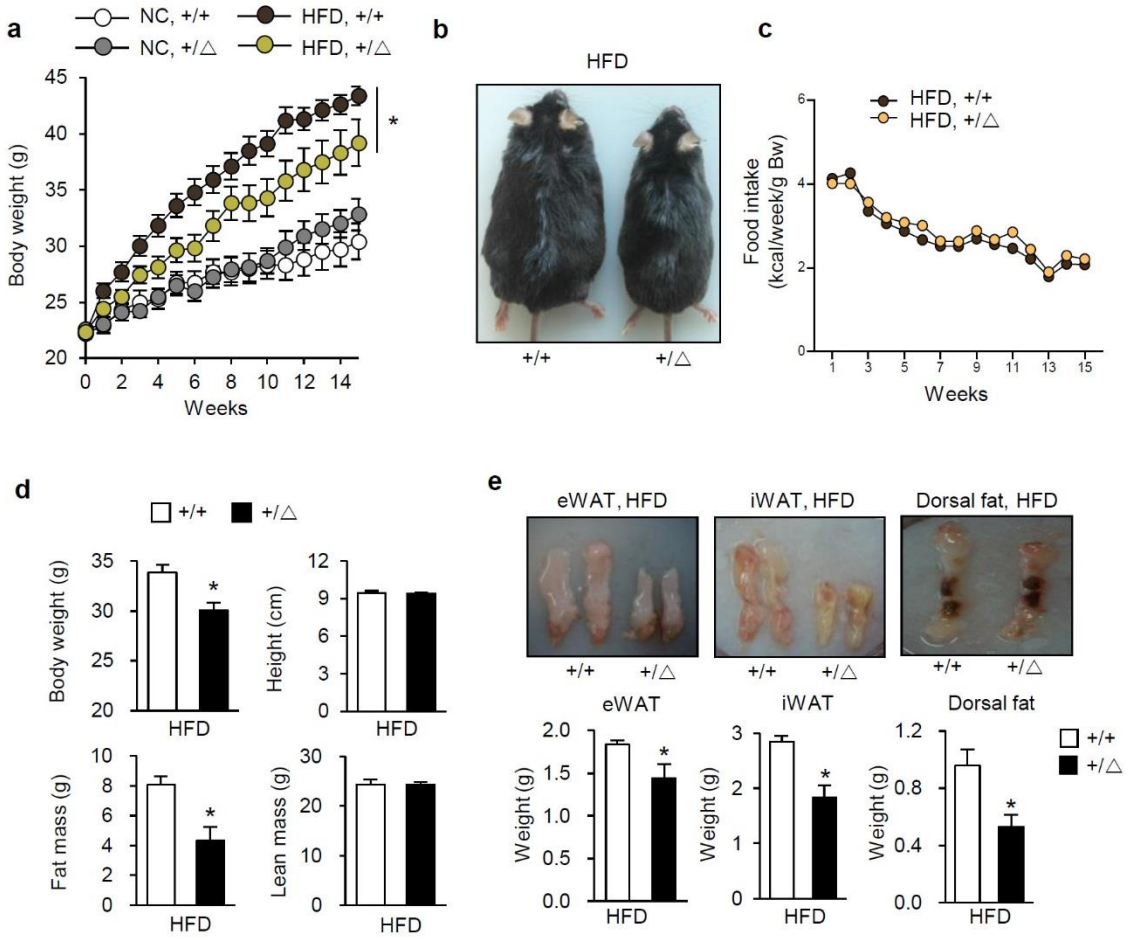

Figure 3-3. TonEBP haplo-deficient mice resist the development of obesity

(a) Body weights of male WT (*TonEBP* +/+) and TonEBP haplo-insufficient (*TonEBP +/Δ*) mice on a C57BL/6 background, fed either a NC or a HFD (n = 7–10 mice per group). (b) Representative photographs of HFD-fed *TonEBP* +/+ and *+/Δ* mice. (c) Food intake was measured in TonEBP haplo-deficient mice fed with HFD (n = 5–7 mice per group). (d) Body composition and length of HFD-fed male *TonEBP* +/+ and *+/Δ* mice determined by echo MRI (n = 8 mice per group). (e) Representative photographs and weights of fat pads (epididymal, inguinal, and dorsal). All data are representative of four independent experiments and presented as mean + s.e.m. * $p < 0.05$ vs. *TonEBP* +/+, determined using Student's t test.

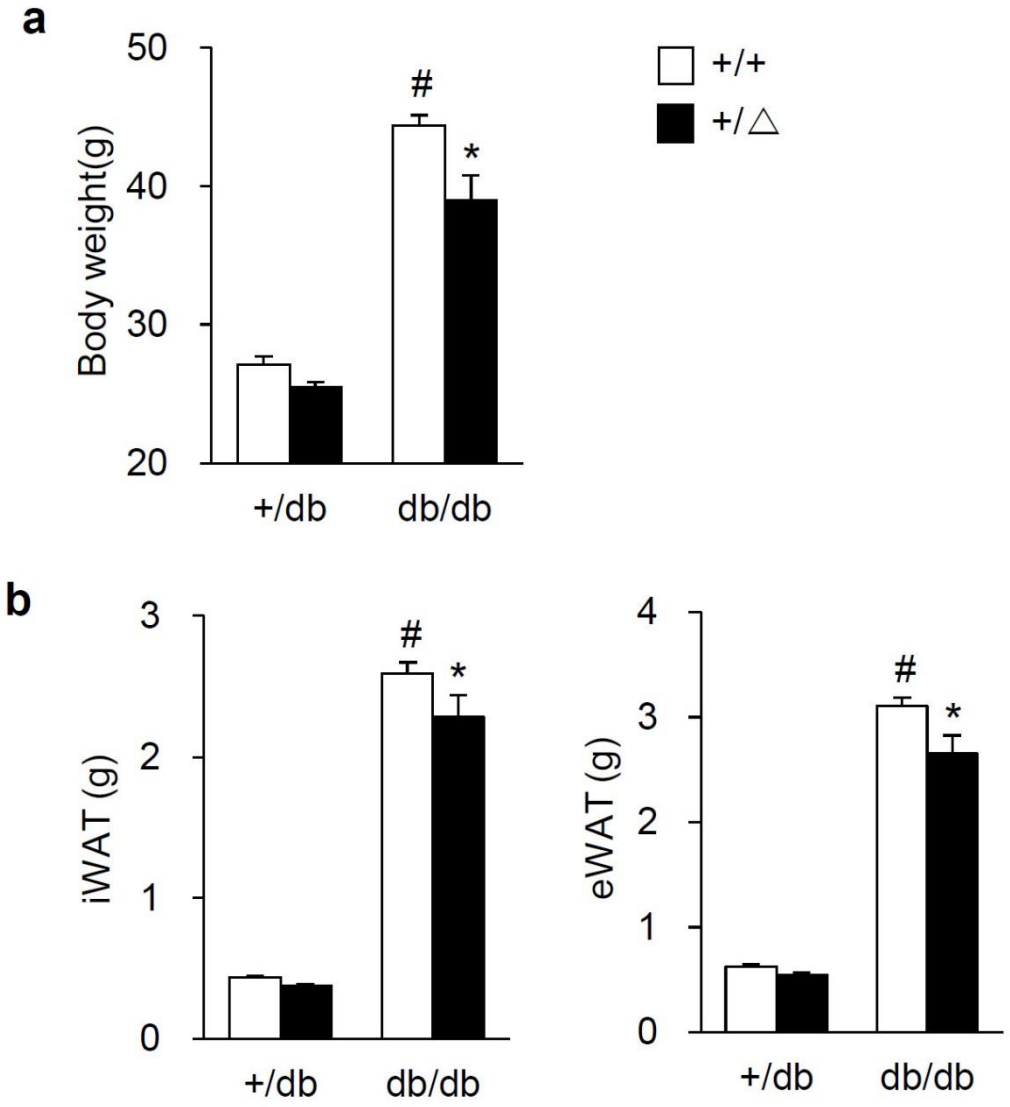

Figure 3-4. TonEBP deficiency protects obesity in *db/db* mice

(a) Body weight of male WT (*TonEBP* +/+) and TonEBP haplo-insufficient (*TonEBP +/Δ*) mice on a C57BL/6 background on *+/db* or *db/db* (n = 7–10 mice per group). (b) Weights of fat pads. All data are representative of two independent experiments and presented as mean + s.e.m. # $p < 0.05$ vs. *+/db* and * $p < 0.05$ vs. *TonEBP* +/+, determined using Student's t test

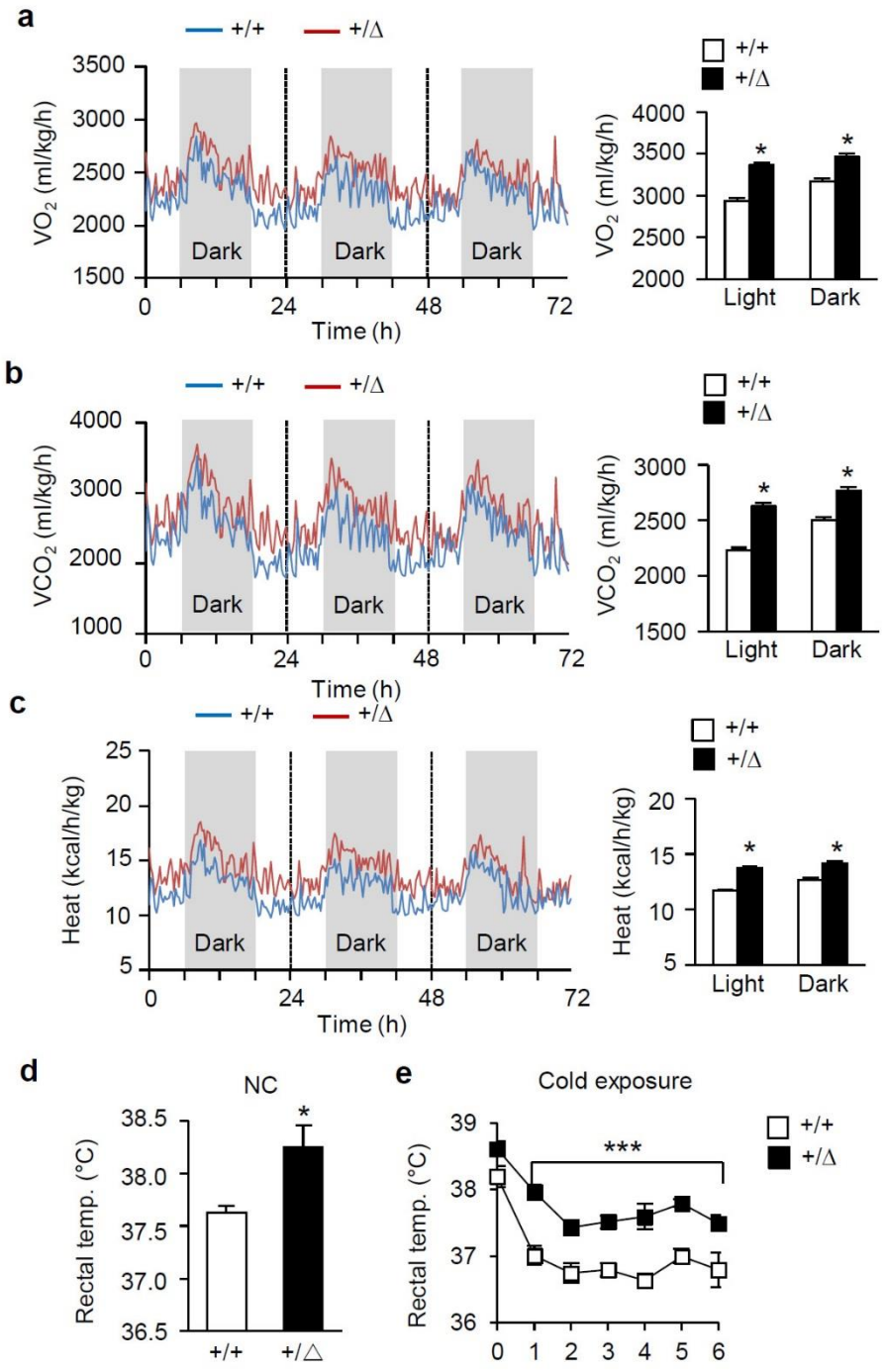

Figure 3-5. TonEBP deficiency promotes energy expenditure

(a-c) (a)VO_2, (b) VCO_2, and (c) heat production analyzed by indirect calorimetry in HFD-fed *TonEBP* +/+ and *+/Δ* mice (n = 6 mice per group). (d and e) Rectal temperature (temp) measured in NC-fed *TonEBP* +/+ and *+/Δ* mice at (d) room temperature and after (e) cold exposure (4℃) (n = 6 mice per group). All data are representative of three independent experiments and presented as mean + s.e.m. * $p < 0.05$ vs. *TonEBP* +/+ determined by Student's t test.

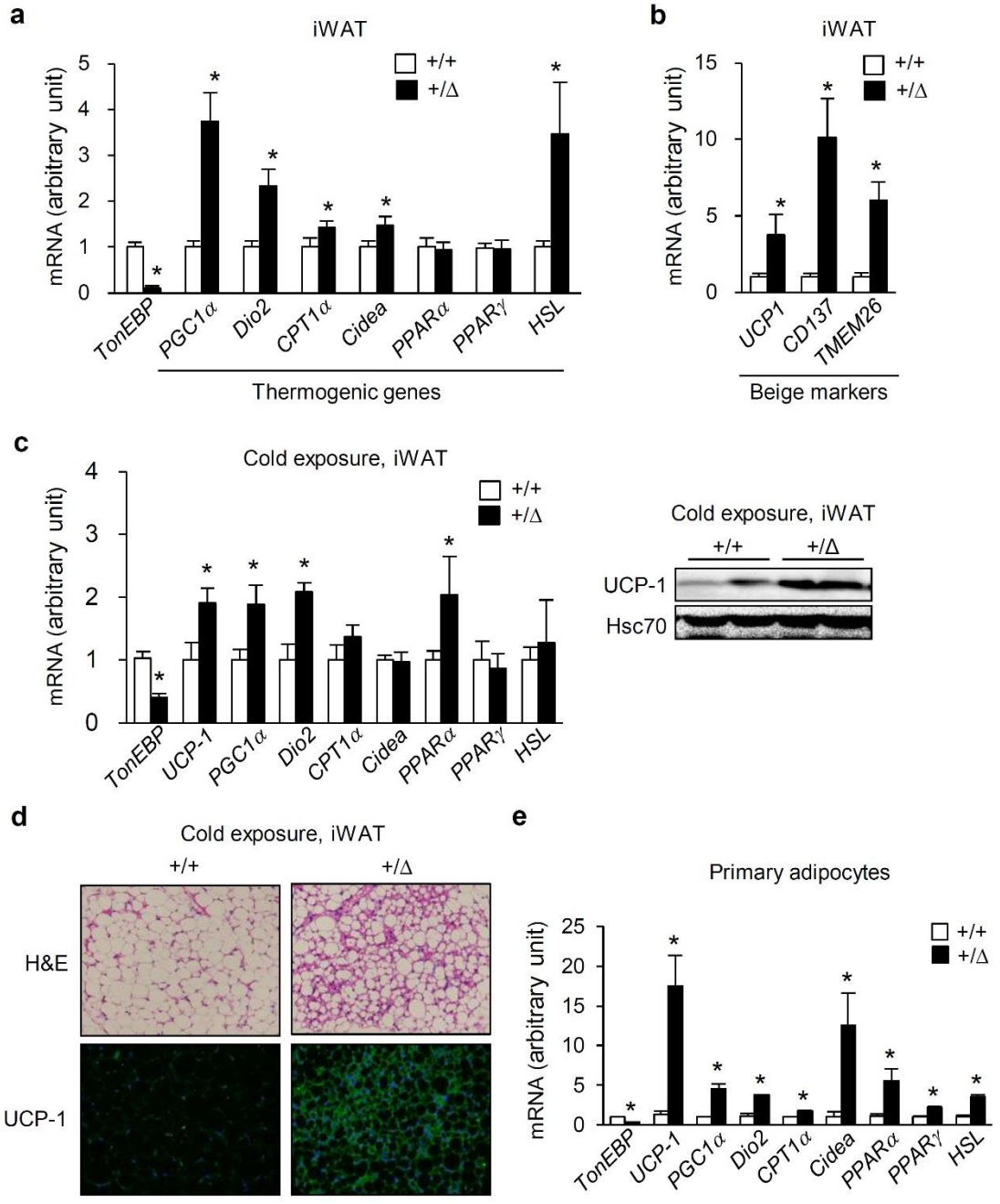

Figure 3-6. TonEBP deficiency enhances thermogenesis and beiging of WAT

(a and b) (a) Thermogenic gene and (b) beiging marker gene mRNA expression in iWAT of HFD-fed *TonEBP* +/+ or *+/Δ* mice (n = 6 mice per group). (c) Thermogenic gene mRNA (left) and UCP-1 protein level (right) in iWAT of TonEBP +/+ or +/Δ mice exposed to cold (4°C) (n = 10 mice per group). (d) Representative images of H&E and UCP-1 stained iWAT from WT or TonEBP haplo-deficient TonEBP mice exposed to cold (4℃). (e) Thermogenic gene mRNA levels in primary adipocytes differentiated from the stromal vascular fraction of *TonEBP* +/+ or *+/Δ* mice (n = 4). All data are presented as mean + s.e.m. * $p < 0.05$ vs. *TonEBP* +/+ determined by Student's t test.

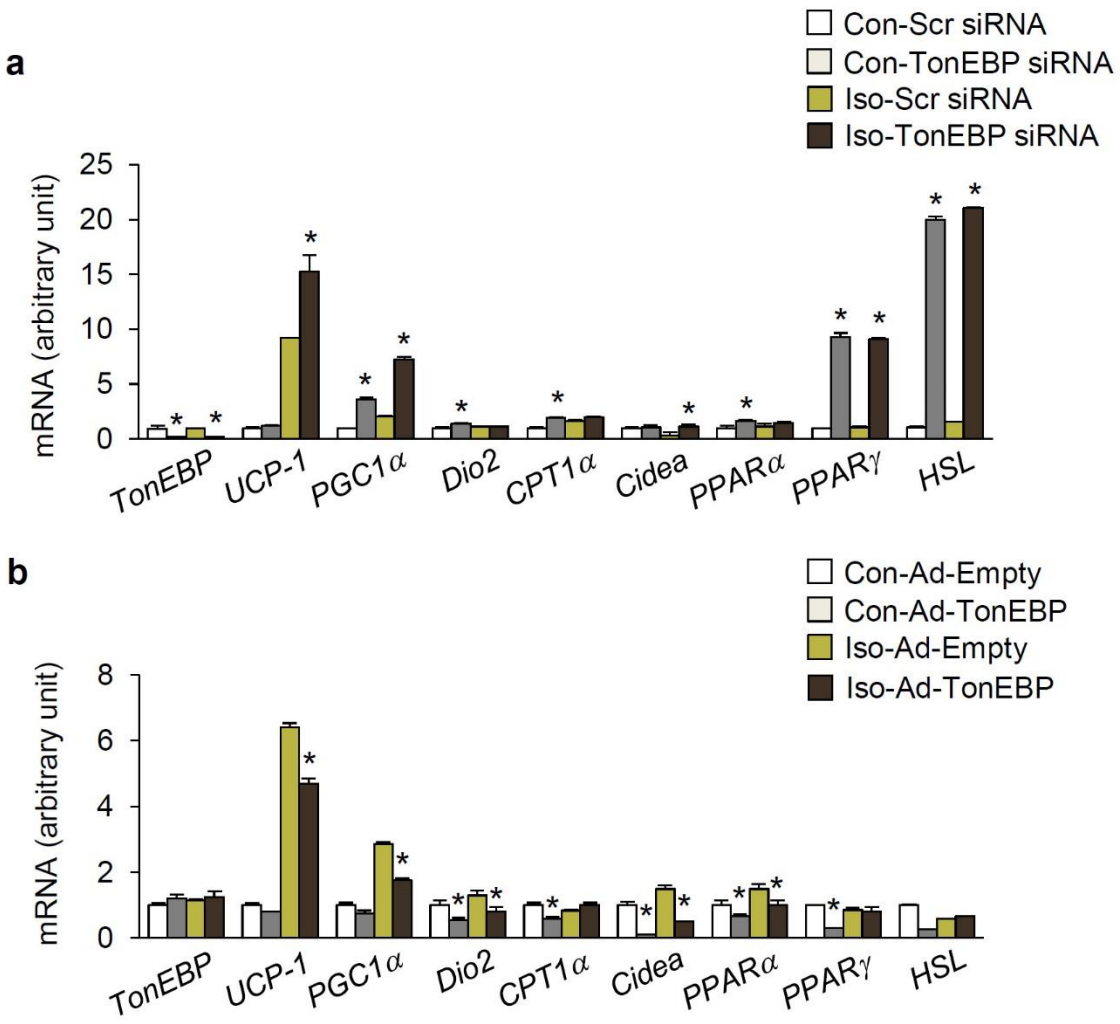

Figure 3-7. Effects of TonEBP knockdown or overexpression on thermogenic gene expression in 3T3-L1 cells

(a) Thermogenic gene mRNA on siRNA-mediated TonEBP knockdown (siTonEBP) and (b) adenovirus-mediated TonEBP overexpression (AdTonEBP) in 3T3-L1 stimulated with or without isoproterenol (Iso) (n = 4). All data are representative of four independent experiments and presented as the mean + s.d. *$p<0.05$ vs. scr siRNA or Ad-Empty determined by Student's t test.

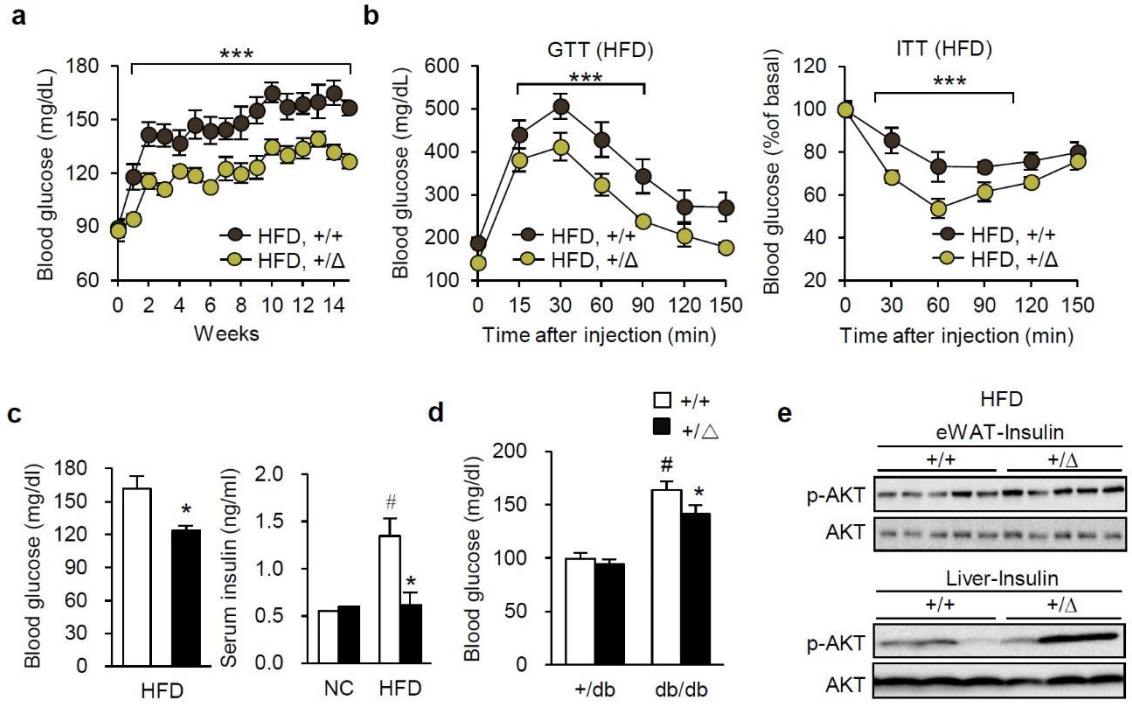

Figure 3-8. TonEBP deficiency ameliorates obesity-induced insulin resistance

(a) Fasting blood glucose level in serum from HFD-fed *TonEBP* +/+ and *+/Δ* mice (n = 7–10 mice per group). (b) Glucose tolerance (left) and insulin tolerance (right) test data for *TonEBP* +/+ and *+/Δ* mice after 9 weeks of HFD feeding. (c) Fasting blood glucose (left) and insulin (right) level in serum from HFD-fed *TonEBP* +/+ and *+/Δ* mice. (d) Fasting blood glucose level of male *TonEBP* +/+ and TonEBP haplo-insufficient *TonEBP +/Δ* mice on a C57BL/6 background on *+/db* or *db/db* (n = 7–10 mice per group). (e) Phosphorylation of AKT in eWAT and liver after insulin injection. All data are representative of two or three independent experiments and presented as mean + s.e.m. # $p < 0.05$ vs. NC or *+/db*, * $p < 0.05$ vs. *TonEBP* +/+ determined by Student's t test.

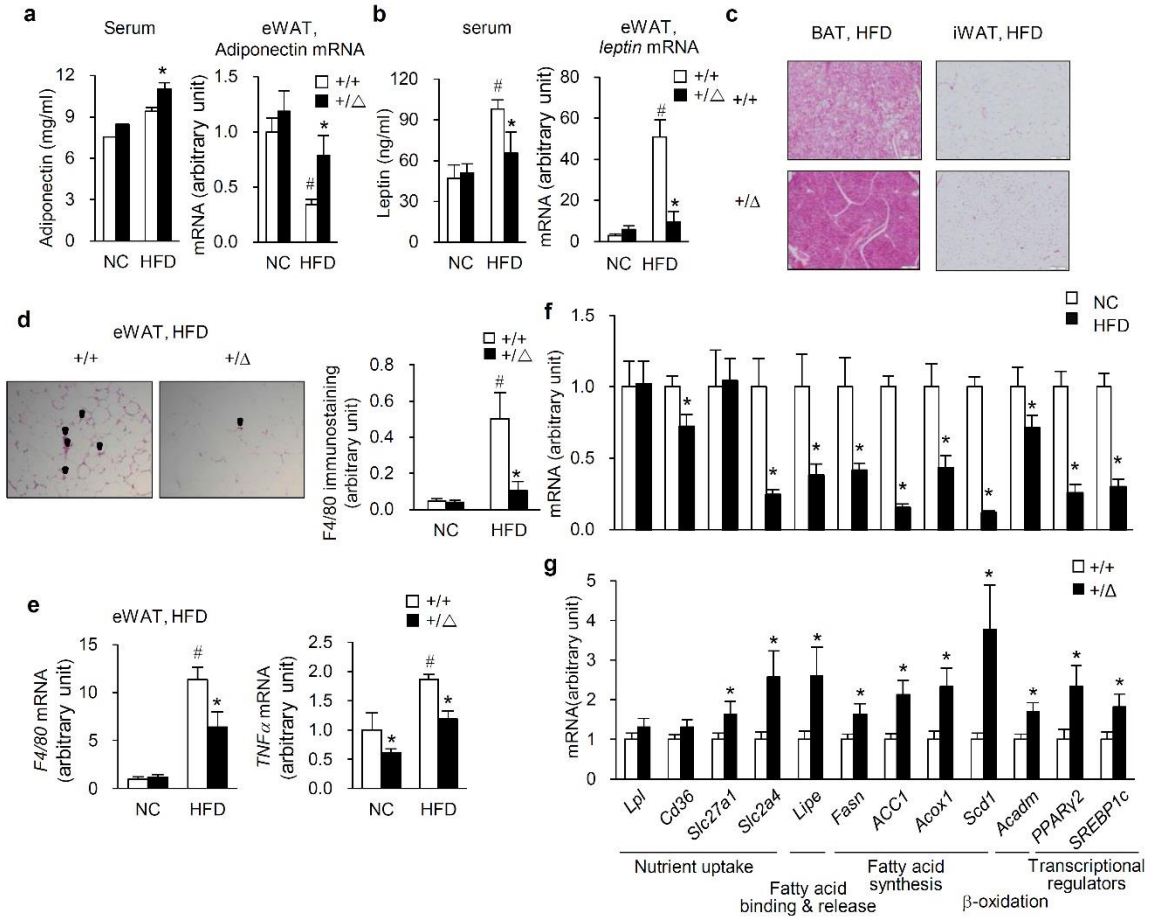

Figure 3-9. TonEBP deficiency ameliorates obesity-induced metabolic dysfunction

(a and b) (a) Serum concentration and iWAT mRNA expression of adiponectin and (b) leptin in *TonEBP* +/+ and *+/Δ* mice fed a HFD. (c and d) (c)Representative images of H&E stained sections of BAT and iWAT and (d) H&E staining and F4/80 immunostaining of eWAT from *TonEBP* +/+ and *+/Δ* mice fed a HFD. (e) *F4/80* and *TNFα* mRNA levels in eWAT from HFD-fed *TonEBP* +/+ and *+/Δ* mice (n = 7–10). (f) Adipocyte function related genes mRNA levels in iWAT from C57BL/6J mice fed a NC or a HFD (n = 5–7 mice per group). (g) mRNA levels of adipocyte function related gene in eWAT from HFD-fed *TonEBP* +/+ and *+/Δ* mice (n = 7–10). All data are representative of three independent experiments and presented as mean + s.e.m. # $p < 0.05$ vs. NC, * $p < 0.05$ vs. *TonEBP* +/+ or NC determined by Student's t test.

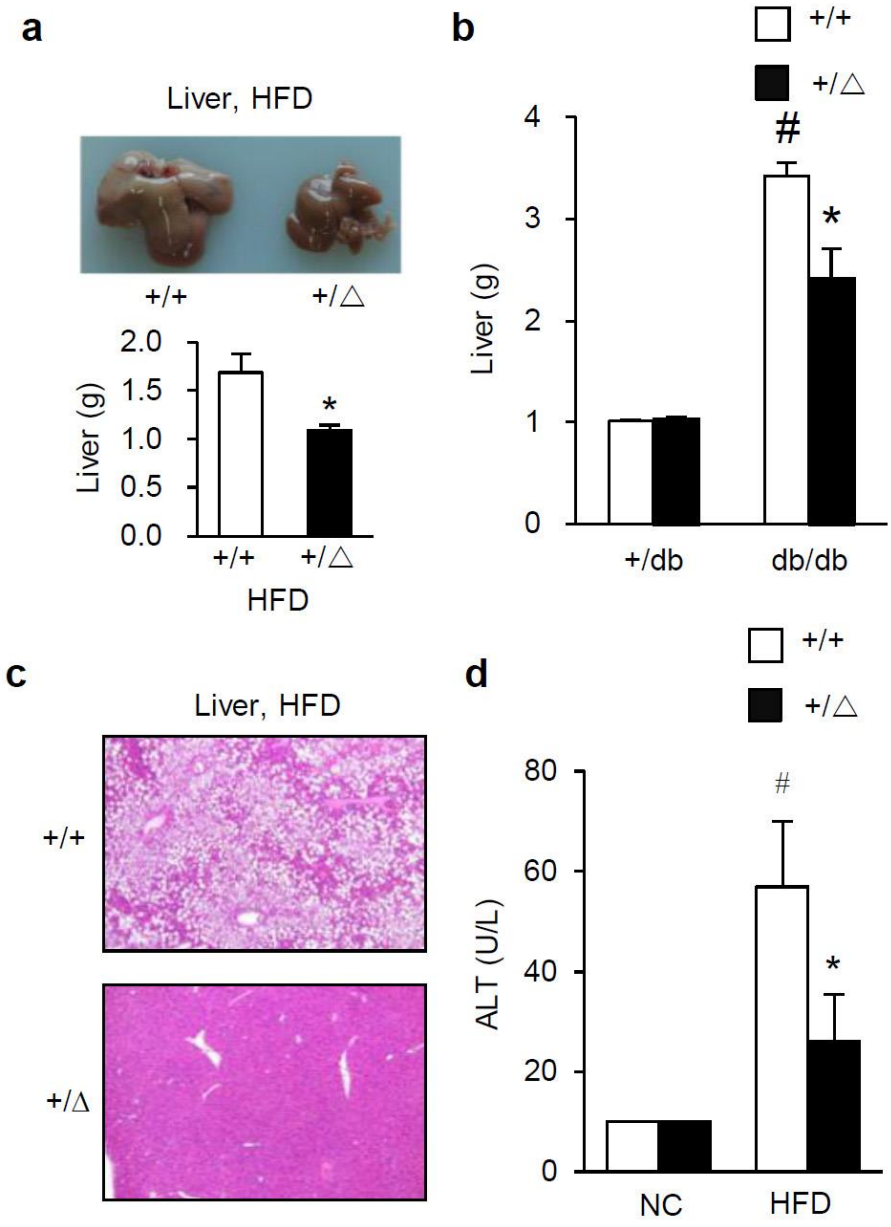

Figure 3-10. TonEBP deficiency protects fatty liver in obesity

(a) Representative images and mass of liver from HFD-fed *TonEBP* +/+ and *+/Δ* mice. (b) Weight of liver of male *TonEBP* +/+ and *TonEBP +/Δ* mice on a C57BL/6 background on *+/db* or *db/db* (n = 7–10 mice per group). (c) Representative images of H&E stained sections of liver from *TonEBP* +/+ and *+/Δ* mice fed with a HFD. (d) ALT concentration in serum from *TonEBP* +/+ and *+/Δ* mice fed a HFD. All data are representative of four independent experiments and presented as mean + s.e.m. # $p < 0.05$ vs. NC, *TonEBP* +/+ * $p < 0.05$ vs. *TonEBP* +/+ determined by Student's t test.

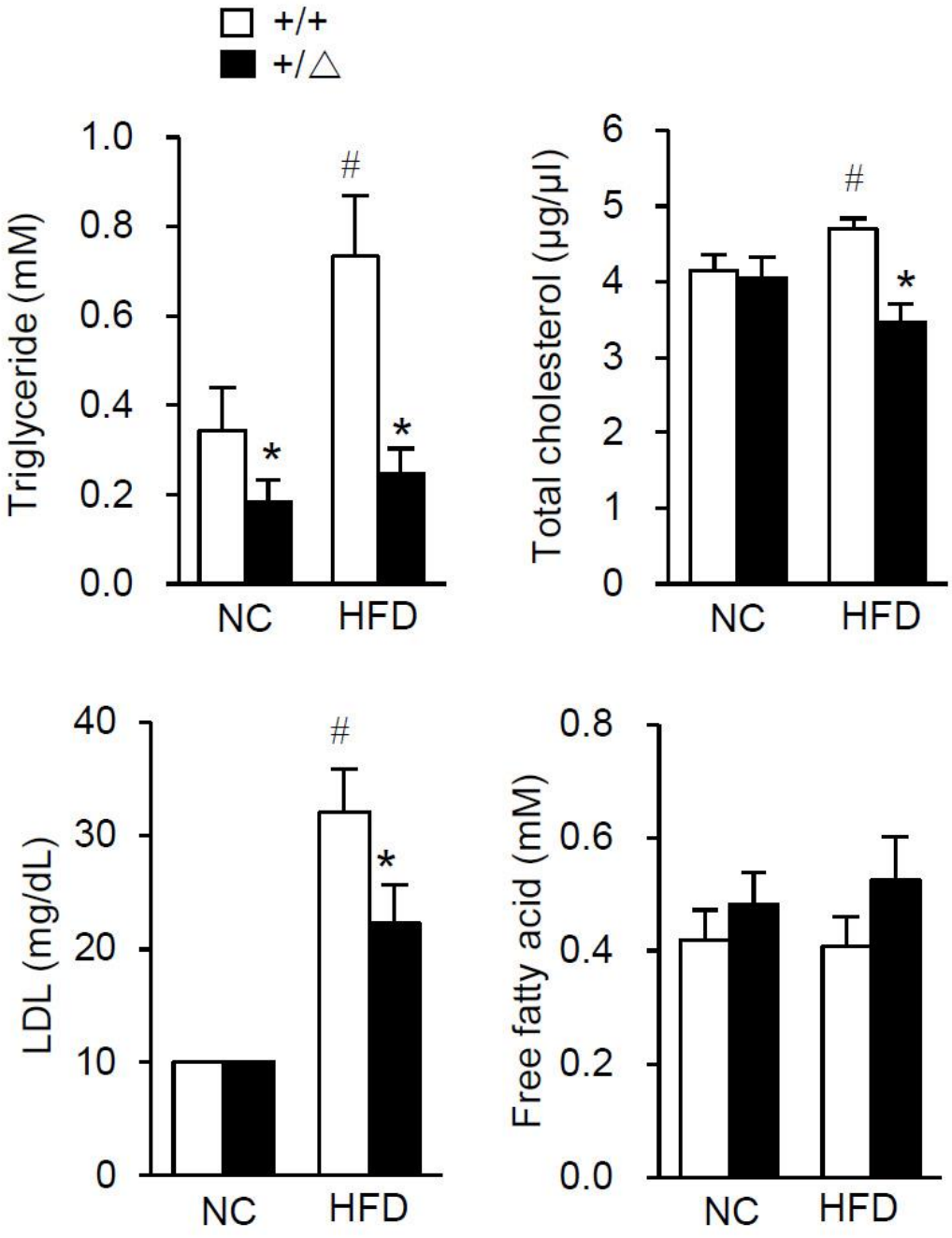

Figure 3-11. TonEBP deficiency ameliorates obesity-induced hyperlipidemia

Cholesterol (total and LDL), triglyceride, and free fatty acid levels, in serum from *TonEBP* +/+ and +/Δ mice fed a HFD. All data are presented as mean + s.e.m. # $p < 0.05$ vs. NC, *TonEBP* +/+ * $p < 0.05$ vs. *TonEBP* +/+ determined by Student's t test.

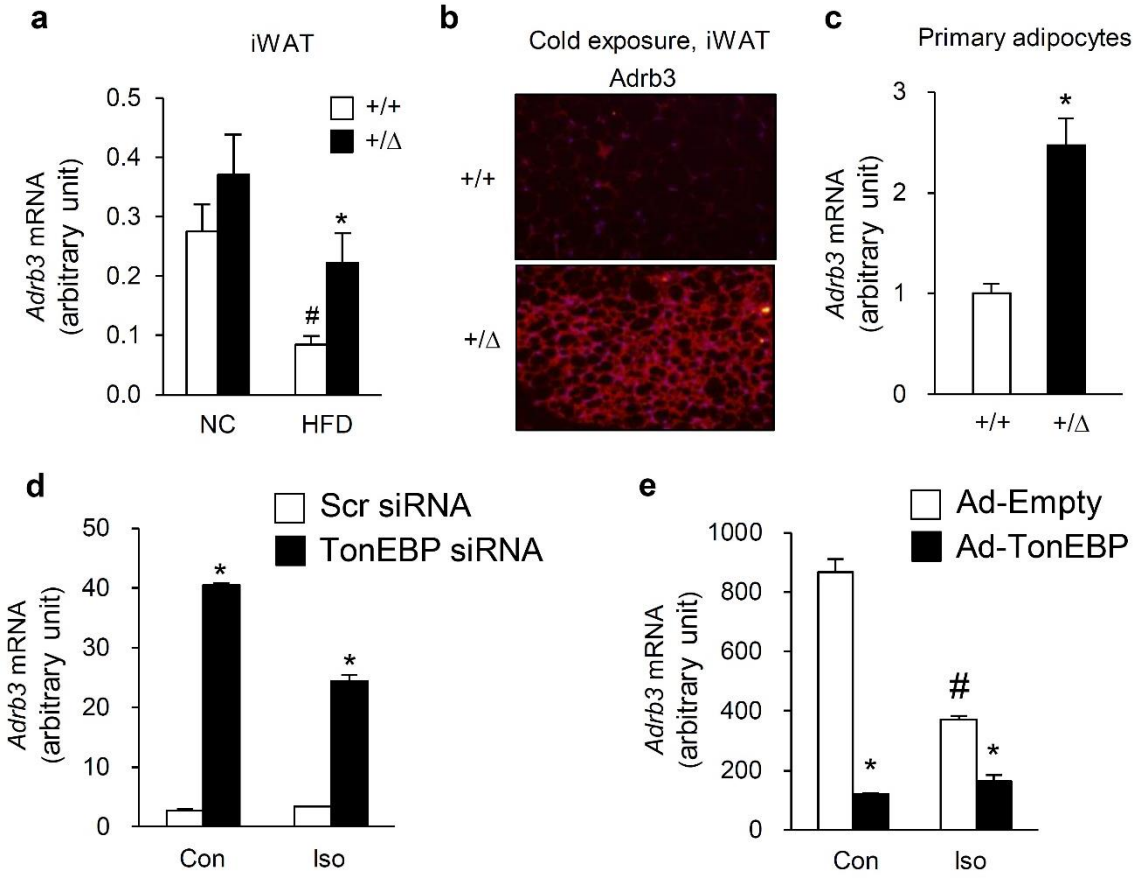

Figure 3-12. TonEBP suppresses *Adrb3* gene expression

(a) *Adrb3* mRNA level in iWAT from *TonEBP* +/+ and *+/Δ* mice fed with a HFD. (b) Adrb3 immunostaining in iWAT from *TonEBP* +/+ and *+/Δ* mice exposed to cold (4℃) (n = 8–10). (c) *Adrb3* mRNA level in primary adipocytes from *TonEBP* +/+ and *+/Δ* mice (n = 4). (d) *Adrb3* mRNA in 3T3-L1 adipocytes with siRNA-mediated TonEBP knockdown (TonEBP siRNA) or (e) adenovirus-mediated TonEBP overexpression (Ad-TonEBP) (n = 4). All data are representative of three independent experiments and presented as the mean + s.e.m. # $p<0.05$ vs. NC or Con * $p < 0.05$ vs. *TonEBP* +/+ or scr siRNA or Ad-Empty determined by Student's t test.

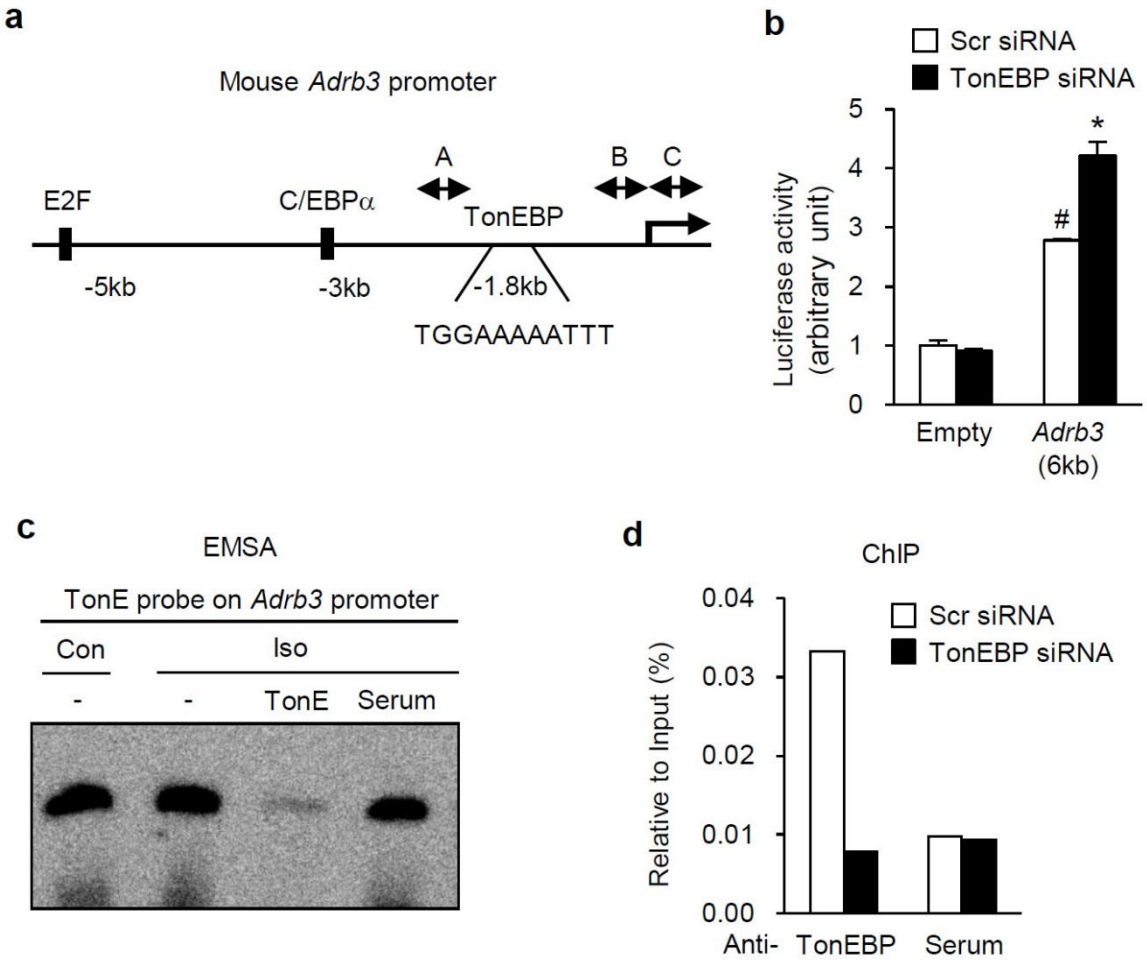

Figure 3-13. TonEBP suppresses *Adrb3* promoter activity by binding to TonE element

(a) Schematic representation of *Adrb3* promoter region, including the TonEBP binding element. (b) Luciferase reporter assay for *Adrb3* promoter in 3T3-L1 adipocytes subjected to siRNA-mediated TonEBP knockdown (TonEBP siRNA) (n = 4). (c and d) TonEBP binding to the putative TonEBP binding site in the Adrb3 promoter using (c) EMSA and (d) ChIP assay. All data are representative of four independent experiments and presented as the mean + s.d. #p<0.05 vs. NC, * p < 0.05 vs. scr siRNA determined by Student's t test.

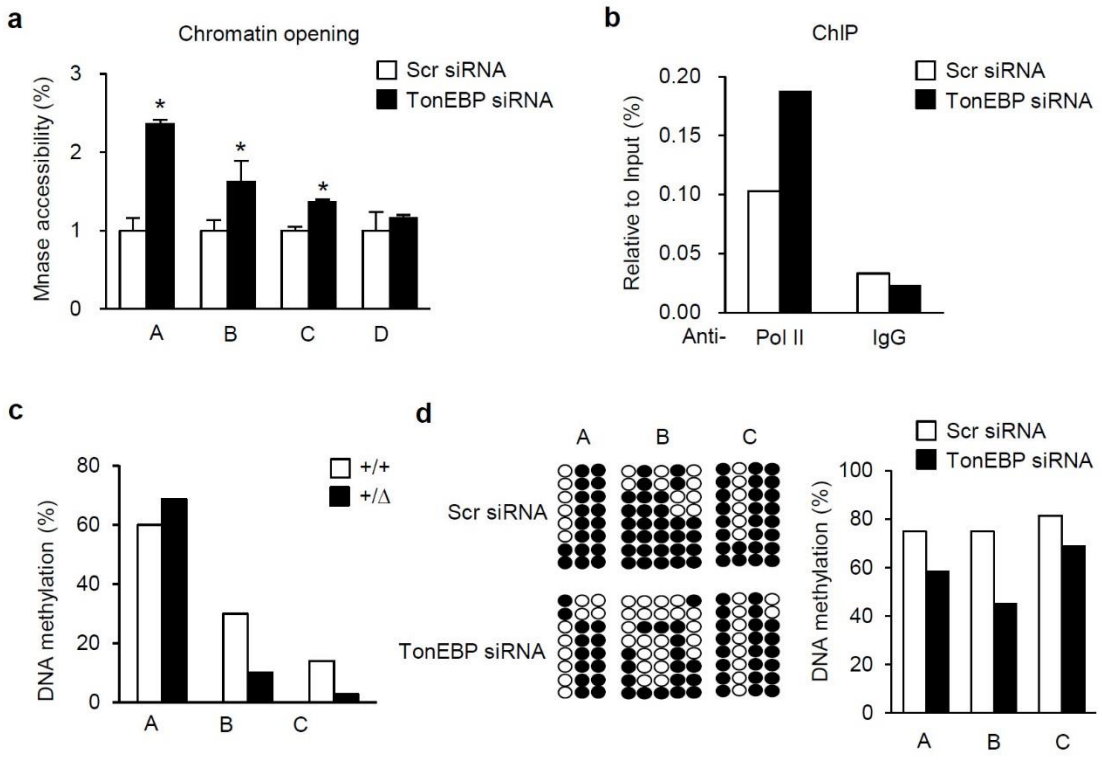

Figure 3-14. TonEBP promotes DNA methylation on *Adrb3* promoter

(a and b) (a) Chromatin accessibility, and (b) ChIP assay for RNA polymerase II (Pol II), on the *Adrb3* promoter region of 3T3-L1 adipocytes subjected to siRNA-mediated TonEBP knockdown.

(c and d) DNA methylation analysis of the *Adrb3* promoter using bisulfite sequencing in (c) iWAT and (d) 3T3-L1 adipocytes. All data are representative of two independent experiments and presented as the mean + s.d. * $p < 0.05$ vs. scr siRNA determined by Student's t test.

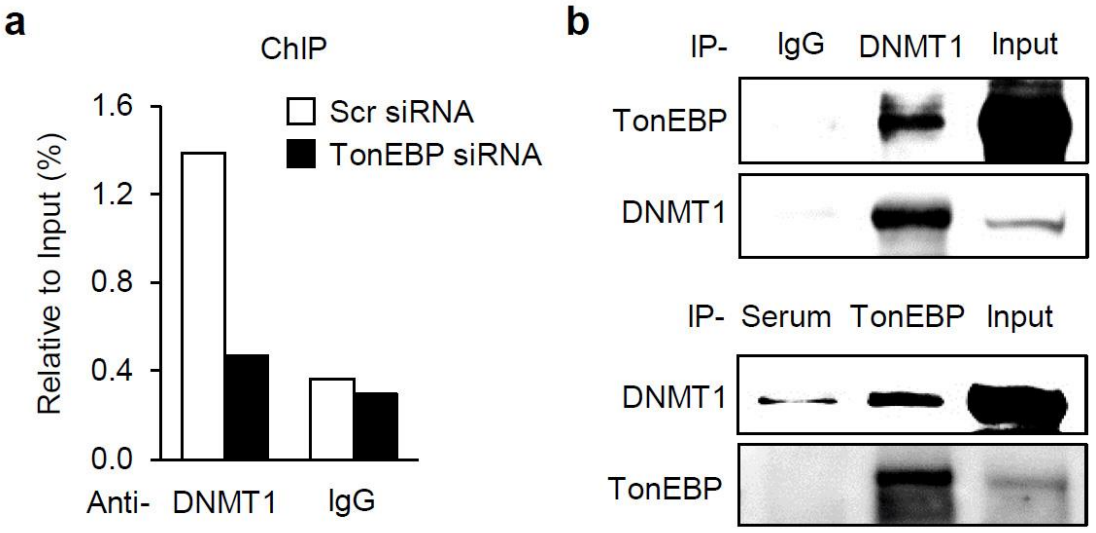

Figure 3-15. TonEBP recruits DNMT1 to *Adrb3* promoter through the interaction

(a) ChIP assay for DNMT1 on the *Adrb3* promoter in 3T3-L1 adipocytes subjected to siRNA-mediated TonEBP knockdown. (b) Immunoprecipitation for TonEBP to demonstrate the DNMT1 interaction. All data are representative of two independent experiments.

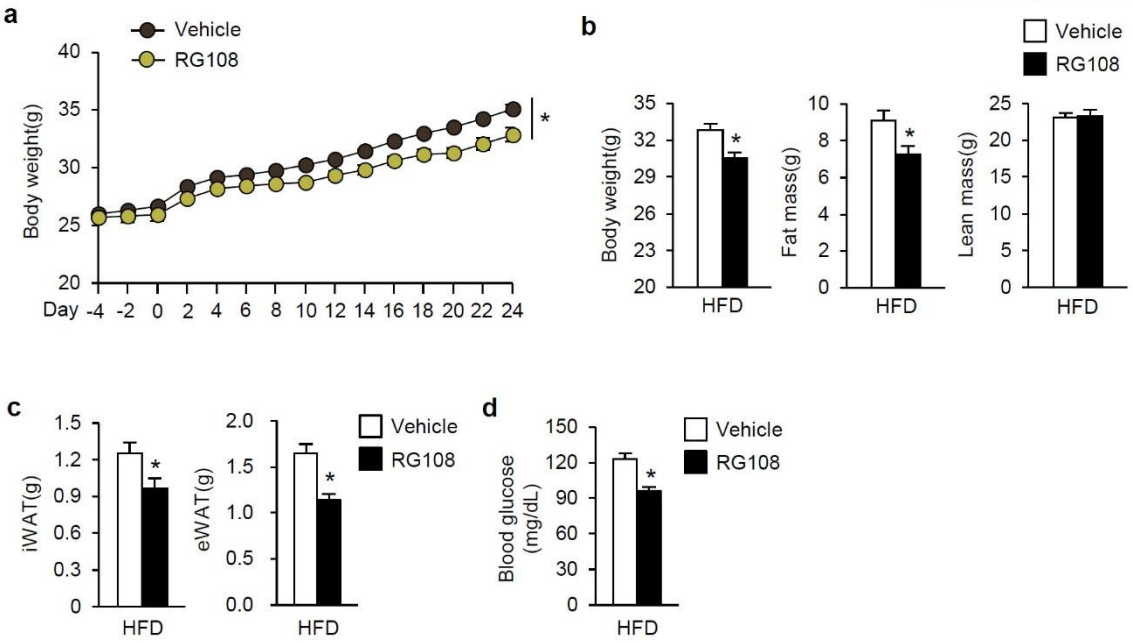

Figure 3-16. DNMT inhibition protects HFD-induced obesity

(a-d) (a) Body weight, (b) body composition by echo MRI, (c) fat pad mass (epididymal and inguinal), and (d) fasting blood glucose level in HFD-fed mice intraperitoneally injected with PBS (vehicle) or RG108 (12 mg/kg) (n = 5 mice per group). All data are representative of two independent experiments and presented as mean + s.e.m. * $p < 0.05$ vs. vehicle determined by Student's t test.

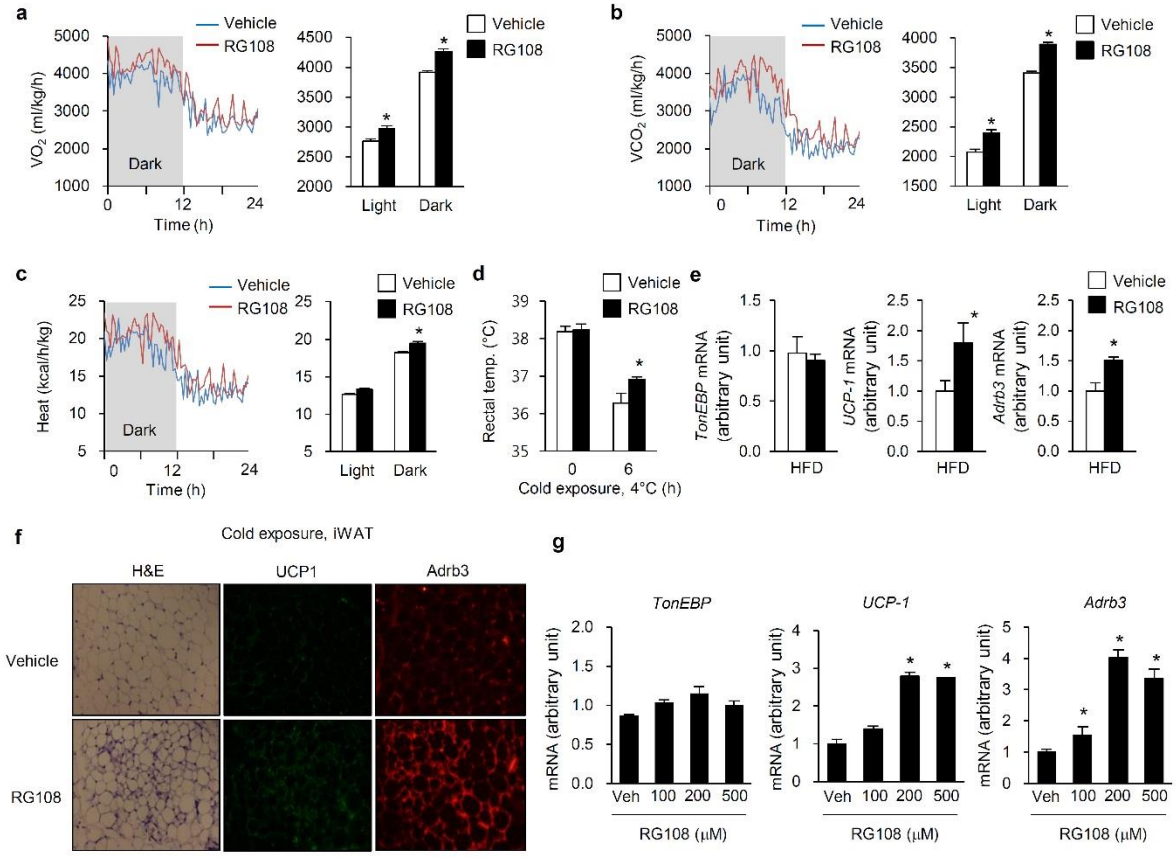

Figure 3-17. DNMT inhibition enhances energy expenditure by inducing WAT beiging and Adrb3 expression

(a-d) (a) VO_2, (b) VCO_2, (c) heat production, and (d) rectal temperature in mice injected with PBS or RG108. (e and f) (e) *TonEBP*, *UCP-1*, and *Adrb3* mRNA, and H&E and (f) immunostaining for UCP-1 and Adrb3, in iWAT from HFD-fed mice intraperitoneally injected with PBS or RG108. (g) *TonEBP*. *UCP-1* and *Adrb3* mRNA in 3T3-L1 adipocytes treated with RG108 for 24 h. All data are representative of two independent experiments and presented as mean + s.e.m. * $p < 0.05$ vs. vehicle determined by Student's t test.

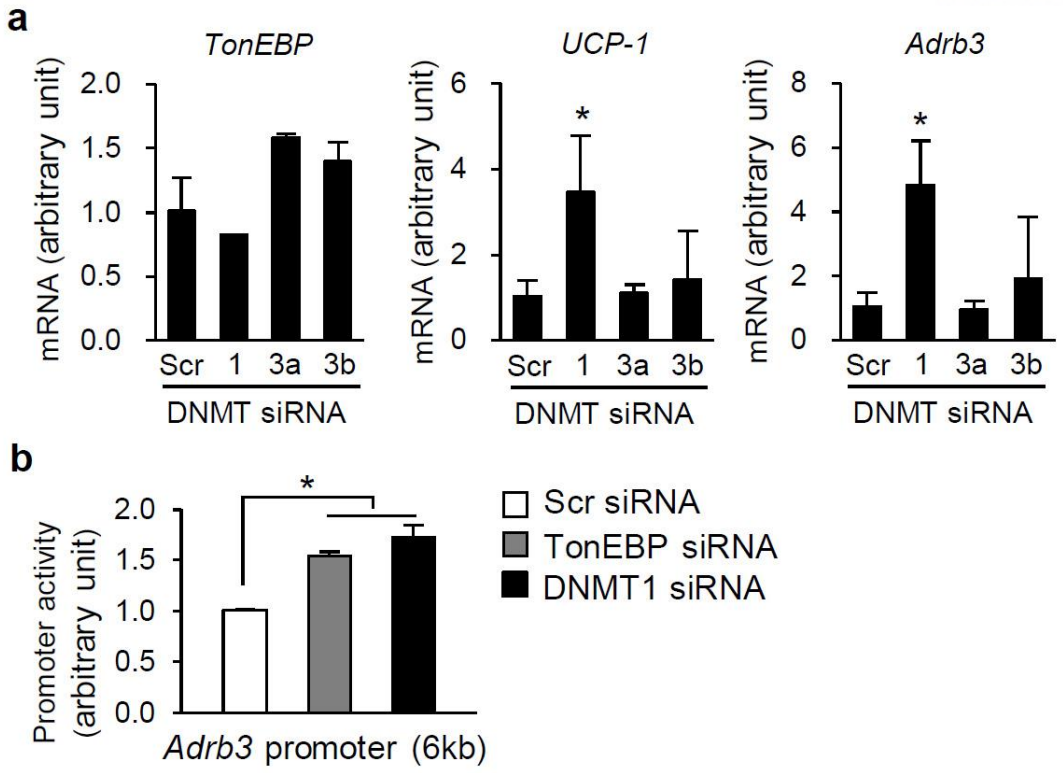

Figure 3-18. DNMT1 deficiency increases Adrb3 expression

(a) *TonEBP, UCP-1* and *Adrb3* mRNA expression in DNMT1, DNMT3a, or DNMT3b siRNA-transfected 3T3-L1 cells. (b) *Adrb3* promoter activity in TonEBP- or DNMT1-silenced 3T3-L1 cells. All data are representative of three independent experiments and presented as mean + s.e.m. * $p < 0.05$ vs. scr siRNA determined by Student's t test.

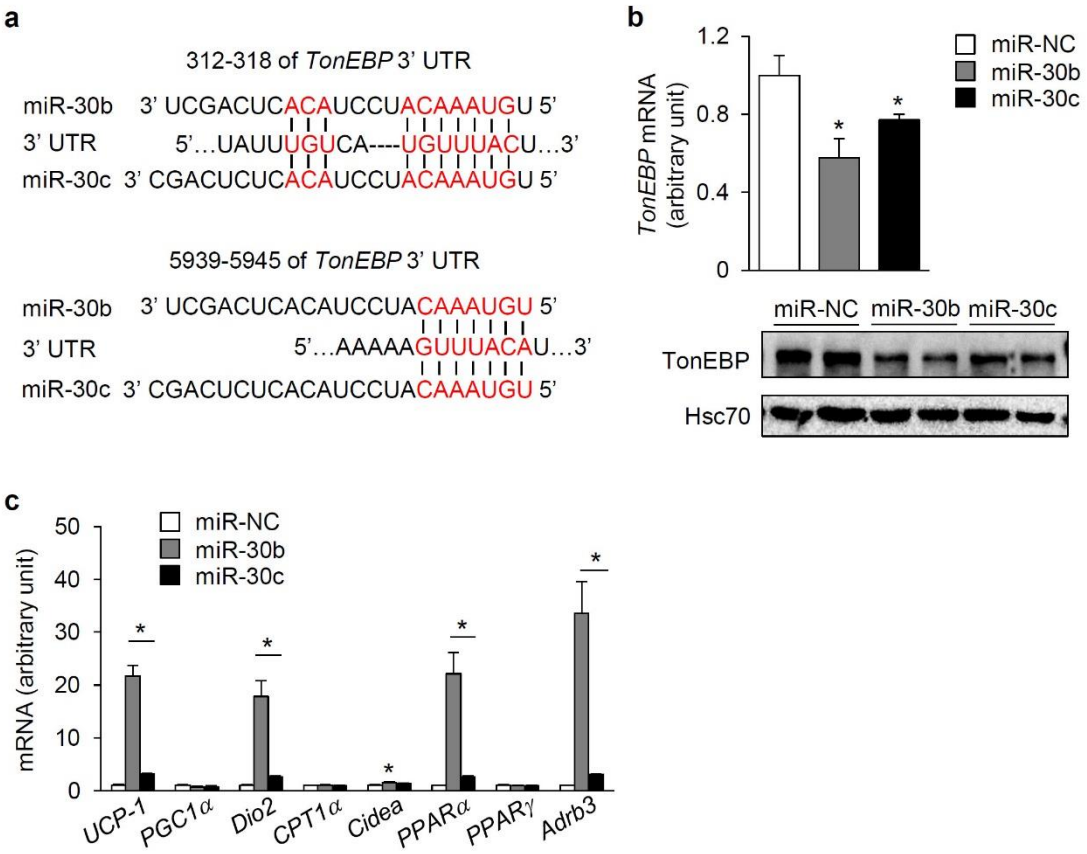

Figure 3-19. TonEBP is a direct target of miR-30b and miR-30c.

(a) Schematic representation of the complementary site of miR-30b and miR-30c on *TonEBP* 3'-UTR. (b) *TonEBP* mRNA and (c) thermogenic gene mRNA in 3T3-L1 adipocytes transfected with miR-NC, miR-30b or miR-30c (n = 4). All data are representative of three independent experiments and presented as mean + s.e.m. * $p < 0.05$ vs. miR-NC determined by Student's t test.

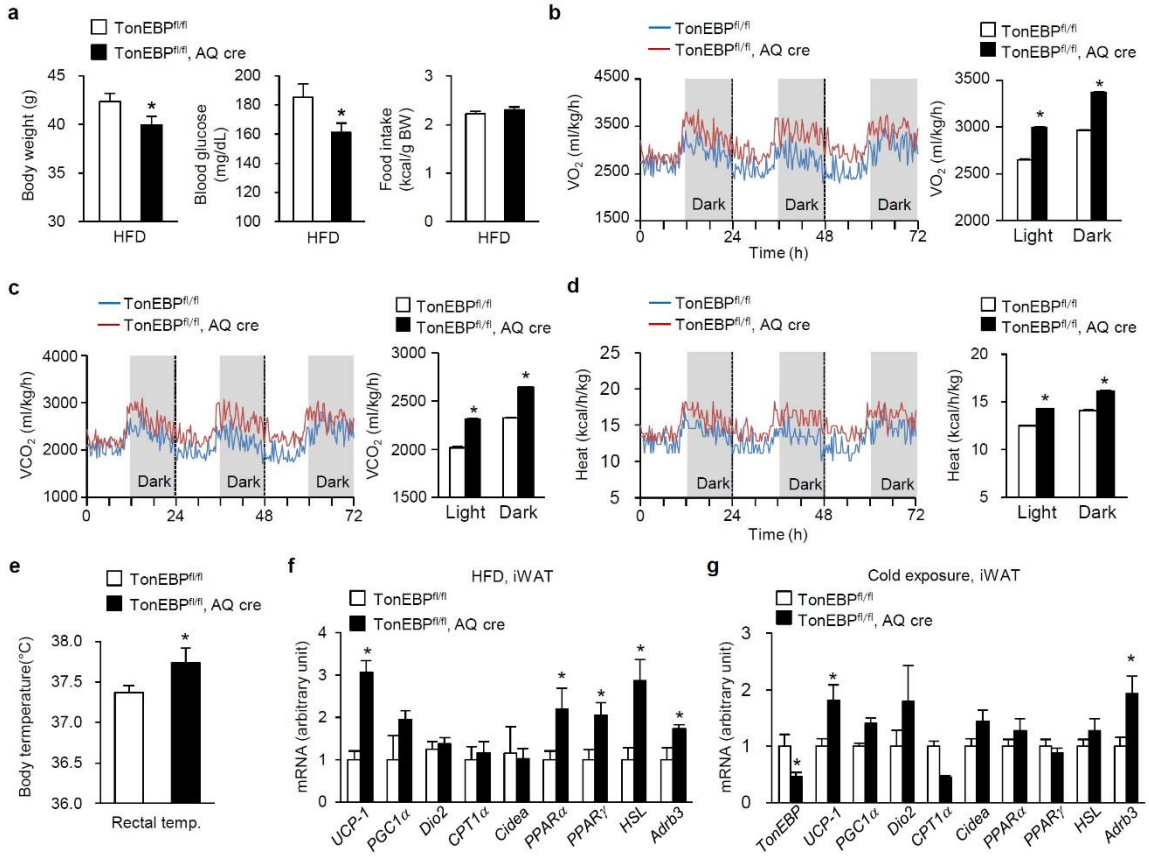

Figure 3-20. Improved metabolic phenotype of adipocyte-specific TonEBP knockout mice

(a) Body weight, fasting blood glucose, and food intake by adipocyte-specific TonEBP knockout mice (*TonEBP* $^{fl/fl}$, *AQ cre*) and control mice (*TonEBP* $^{fl/fl}$) fed with a HFD (n = 9–10 mice per group). (b-e) (b) VO_2, (c) VCO_2, (d) heat production, and (e) rectal temperature analyzed in adipocyte-specific TonEBP knockout mice and control mice fed with a HFD (n = 8 mice per group). (f-g) mRNA expression of thermogenic genes in iWAT from adipocyte-specific TonEBP knockout and control mice fed with a (f) HFD or (g) exposed to cold conditions. All data are representative of two independent experiments and presented as mean + s.e.m. * $p < 0.05$ vs. *TonEBP* $^{fl/fl}$ determined by Student's t test.

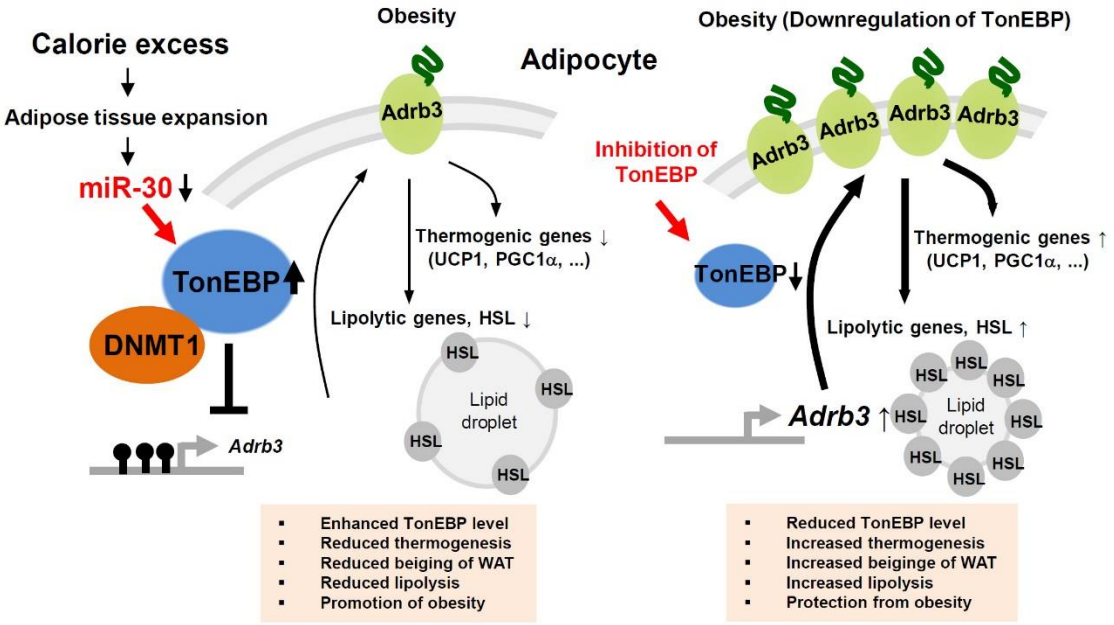

Figure 3-21. Schematic model for the role of TonEBP in obesity

3-5. References

1. Ouchi, N., Parker, J.L., Lugus, J.J. and Walsh, K. 2011 Adipokines in inflammation and metabolic disease. *Nat. Rev. Immunol.* 11: 85-97
2. Trayhurn, P. 2014. Hypoxia and adipocyte physiology: implications for adipose tissue dysfunction in obesity. *Annu. Rev. Nutr.* 34: 207-36
3. Wu, J., Boström, P., Sparks, L.M., Ye, L., Choi, J.H., Giang, A.H., Khandekar, M., Virtanen, K.A., Nuutila, P., Schaart, G., Huang, K., Tu, H., van Marken Lichtenbelt, W.D., Hoeks, J., Enerbäck, S., Schrauwen, P. and Spiegelman, B.M. 2012. Beige adipocytes are a distinct type of thermogenic fat cell in mouse and human. *Cell* 150: 366-76
4. Harms, M. and Seale, P. 2013, Brown and beige fat: development, function and therapeutic potential. *Nat. Med*. 19: 1252-63
5. Miyakawa, H., Woo, S.K., Dahl, S.C., Handler, J.S. and Kwon, H.M. 1999. Tonicity-responsive enhancer binding protein, a rel-like protein that stimulates transcription in response to hypertonicity. *Proc. Natl Acad. Sci. USA.* 96: 2538–2542
6. Lopez-Rodriguez, C., Aramburu, J., Rakeman, A.S. and Rao, A. 1999. NFAT5, a constitutively nuclear NFAT protein that does not cooperate with Fos and Jun. *Proc. Natl Acad. Sci. USA.* 96: 7214–7219
7. Aramburu, J., Drews-Elger, K., Estrada-Gelonch, A., Minguillón, J., Morancho, B., Santiago, V. and López-Rodríguez, C. 2006. Regulation of the hypertonic stress response and other cellular functions by the Rel-like transcription factor NFAT5. *Biochem. Pharmacol*. 72: 1597–1604
8. Lee, S.D., Choi, S.Y., Lim, S.W., Lamitina, S.T., Ho, S.N., Go, W.Y. and Kwon, H.M. 2007. TonEBP stimulates multiple cellular pathways for adaptation to hypertonic stress: organic osmolyte-dependent and -independent pathways. *Am. J. Physiol Renal. Physiol.* 300: F707–715
9. Go, W.Y., Liu, X., Roti, M.A., Liu, F. and Ho, S.N. 2004. NFAT5/TonEBP mutant mice define osmotic stress as a critical feature of the lymphoid microenvironment. *Proc. Natl Acad. Sci.* USA. 101, 10673–10678
10. Buxadé, M., Lunazzi, G., Minguillón, J., Iborra, S., Berga-Bolaños, R., Del Val, M., Aramburu, J. and López-Rodríguez, C. 2012 Gene expression induced by Toll-like receptors in macrophages requires the transcription factor NFAT5. *J. Exp.Med.* 209: 379–393
11. Yoon, H.J., You, S., Yoo, S.A., Kim, N.H., Kwon, H.M., Yoon, C.H., Cho, C.S., Hwang, D. and Kim, W.U. 2011. NFAT5 is a critical regulator of inflammatory arthritis. *Arthritis Rheum.* 63: 1843–1852.
12. Halterman, J.A., Kwon, H.M., Leitinger, N. and Wamhoff, B.R. 2012. NFAT5 expression in bone marrow-derived cells enhances atherosclerosis and drives macrophage migration. *Front. Physiol.*

3, 1–7

13. Kleinewietfeld, M., Manzel, A., Titze, J., Kvakan, H., Yosef, N., Linker, R.A., Muller, D.N. and Hafler, D.A. 2013. Sodium chloride drives autoimmune disease by the induction of pathogenic TH17 cells. *Nature*. 496: 518–522
14. Lee, J.H., Lee, H.H., Ye, B.J., Lee-Kwon, W., Choi, S.Y., Kwon, H.M. 2015. TonEBP suppresses adipogenesis and insulin sensitivity by blocking epigenetic transition of PPARγ2. *Sci. Rep*. 5: 10937
15. Hotta, K., Funahashi, T., Arita, Y., Takahashi, M., Matsuda, M., Okamoto, Y., Iwahashi, H., Kuriyama, H., Ouchi, N., Maeda, K., Nishida, M., Kihara, S., Sakai, N., Nakajima, T., Hasegawa, K., Muraguchi, M., Ohmoto, Y., Nakamura, T., Yamashita, S., Hanafusa, T. and Matsuzawa, Y. 2000. Plasma concentrations of a novel, adipose-specific protein, adiponectin, in type 2 diabetic patients. *Arterioscler. Thromb. Vasc. Biol*. 20: 1595–1599
16. Rosenbaum, M. and Leibel, R.L. 1999. The role of leptin in human physiology. *N. Engl. J. Med.* 341: 913–915
17. Schenk, S., Saberi, M. and Olefsky, J.M. 2008. Insulin sensitivity: modulation by nutrients and inflammation. *J. Clin. Invest*. 118: 2992–3002
18. Postic, C. and Girard, J. 2008. Contribution of de novo fatty acid synthesis to hepatic steatosis and insulin resistance: lessons from genetically engineered mice. *J. Clin. Invest.* 118: 829–838
19. Hotamisligil, G.S. 2006. Inflammation and metabolic disorders. *Nature* 444: 860–867
20. Jung, R.T., Shetty, P.S., James, W.P., Barrand, M.A. and Callingham, B.A. 1979. Reduced thermogenesis in obesity. *Nature.* 279: 322–323
21. Mottillo, E.P., Shen, X. J. and Granneman, J.G. 2007. Role of hormone-sensitive lipase in β-adrenergic remodeling of white adipose tissue. *Am. J. Physiol. Endocrinol. Metab.* 293: E1188–E1197
22. Hu, F., Wang, M., Xiao, T., Yin, B., He, L., Meng, W., Dong, M. and Liu, F. 2015. miR-30 promotes thermogenesis and the development of beige fat by targeting RIP140. *Diabetes.* 64: 2056-2068
23. Xie, H., Lim, B. and Lodish, H.F. 2009. MicroRNAs induced during adipogenesis that accelerate fat cell development are downregulated in obesity. *Diabetes.* 58: 1050-1057
24. Bartel, D.P. 2004. MicroRNAs: genomics, biogenesis, mechanism, and function. *Cell.* 116: 281-297
25. Bartel, D.P. 2009. MicroRNAs: target recognition and regulatory functions. *Cell.* 136: 215-233
26. Rosen, E.D. and Spiegelman, B.M. 2006. Adipocytes as regulators of energy balance and glucose homeostasis. *Nature* 444: 847–853
27. Xie, H., Sun, L. and Lodish, H.F. 2009. Targeting microRNAs in obesity. *Expert. Opin. Ther. Targets*. 13, 1227–1238

28. Heneghan, H.M., Miller, N. and Kerin, M.J. 2010. Role of microRNAs in obesity and the metabolic syndrome. *Obes. Rev.* 11: 354–361
29. McGregor, R.A. and Choi, M.S. 2011. microRNAs in the regulation of adipogenesis and obesity. *Curr. Mol. Med.* 11: 304–316
30. Toperoff, G., Aran, D., Kark, J.D., Rosenberg, M., Dubnikov, T., Nissan, B., Wainstein, J., Friedlander, Y., Levy-Lahad, E., Glaser, B. and Hellman, A. 2012. Genome-wide survey reveals predisposing diabetes type 2-related DNA methylation variations in human peripheral blood. *Hum. Mol. Genet.* 21: 371–383
31. Petronis, A. 2010. Epigenetics as a unifying principle in the aetiology of complex traits and diseases. *Nature.* 465: 721–727
32. Fujisaka, S., Usui, I., Bukhari, A., Ikutani, M., Oya, T., Kanatani, Y., Tsuneyama, K., Nagai, Y., Takatsu, K., Urakaze, M., Kobayashi, M. and Tobe, K. 2009. Regulatory mechanisms for adipose tissue M1 and M2 macrophages in diet-induced obese mice. *Diabetes.* 58: 2574-2582

Conclusion

Adipose tissues have been the target of intense investigation because of the emergence of obesity and type 2 diabetes as a serious public health problem. Adipocytes and macrophages in the adipose tissues are crucial integrators of various physiological pathways regulating whole-body glucose and energy homeostasis. One of the most reliable links between obesity and its complication is inflammation in the adipose tissues. Obesity induces low-grade inflammation in the adipose tissues, which in turn, causes systemic insulin resistance by inhibiting insulin signal transduction.

Adipose tissues are also capable of transforming the chemical energy of fat into heat, thus preventing excessive fat accumulation, through the activity of specialized thermogenic adipocytes. In addition to the classical brown adipocytes that largely comprise brown adipose tissue, and which constitutively express thermogenic genes, 'brown-like' adipocytes, known as beige cells, are also present in white adipose tissues, and thermogenesis can be induced in these cells in response to sympathetic activation. Activation of the thermogenic gene program in brown or beige adipocytes increases systemic energy expenditure and can ameliorate or prevent the development of obesity-associated metabolic disorders as a result. Thus, efforts aimed at gaining a deeper understanding of the regulation of energy storage, mobilization, and use by adipocytes may lead to the identification of potential future therapies for metabolic disease.

In this study, I discovered that TonEBP is a critical regulator of inflammation and the beiging process of WAT:

1. I have investigated the role of macrophage TonEBP in inflammation and insulin resistance. I find that TonEBP is required for the recruitment of p300 to NFκB in M1 macrophage activation and inflammation. In addition, I find that cerulenin is a powerful inhibitor of NFκB with minimal toxicity due to the disruption of the p300 recruitment to NFκB without affecting its nuclear localization or phosphorylation. In addition, TonEBP represses M2 polarization of macrophages *via* the suppression of PPARγ expression. Consistent with the dual regulation of M1/M2 polarization by TonEBP, myeloid specific-TonEBP deficient mice fed with high fat diet showed improved insulin resistance without changes in body weight. Their adipose tissues contain fewer M1 macrophages and more M2 macrophages leading to reduced adipose inflammation. These findings reveal the functions of macrophage TonEBP to promote insulin resistance through the regulations of both NFκB activity (stimulation) and PPARγ expression (suppression).

2. I have also investigated the TonEBP actions in adipocytes. In mice, TonEBP expression is specifically increased in eWAT and iWAT in response to feeding with HFD. Moreover, genetic TonEBP deficiency in adipocytes causes lower body weight and improved insulin resistance with

higher energy expenditure. Their white adipose tissue has elevated thermogenic activity and beiging phenotype with multi-locular lipid droplets and expression of UCP1 in iWAT. In addition, TonEBP haplo-deficient mice were resistant to hypothermia in response to cold exposure. These observations demonstrate that TonEBP is a key regulator (suppressor) of WAT thermogenesis and beiging.

In sum, I have discovered that TonEBP regulates multiple processes including inflammation and thermogenesis and beiging of WAT. Elevated expression of TonEBP in adipose tissue including macrophage and adipocyte of obese mice promotes insulin resistance and obesity (see graphical summary below). These findings raise the possibility that TonEBP is an attractive target for future therapeutics in the treatment of obesity and type 2 diabetes.

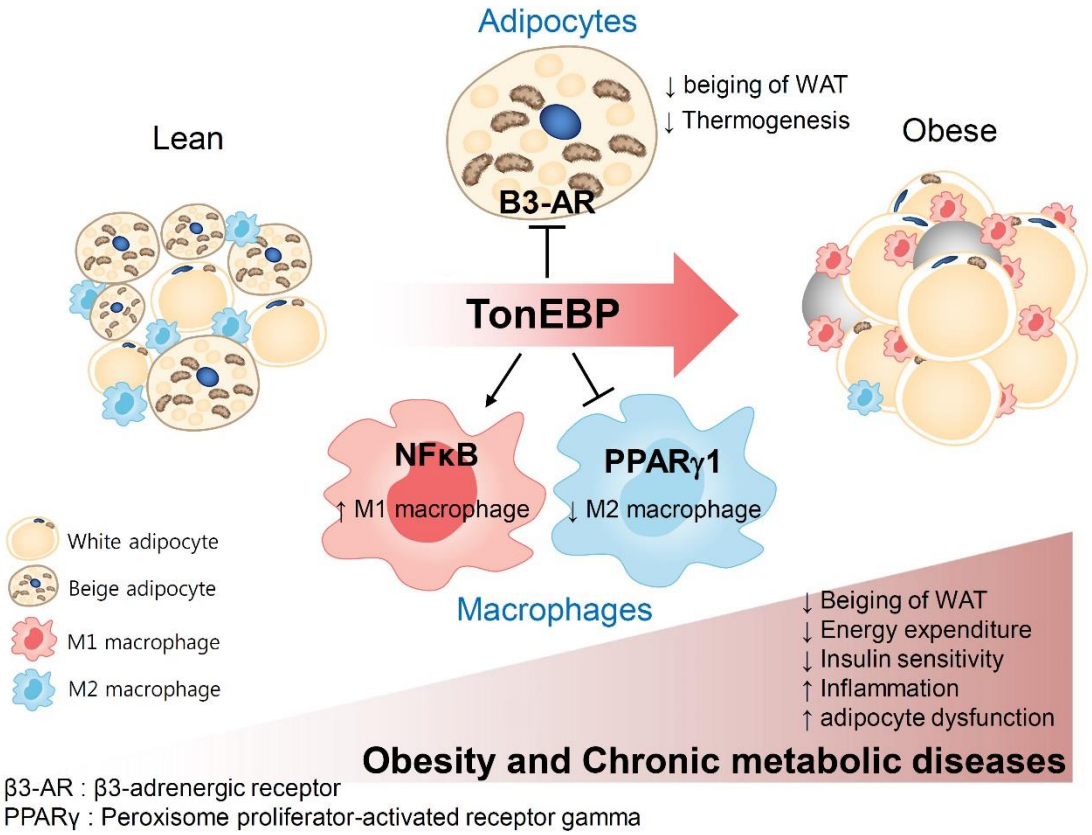

Graphical summary

Acknowledgement (감사의 글)

처음 유니스트 대학원에 진학하면서 졸업은 까마득히 멀고 먼 미래의 일이라 느꼈었습니다. 그러나 석박사 통합과정 5 년이 지난 지금 학위 논문을 마무리 하고 있는 제 자신을 보면 꿈만 같습니다. 처음 실험실에 들어왔을 때, 아무 것도 몰랐던 제가 박사학위를 마치기까지는 지도교수님이신 권혁무 교수님께서 계셨기에 가능했습니다. 바쁘신 중에도 연구뿐만 아니라 연구자에게 필요한 다양한 부분들에 대해 꼼꼼하게 지도를 해주시고, 항상 조급해하지도 느슨해지지도 않고 일관되도록 이끌어 주셔서 졸업이 가능했었던 것 같습니다. 또한, 오랜 학위기간 동안 지치지 않고 열정을 가지고 열심히 할 수 있도록 저를 신뢰해주시고 하고자 하는 연구들을 지원해주신 존경하는 교수님께 정말 감사 드립니다. 교수님의 가르침을 바탕으로 앞으로 좋은 연구자가 될 수 있도록 노력하겠습니다. 그리고 바쁘신 시간 내주시어 학위 논문을 잘 마무리 할 수 있도록 지도해주신 강병헌 교수님, 고명곤 교수님, 박지영교수님, 최장현 교수님께도 감사의 말씀을 전합니다. 이외에도 학위과정 동안 도와주신 이창욱교수님, 이화선교수님, 생명과학부 모든 교수님들께 감사합니다.

또한, 박사 학위기간 동안 교수님만큼 저를 제자로 생각해주시고 많은 가르침과 도움을 주신 최수연 박사님께도 깊은 감사의 말씀을 드립니다. 실험실 생활을 같이하면서 항상 선배로서 모범을 보여준 은진이 누나와 후배로서 불평 한마디 없이 잘 따라준 현제, 준호, 병진이형, 승민이, 규원이, 현이, 그리고 연구에만 집중 할 수 있도록 도와준 나리선생님 등 많은 분들의 도움이 있었기에 학위를 잘 마무리 할 수 있었습니다. 연구 과정에서 혼자라면 할 수 없었던 많은 실험들을 도와준 병진이형, 준호, 승민이를 포함한 IKD 실험실 구성원 모두에게 감사의 말씀을 드립니다.

학교 밖에서도 가장 큰 힘이 되어준 가족들에도 고마움을 전합니다. 오랜 시간 멀리 떨어져서 매일 걱정해주시고 격려해주시고 지원해주시고 응원해주신 부모님, 목표를 향해 열심히 나아가고 있는 기특한 한별이, 집에 갈 때마다 반갑게 맞아주고 오빠 장난도 다 받아주는 지은이 덕분에 모든 과정을 마칠 수 있었습니다. 뿐만 아니라 항상 먼 곳에서도 응원해주시는 할머니, 외할머니, 할아버지, 살아 생전에 항상 저를 자랑스러워 해주신 외할아버지를 포함한 가족 분들께 감사합니다.

언급하지 못하였으나 학위과정 동안 도와주신 많은 분들께도 감사의 마음을 표하며, 앞으로 더욱 열심히 연구에 정진하여 발전하는 모습을 보여드리겠습니다. 감사합니다.